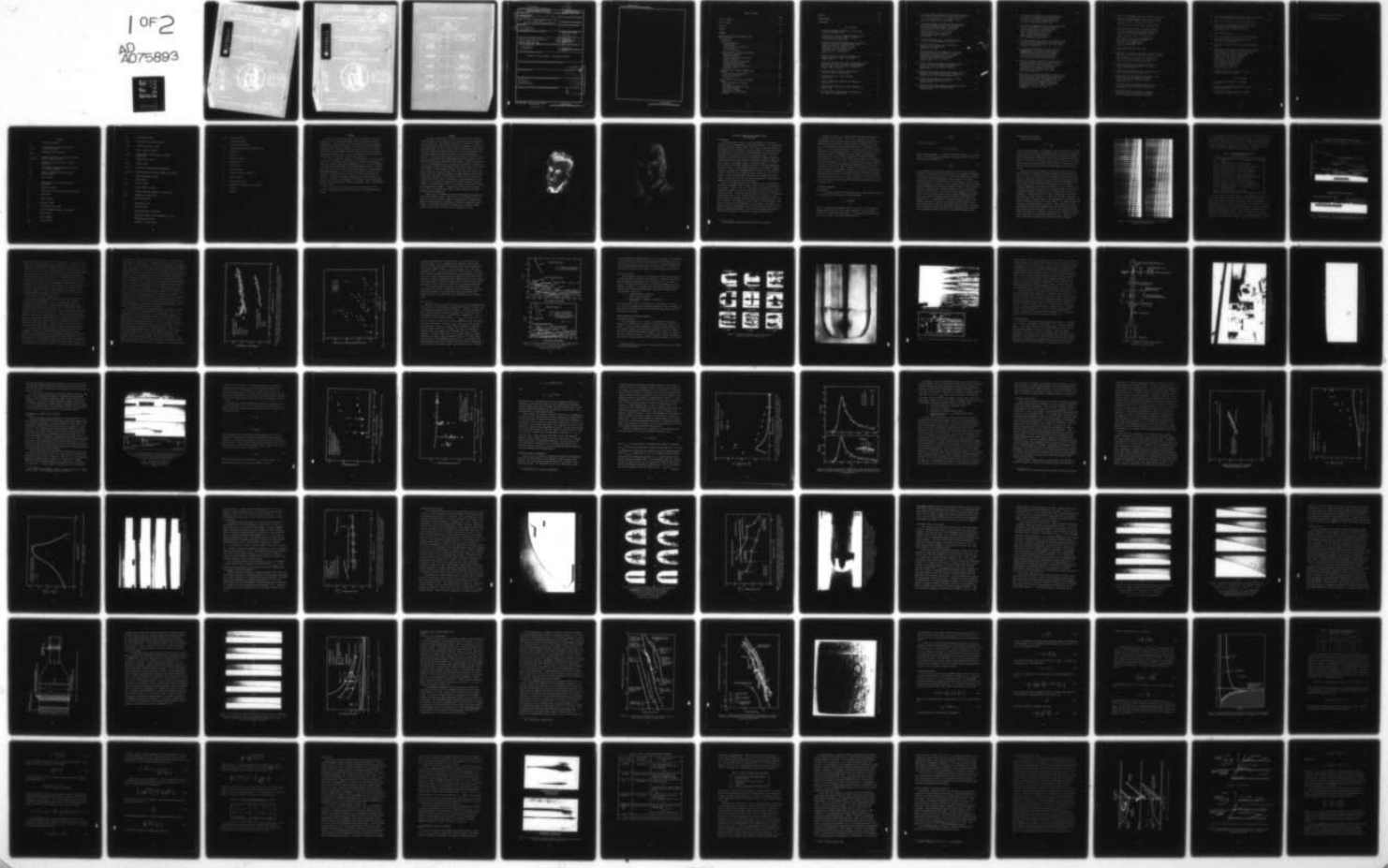


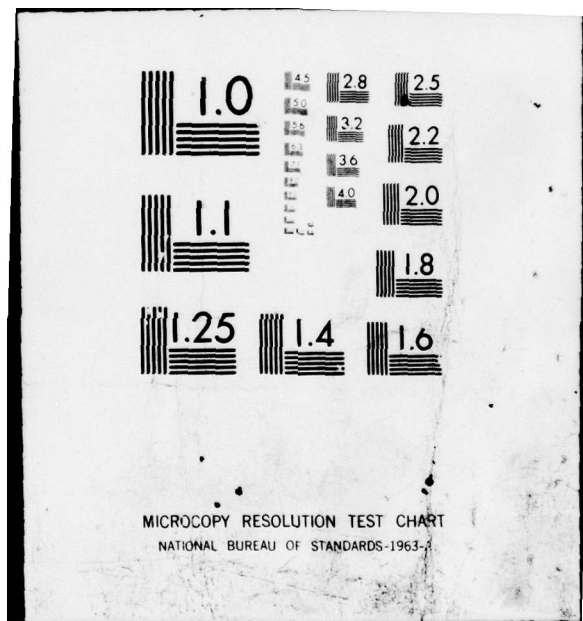
AD-A075 893 DAVID W TAYLOR NAVAL SHIP RESEARCH AND DEVELOPMENT CE--ETC F/G 20/4  
CAVITATION INCEPTION AND INTERNAL FLOWS WITH CAVITATION. THE FO--ETC(U)  
OCT 79 A J ACOSTA

UNCLASSIFIED DTNSRDC-79/011

NL

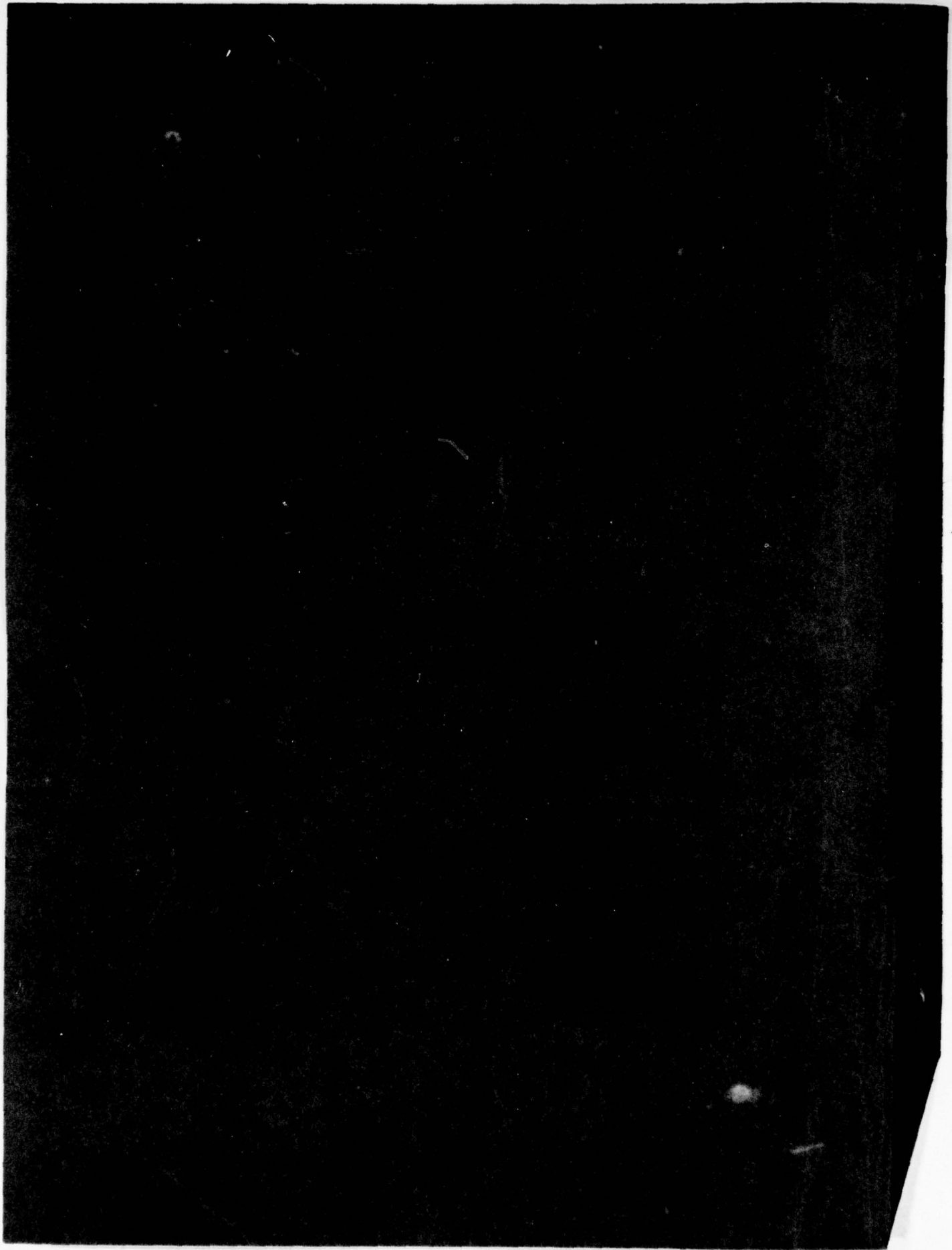
1 OF 2  
AD-A075893





DA075893

DA075893



## UNCLASSIFIED

SECURITY CLASSIFICATION OF THIS PAGE (When Data Entered)

REPORT DOCUMENTATION PAGE		READ INSTRUCTIONS BEFORE COMPLETING FORM																				
1. REPORT NUMBER <i>(14) DTNSRDC-79/011</i>	2. GOVT ACCESSION NO.	3. RECIPIENT'S CATALOG NUMBER <i>(12)</i>																				
4. TITLE (and Subtitle)  CAVITATION INCEPTION AND INTERNAL FLOWS WITH CAVITATION THE FOURTH DAVID W. TAYLOR LECTURE		5. TYPE OF REPORT & PERIOD COVERED																				
7. AUTHOR(S)  <i>(10) Allan J. Acosta</i>		6. PERFORMING ORG. REPORT NUMBER																				
9. PERFORMING ORGANIZATION NAME AND ADDRESS		10. PROGRAM ELEMENT, PROJECT, TASK AREA & WORK UNIT NUMBERS  Work Unit 4-1500-001-41/1509																				
11. CONTROLLING OFFICE NAME AND ADDRESS  David W. Taylor Naval Ship Research and Development Center Bethesda, Maryland 20084		12. REPORT DATE <i>(11) October 1979</i>																				
14. MONITORING AGENCY NAME & ADDRESS (if different from Controlling Office)  <i>(12) 126</i>		13. NUMBER OF PAGES 124																				
15. SECURITY CLASS. (of this report)  UNCLASSIFIED																						
15a. DECLASSIFICATION/DOWNGRADING SCHEDULE																						
16. DISTRIBUTION STATEMENT (of this Report)  APPROVED FOR PUBLIC RELEASE: DISTRIBUTION UNLIMITED																						
17. DISTRIBUTION STATEMENT (of the abstract entered in Block 20, if different from Report)																						
<table border="1"> <tr> <td colspan="2">Accession For</td> </tr> <tr> <td colspan="2">NTIS GRA&amp;I</td> </tr> <tr> <td colspan="2">DDC TAB</td> </tr> <tr> <td colspan="2">Unannounced</td> </tr> <tr> <td colspan="2">Justification _____</td> </tr> <tr> <td colspan="2">By _____</td> </tr> <tr> <td colspan="2">Distribution/ _____</td> </tr> <tr> <td colspan="2">Availability Codes _____</td> </tr> <tr> <td>Distr</td> <td>Avail and/or special</td> </tr> <tr> <td><i>A</i></td> <td></td> </tr> </table>			Accession For		NTIS GRA&I		DDC TAB		Unannounced		Justification _____		By _____		Distribution/ _____		Availability Codes _____		Distr	Avail and/or special	<i>A</i>	
Accession For																						
NTIS GRA&I																						
DDC TAB																						
Unannounced																						
Justification _____																						
By _____																						
Distribution/ _____																						
Availability Codes _____																						
Distr	Avail and/or special																					
<i>A</i>																						
19. KEY WORDS (Continue on reverse side if necessary and identify by block number)  Cavitation Two Phase Flows Cavitation Scaling																						
20. ABSTRACT (Continue on reverse side if necessary and identify by block number)																						

DD FORM 1 JAN 73 1473

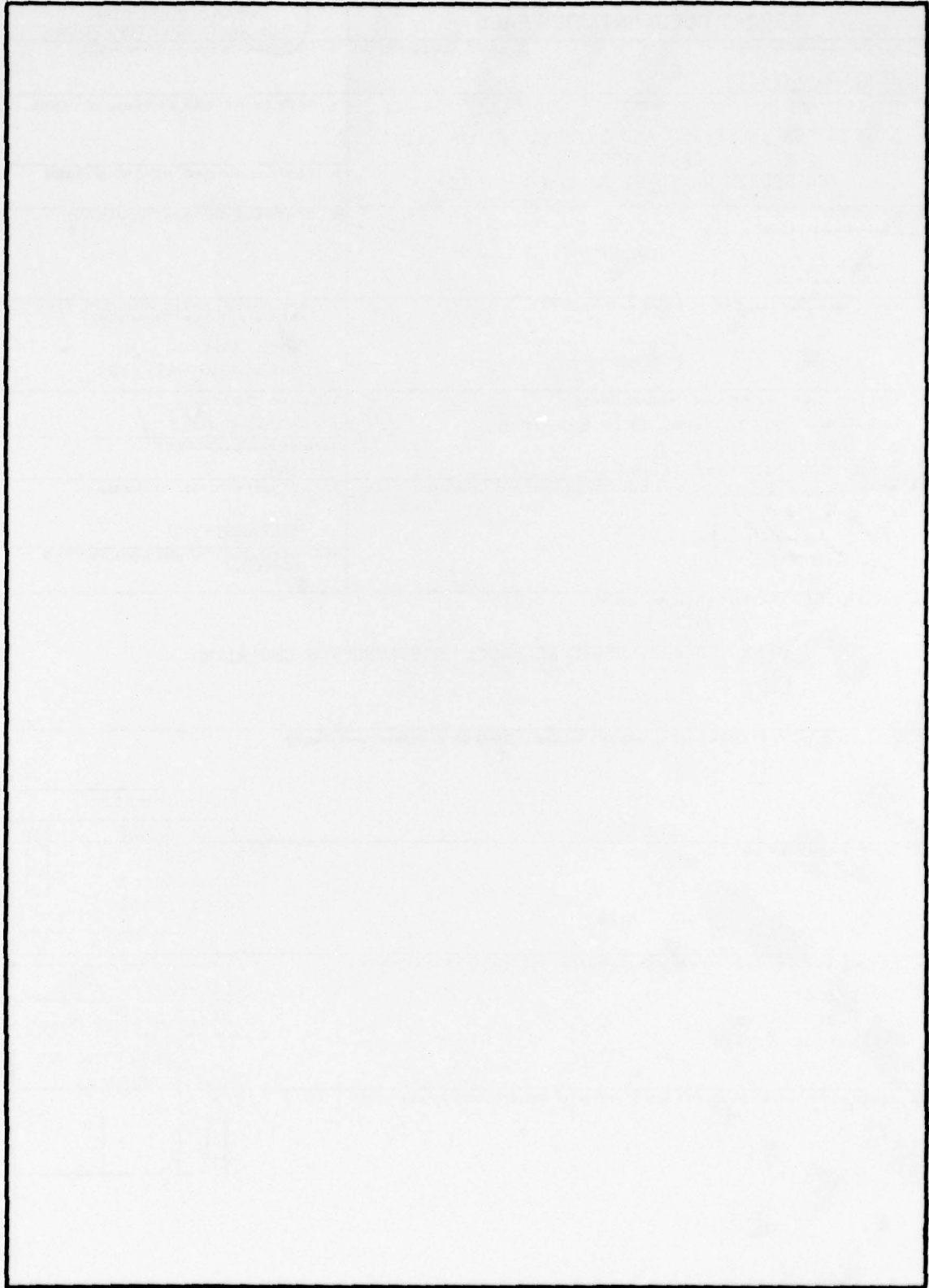
EDITION OF 1 NOV 65 IS OBSOLETE  
S/N 0102-LF-014-6601*387682*

UNCLASSIFIED

SECURITY CLASSIFICATION OF THIS PAGE (When Data Entered), *IP*

**UNCLASSIFIED**

**SECURITY CLASSIFICATION OF THIS PAGE (When Data Entered)**



**UNCLASSIFIED**

**SECURITY CLASSIFICATION OF THIS PAGE (When Data Entered)**

## TABLE OF CONTENTS

	Page
<b>LIST OF FIGURES . . . . .</b>	<b>iv</b>
<b>LIST OF TABLES . . . . .</b>	<b>viii</b>
<b>NOTATION . . . . .</b>	<b>x</b>
<b>PREFACE . . . . .</b>	<b>xiii</b>
<b>FOREWORD. . . . .</b>	<b>xiv</b>
<b>CAVITATION INCEPTION AND INTERNAL FLOWS</b>	
<b>WITH CAVITATION . . . . .</b>	<b>1</b>
INTRODUCTION . . . . .	1
CAVITATION INCEPTION . . . . .	2
Preliminaries . . . . .	2
Scale Effect--Early Results . . . . .	4
The ITTC Tests . . . . .	12
Forms of Cavitation . . . . .	14
VISCOUS EFFECTS ON CAVITATION INCEPTION . . . . .	14
Experimental Methods . . . . .	14
Laminar Separation . . . . .	18
Inception Observations within the Laminar Separation . . . . .	22
Conditions within the Separation . . . . .	27
Transition and Cavitation . . . . .	32
Stimulated Boundary Layers . . . . .	40
The Polymer Effect in Cavitation . . . . .	45
Turbulence Levels . . . . .	49
CAVITATION NUCLEI, BUBBLE MECHANICS AND SCALING . . . . .	54
Nuclei and Their Measurements . . . . .	54
Some Bubble Mechanics . . . . .	59
Scaling Ideas . . . . .	67
FULLY DEVELOPED CAVITATION IN INTERNAL FLOWS . . . . .	68
Analytic Methods for Internal Cavitation . . . . .	73
The Coupling Problem for a Pump . . . . .	74
The Transfer Function . . . . .	79
Application to Pumps . . . . .	80
Experiments in Unsteady Pump Dynamics . . . . .	83

	Page
SUMMARY . . . . .	90
ACKNOWLEDGMENT . . . . .	91
BIBLIOGRAPHY . . . . .	93

#### LIST OF FIGURES

1 - Travelling Bubble Cavitation on a 1.5-Cal Ogive (Knapp and Hollander 1948) . . . . .	5
2 - Cavitation on a Two-Inch Diameter Hemisphere Body: Flow from Right to Left; Speed = 40 ft/sec (From Parkin and Kermene 1953) . . . . .	7
3 - Cavitation Index on Hemispherical and 1.5-Cal Ogive Bodies as a Function of Reynolds Number (From Parkin and Holl 1953: The point of dis- appearance of the cavitation is used as the index in this case and this is termed "desinent" cavitation by Holl.) . . . . .	10
4 - Cavitation Index on a Series of Geometrically Similar Hydrofoils Showing a Size Effect (Parkin 1952) . . . . .	11
5 - Cavitation Inception Index versus Tunnel Speed for Two Dissolved Air Contents on a Flat-Faced Ellipsoidal Body for Various Test Facilities (Lindgren and Johnsson 1966, ITTC Tests) . . . . .	13
6 - Incipient Cavitation on the ITTC Headform in Various Facilities (Johnsson 1969) . . . . .	15
7 - Cavitation Inception on the ITTC Body-- Caltech HSWT . . . . .	16
8 - A Form of Cavitation Inception on a Hydrofoil (Arakeri 1971) . . . . .	17
9 - Schlieren Flow Visualization System (Lindgren and Johnsson 1966) . . . . .	19
10 - The Spark Source, Steady Source, and Collecting Lens Setup in the Caltech LTWT . . . . .	20

11 - A Two-Inch Diameter Hemisphere Showing Laminar Separation and Turbulent Reattachment at a Body Reynolds Number of $2.6 \times 10^5$ (The height of the separation region is about 0.01 inches, Gates et al. 1978) . . . . .	21
12 - The Form and Extent of Cavitation Originating Within the Viscous Separated Region of the Hemispherical Nose at Three Levels of Tunnel Pressure (The freestream speed is 40 ft/sec and the body Reynolds number is $6 \times 10^5$ . The dark patches above the model outline are the cavitating areas. Arakeri and Acosta 1973) . . . . .	23
13 - Inception Observations on a Hemisphere-Nose Body in the Caltech HSWT (Arakeri et al. 1973) . . . . .	25
14 - Inception Observations on the ITTC (Swedish) Headform in the Caltech HSWT (Arakeri et al. 1973) . . . . .	26
15 - Peak and RMS Pressure Fluctuations on a Two-Inch Hemispherical Body (The transducer is located at an arc-diameter ratio of 0.95. The active diameter of the transducer was several times the disturbance wave length. Arakeri 1975b) . . . . .	29
16 - Pressure Fluctuations (Negative Peak Upper and RMS Lower) on a Body of Revolution Downstream of a Laminar Separation Reattachment (Huang and Hannan 1975) . . . . .	30
17 - Comparison of Desinent Cavitation Measurements with the Negative of the Pressure Coefficient at the Site of Calculated Point of Transition (Arakeri 1973) . . . . .	34
18 - Pressure Fluctuations on the Surface of a 1.5-Cal Ogive at the Arc-Diameter Ratio of 1.3 (Arakeri 1975b) . . . . .	35
19 - Comparison of Measured Frequency Distribution with that Calculated from Linear Stability Results (Arakeri 1975b) . . . . .	36

20 - Flow from Left to Right Shows: (a) Some Details of Transition on a Two-Inch 1.5-Cal Ogive Body at 30 ft/sec, (b) Desinent Cavitation at the Same Velocity, and (c) and (d) Similar Results at 40 ft/sec. (Arakeri and Acosta 1974) . . . . .	37
21 - Inception and Desinent Cavitation Index for the NSRDC Body in the Caltech HSWT at an Air Content of 10.4 ppm (The numbers in parentheses represent the number of data points and the height of the bars, the range of the data.) Laminar separation was not observed greater than about 28 ft/sec. (Arakeri and Acosta 1976) . . . . .	39
22 - A Tripped Boundary Layer on a Two-Inch Hemisphere Body at a Subcritical Reynolds Number (The trip is located 30 degrees from the nose and is 0.012 inches high, Arakeri and Acosta 1976) . . . . .	41
23 - A Two-Inch Hemisphere Body with Trips Showing the <u>Disappearance</u> of Cavitation as Tunnel Speed is Increased and the Cavitation Index Decreased (The left side sequence has a trip height of 0.012 inches and the right side has a trip of 0.005 inches, Arakeri and Acosta 1976) . . . . .	42
24 - Cavitation Inception Index versus Tunnel Speed for a 1.81-Inch Hemisphere Body with a 0.005-Inch Trip (The water tunnel is the Caltech HSWT: in every case inception occurs as an attached cavity. The numbers are the number of data points and the bars show the experimental range, Arakeri and Acosta 1976) . . . . .	43
25 - Cavitation on a Two-Inch Hemisphere Body (Speed = 43.5 ft/sec with a 0.014-inch trip located 30 degrees from the nose spanning one-half the circumference. The cavitation index is 0.56. Downstream of the trip there is no cavitation (upper portion) and on the lower portion of the body the normal band cavitation can be seen. Photo courtesy of Professor J. W. Holl, Penn State University) . . . . .	44

	Page
26 - Flow Past the Hemisphere Body with Injection of 100 wppm Polyox at a Reynolds Number of $3.9 \times 10^5$ (The dimensionless injectant rates are, respectively: (a) no injection, (b) $0.5 \times 10^{-6}$ , (c) $1.1 \times 10^{-6}$ , (d) $1.7 \times 10^{-6}$ , and (e) $2.9 \times 10^{-6}$ , Gates and Acosta 1978) . . . . .	47
27 - Flow Past the Schiebe Body at a Reynolds Number of $4.2 \times 10^6$ with Injection of 500 wppm Polyox (The dimensionless injection parameters are respectively: (a) zero, (b) $2.3 \times 10^{-6}$ , (c) $1.5 \times 10^{-5}$ , and (d) $2.9 \times 10^{-5}$ . The photographs are each 0.2 body diameters in length centered on arc lengths of 0.82, 0.75, 0.6, 0.53, respectively, Gates and Acosta 1978) . . . . .	48
28 - Caltech Low Turbulence Water Tunnel (Gates 1977) . . . . .	50
29 - The Effect of Freestream Turbulence on the Flow Past the NSRDC Body (The flow is from right to left at a body Reynolds number of $1.6 \times 10^5$ . The turbulence intensity is: (a) 0.05 percent, (b) 0.65, (c) 1.1, (d) 2.3, and (e) 3.6 percent, Gates 1977) . . . . .	52
30 - Comparison of Observed Transition Locations with Values Predicted by the Amplification Method (Wazzan and Gazley 1978) . . . . .	53
31 - Freestream Nuclei Number Density Distributions from Various Sources (Gates and Acosta 1978) . . . . .	56
32 - Nuclei Distributions Measured by Holography in the Caltech LTWT (All Microbubbles) and HSWT (Essentially All Solid Particles) (Gates and Acosta 1978) . . . . .	57
33 - TV Monitor Showing Holographic Reconstruction of a 20-Micrometer Particle and 200-Micrometer Bubble (Katz 1978) . . . . .	58
34 - Equilibrium Radius for Constant Gas Content K (Arbitrary Units) Showing Stable and Unstable Regions (Adapted from Knapp et al. (1970)) . . . . .	62

	Page
35 - Cavitation on the Same (Schiebe) Body in the Caltech LTWT and the Caltech HSWT (Gates and Acosta 1978) . . . . .	69
36 - Forms of Cavitation in an Inducer Pump Blade Row . . . . .	75
37 - Representation of Unsteady Cavitating Flow Through a Cascade of Inducer Blades Together with Linearized Boundary Conditions (Kim and Acosta 1975) . . . . .	76
38 - Pump Performance Curves . . . . .	81
39 - Cavitation Compliance $K_B$ Estimated from Microbubble Populations Measured in Water Tunnels versus Cavitation Index (Brennen 1973) . . . . .	84
40 - Test Loop for Dynamic Transfer Function Measurement (Ng 1976) . . . . .	86
41 - Transfer Function for an Axial Inducer Pump at a Flow Coefficient of 0.07 (Inlet Value) (The value of the total pressure coefficient is about 0.05. The inducer consists of four cambered blades having a tip inlet angle of 7 degrees followed by 12 more heavily loaded tandem blades. The real part of the coefficients are shown solid and the imaginary dotted. Two sets of data are shown, fully wetted and for a cavitation index $\sigma = 0.046$ ) . . . . .	87
42 - Cavitation in the Pump of Figure 41 at the Cavitation Index of $\sigma = 0.040$ . . . . .	89

#### LIST OF TABLES

1 - Some Chronological Events in Cavitation Inception . . . . .	6
2 - Some Values of Natural Frequency and Critical Radius for Bubbles . . . . .	63
3 - Comparison of Thermal Parameters for Water $U_o = 10 \text{ m/s}$ , $L = 3 \text{ cm}$ . . . . .	66

Page

4 - Types of Cavitation Inception Phenomena . . . . .	70
5 - Types of Internal Flow Cavitation . . . . .	71

### NOTATION

$c_p$	Pressure coefficient
$c_{p_{loc}}$	Local pressure coefficient at point of cavitation inception
$c_{p_{min}}$	Minimum pressure coefficient
$c_{p_{reattach}}$	Pressure coefficient at reattachment point of laminar separation bubble
$c_{p_s}$	Pressure coefficient at point of laminar separation
$c_{p_t}$	Fluctuating pressure coefficient at location of cavitation inception
$c_{p_{tr}}$	Pressure coefficient at boundary-layer transition point
$E_k$	Eckert number
$e^n$	Amplification factor for boundary layer disturbances
$j$	Imaginary constant
$K$	Proportionality constant for gas within bubble
$k_c$	Conductivity
$k_s$	Spring constant
$L$	Reference length
$\ell(t)$	Fluctuating cavity length
$N$	Velocity component normal to cascade axis
$P_e$	Peclet number
$p$	Static pressure
$p_{cav}$	Cavity pressure

$p_g$	Gas partial pressure
$p_{\min}$	Minimum value of static pressure
$p_{\text{sat}}$	Saturation pressure of gas
$p_v$	Vapor pressure of liquid
$p_v(T_\infty)$	Vapor pressure of pure liquid at ambient temperature
$p_\infty$	Ambient static pressure
$p_\infty(t)$	Pressure field
$\hat{p}_1, \hat{p}_2$	Additional complex fluctuating pressures
$p_{1s}, p_{2s}$	Steady pressures across the cascade with no motion
$q$	Freestream dynamic pressure
$R$	Bubble radius
$R_{\text{crit}}$	Critical radius
$R_0$	Initial radius of bubble
$T$	Velocity component tangential to cascade axis
$T(R)$	Temperature on bubble wall
$T_\infty$	Ambient temperature
$t^*$	Dimensionless time
$U_0$	Reference speed
$\hat{u}_n$	Fluctuating velocity components
$v$	Perturbation normal velocity component on cavity
$x$	Distance along the chord
$y$	Coordinate in linear theory

[z]	Transfer function
$\alpha$	Thermal diffusivity
$\delta$	Heat diffusion distance
$\varepsilon(t)$	Linearization function for bubble radius
$\zeta$	Latent heat
$\mu$	Viscosity
$\nu$	Viscosity constant
$\rho$	Liquid density
$\rho_v$	Vapor density
$\sigma$	Cavitation number
$\sigma_i$	Cavitation number at inception
$\sigma_s$	Surface tension
$\phi$	Nondimensional speed
$\psi$	Nondimensional pressure across cascade
$\Omega$	Frequency
$\omega$	Frequency

#### PREFACE

The David W. Taylor Lectures were conceived to honor our founder in recognition of his many contributions to naval architecture and naval hydrodynamics. Admiral Taylor had a keen devotion to both experimental evaluations and theoretical analysis for the solution of naval problems. He established a tradition of applied scientific research at the "Model Basin" which has been carefully nurtured through the decades and which we treasure and maintain today. It is in this spirit that we have invited Prof. Allan J. Acosta to be a David W. Taylor Lecturer.

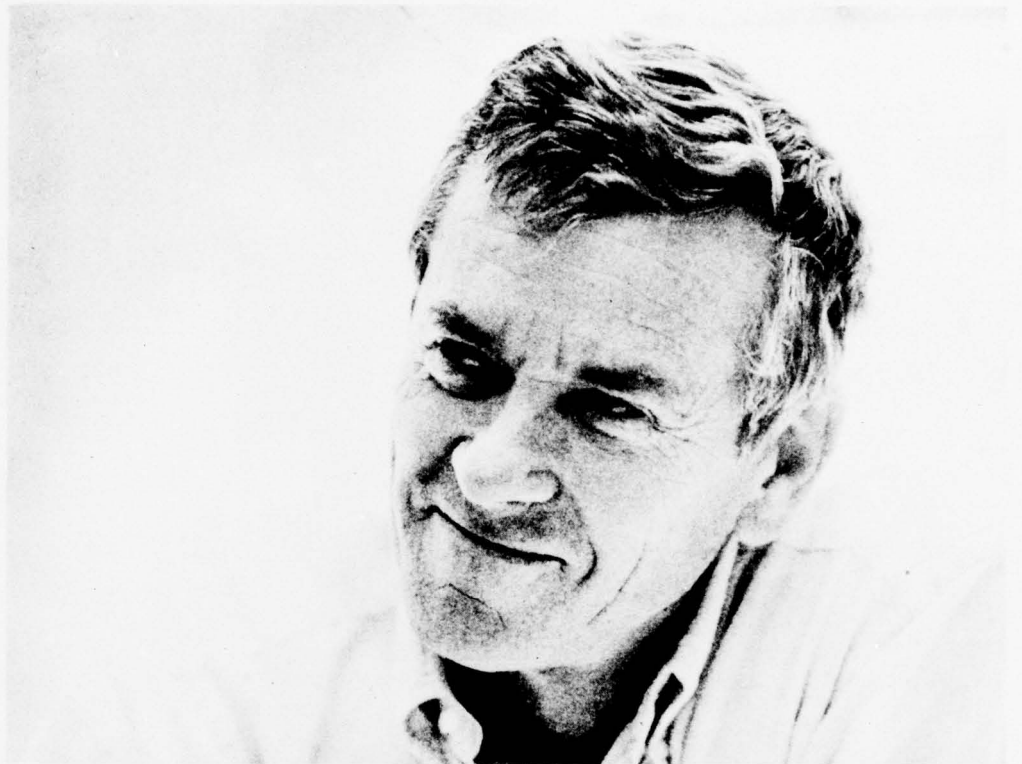
Dr. Acosta received his Bachelor of Science Degree from the California Institute of Technology in 1945, followed by a Master of Science Degree (1948) and the Ph.D. (Mechanical Engineering) in 1952. For the following two years, he was Section Chief of the Hydrodynamics Laboratory. During the period 1954-58, Dr. Acosta was Assistant Professor in the Mechanical Engineering Department at the California Institute of Technology, was promoted to Associate Professor in 1958, and since 1966 has been full professor. Currently, he teaches thermodynamics, fluid mechanics, heat transfer, and advanced turbomechanics. His research areas include hydrodynamics of cavitating flows, hydrofoils, underwater bodies, turbomachines and heat transfer.

Prof. Acosta lives near the beach and is an avid sailor. He is currently completing construction of a sailboat for an around-the-world voyage.

#### FOREWORD

It has been a great honor to deliver the fourth in this series of lectures because of the prestige of this laboratory and the distinguished lecturers before me. The previous lectures have all been of a rather theoretical nature; I have been asked instead to emphasize problems from a more applied point of view. On the one hand, this appears to be an easy course to follow, since many important areas of naval hydrodynamics lack the precise physical description required for detailed mathematical analysis. On the other hand, there is a real problem of selection, since so much of the present work in hydrodynamics has originated here at the Naval Ship Research and Development Center (NSRDC). With this caveat then, it will be understandable that I have chosen for discussion a subject of long standing interest in naval hydrodynamics, generally, and one of particular interest to this laboratory, namely, cavitation. Even this is too broad a topic for only a few lectures and I have restricted myself to two topics; these are, cavitation inception on smooth bodies and some effects of developed cavitation in internal flows. There are many instances of cavitation in internal flows. The testing of cavitating bodies in water tunnels is one, and that of cavitation in a ducted propulsion system is another. In both situations the flow is internally confined and is, therefore, geometrically complex. System interactions can then occur which, particularly for unsteady flows, leads to great difficulties of experimentation and interpretation.

I would like to acknowledge the help and stimulating discussions with many of the laboratory staff. These are too many to mention here, but I would like to reserve special thanks to Justin McCarthy, William Morgan, and Mrs. Shirley Childers for making my lectureship a memorable occasion. Finally, I would like to express my gratitude to my friend and former teacher, Milton Plesset, for his witty and insightful counsel.





## CAVITATION INCEPTION AND INTERNAL FLOWS WITH CAVITATION

### INTRODUCTION

Cavitation has been a topic of unique importance in naval hydrodynamics since the introduction of high speed propellers. The interesting historical survey by Johnson (1972)\* shows that the principal features of cavitation as a source of noise, vibration, damage, and reduced performance were experienced at the outset in ship propulsion in a pattern that has continued to be repeated in the most current applications. These undesirable features of cavitation were highlighted in Knapp's well-known Clayton Lecture before the Institute of Mechanical Engineers (Knapp 1952) and is echoed in the summary volume on cavitation (Knapp et al. 1970). The inception of cavitation announces the start of the phase change that may lead, in turn, to these unwanted effects and is therefore a boundary between fully wetted and cavitating modes of flow that is very desirable to know. But the onset of cavitation, when it does occur, does so in a variety of forms which may differ from facility to facility on similar bodies. Even on one test body, the various appearances of cavitation may change with flow speed and liquid environment.

Thus, this inception process does not appear to be a well-defined, unique kind of physical event for which there are clear-cut simple governing relations. Indeed, as in all fluid mechanics the presence of cavitation requires appeal to all three of the basic conservation laws (mass, momentum, energy). Cavitation inception appears to be one of those physical problems which does not yet seem well posed for the laboratory; experimental results on supposedly similar tests show wide variability and, even for one specific test condition, a wide "scatter" is often observed. This state of affairs was not helped much, in early years, by the absence of a detailed scientific description of the flow (with some exceptions) at the moment of cavitation inception. It was then not surprising that many of the theoretical attempts to explain the "scaling laws" fell short.

---

\*A bibliographic listing of references is given on page 93.

Cavitation inception as a separate topic of study has seemed then to be a somewhat "messy" subject. Yet, it is an important one in fluid engineering, and recently there has been some substantial progress by the combined efforts of workers in several countries including this Center, both in understanding the basic flows involved, and in laboratory techniques. In the remaining sections, we will review, briefly, some of these findings and recent experimental work. To appreciate the point of view of many of the workers in cavitation we need to survey the highlights of bubble mechanics, the most common denominator in cavitation-inception scaling theories. At the root of all phase change processes in cavitation is a "nucleating source"--or simply a cavitation nucleus--since technical fluids do not exhibit the large tensions required of pure liquids prior to cavitation. These nuclei, long the subject of speculation, are now becoming accessible to measurement, although there is still an observational gap connecting these sources of cavitation and the macroscopic cavitation ultimately seen on bodies. Some of these findings are reviewed in light of current laboratory practice. Finally, we discuss, in a preliminary way, some of the special problems posed by developed cavitation when this occurs in confined flows.

#### CAVITATION INCEPTION

##### Preliminaries

It is common to express the ambient pressure at which cavitation occurs in a coefficient form called the "cavitation number"

$$\sigma \equiv \frac{p_{\infty} - p_v(T_{\infty})}{q} \quad (1)$$

where  $q$  is the freestream dynamic pressure,  $1/2 \rho U_{\infty}^2$ ,  $p_{\infty}$  is the ambient static pressure and  $p_v(T_{\infty})$  is the vapor pressure of the pure liquid at ambient (i.e., freestream) temperature. At the same time the static pressure,  $p$ , on a body is put into dimensionless form

$$c_p \equiv \frac{p - p_\infty}{q} \quad (2)$$

so that the pressure is

$$p = p_v(T_\infty) + q(\sigma + c_p) \quad (3)$$

When the fluid pressure,  $p$ , is less than the vapor pressure,  $p_v$ , we expect vapor to form and, hence, we may expect cavitation to begin. Thus, as a first guess, we estimate that

$$\sigma \leq -c_{p_{\min}} \quad (4)$$

is the condition for the onset of cavitation. We follow Holl (1969) in calling the cavitation that occurs when  $p_{\min} < p_v(T_\infty)$  vaporous cavitation as we expect the cavitation process to be one of the formation and collapse of cavitation voids filled primarily with the vapor of the liquid. Observations show (Holl ibid) that it is also possible for  $p_{\min}$  to exceed the vapor pressure at inception. This can happen wherever the test liquid contains dissolved gas and the local pressure is below the gas saturation pressure or bubble point. Cavitation inception, when so dominated by diffusion of the gas into a cavity void, is termed gaseous cavitation by Holl. As he has shown, this may be quite common in hydrodynamic applications (see also the reviews by Acosta and Parkin 1975, Morgan and Peterson 1977). A further type of cavitation inception termed by Holl "pseudo cavitation," is said to occur when entrained bubbles of gas or vapor respond quasi-statically to an imposed pressure history. This feature of cavitation is more characteristic of bubbly two-phase flow than it is of cavitation inception and will not be considered further herein.

Scale Effect--Early Results  
Departures from the rule

$$\sigma_i = -c_{p_{\min}} \quad (5)$$

for the cavitation number at inception are called "scale effects." Indeed, almost from the very start of experimentation in cavitation, discrepancies from this rule were so prevalent that this became an important research topic, particularly for laboratory work where the discrepancies were more evident. The thrust of the earlier studies was, as it is now, to obtain a more detailed microscopic picture of the formation of cavitation in the hope that this would lead to a better physical model for describing the process.

Among the very most influential of these works were the beautiful motion pictures of growing and collapsing bubbles travelling on the surface of a body of revolution made by R.T. Knapp of Caltech in about 1946. These were sensational pictures at the time which, when coupled with the brilliantly successful analysis of Plesset (see Knapp and Hollander 1948, Plesset 1949), firmly established bubble mechanics as the essential scientific component of this type of cavitation. In fact, because of the time-delay required for the growth of a travelling bubble to visible size, it appeared reasonable to expect the scale effect to follow from this mechanism. A reproduction of one of Knapp's photographs of these travelling bubbles is shown in Figure 1. There, then, followed in the early 1950's a period of intense activity, both experimental and theoretical, devoted to settling the cause for the scale effect. To a latter day observer it appears that bubble mechanics, already of vital importance in underwater acoustics, became the paradigm through which experiments on cavitation inception were to be explained. As we will see, growing travelling bubbles are one form of cavitation characteristic of inception but they are not the only form, nor necessarily the dominant form. However, at this time in 1950 these differences were largely overlooked or unknown.

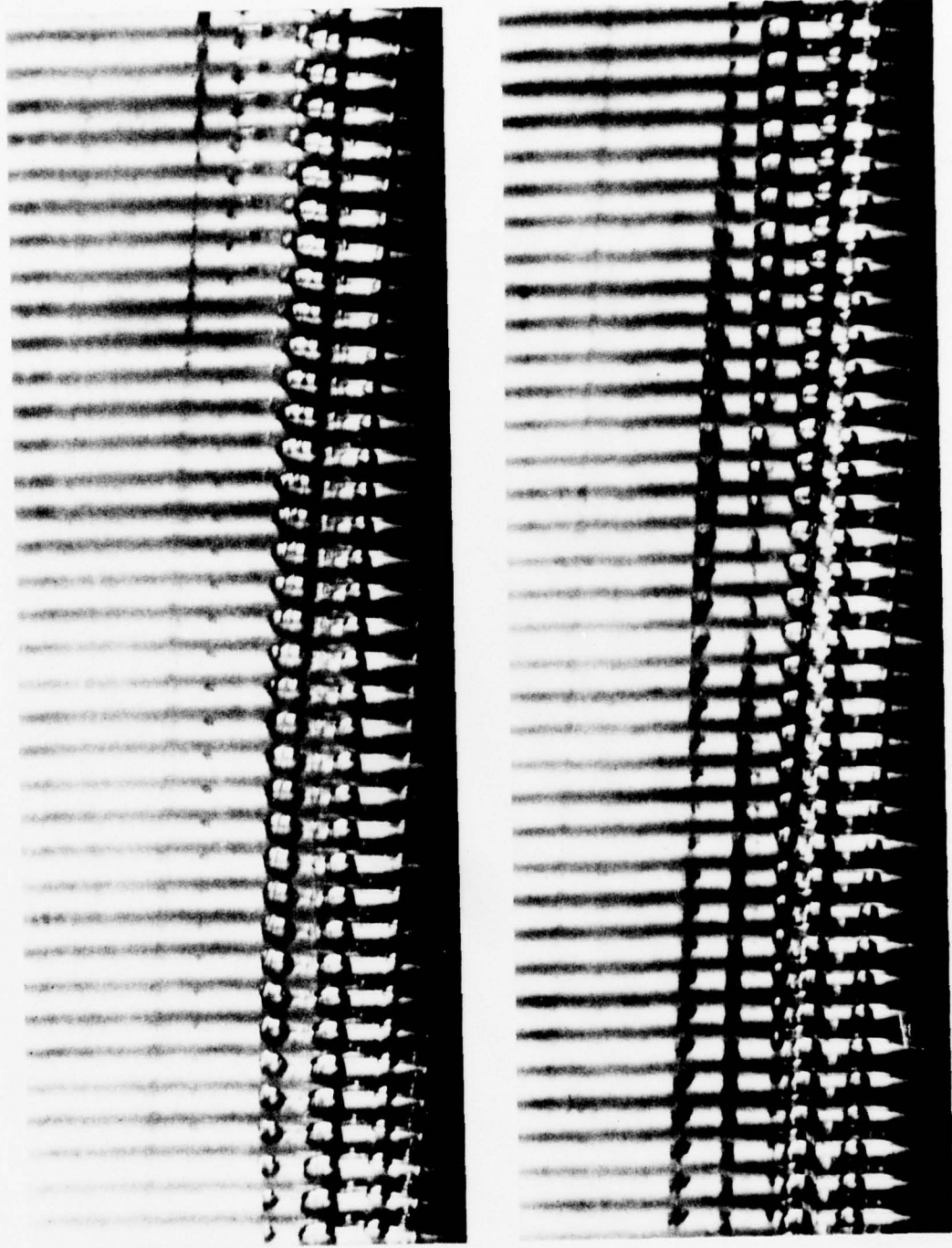


Figure 1 - Travelling Bubble Cavitation on a 1.5-Cal Ogive  
(Knapp and Hollander 1948)

A good account of cavitation in this period may be found in the book "Cavitation" (Knapp et al. 1970) through about 1969. This, together with the volume "Cavitation State of Knowledge," provides an excellent summary to that time. In the present context, some of the events of this period that seem significant are summarized in Table 1. This tabulation stops in 1969 deliberately to emphasize progress made since then.

TABLE 1 - SOME CHRONOLOGICAL EVENTS IN  
CAVITATION INCEPTION

1947	Knapp's movies of growth and collapse of travelling bubbles
1949	Plesset's analysis of bubble motion
1953	Parkin and Kermeen - Boundary Layer Inception
1955	Plesset and Zwick - Vapor Bubble Dynamics
1956	Daily and Johnson - Shear Flow Inception
1959	Ripkin and Killen - Nuclei Measurements
1962	van der Walle - "Stabilized" Bubble Cavitation
1966	Johnson and Hsieh - Bubble Screening
1966	Schiebe - Cavitation Occurrence Counting
1966	Lindgren and Johnsson - ITTC Comparative Tests
1969	Holl and Kornhauser - Thermodynamic Effects on Scaling Inception
1969	"Cavitation State of Knowledge"

One of the most influential events of this tabulation is the experimental work of Parkin and Kermeen (1953). They focus more sharply on the small bubbles seen within the boundary layer of smooth bodies as this appeared to be the crucial region of flow. Their impressive photographs showed that, on a hemispherically nosed body, the region of visible cavitation was preceded by a region of "microscopic cavitation bubbles which grow in the boundary layer." Figure 2, taken from their report, shows these small bubbles upstream of the more readily visible macroscopic cavitation. Also shown on the figure, is their interpretation of the flow

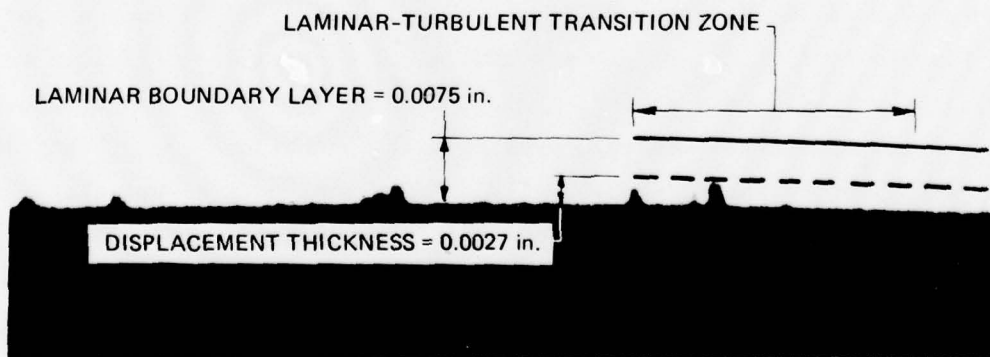
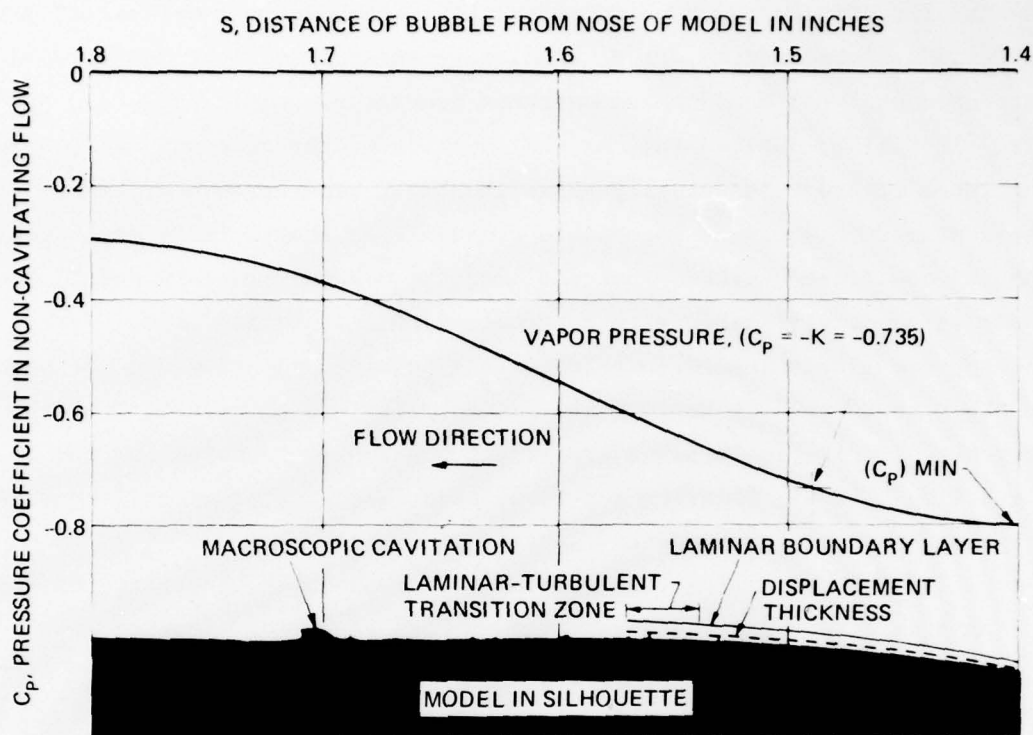


Figure 2 - Cavitation on a Two-Inch Diameter Hemisphere Body: Flow from Right to Left; Speed = 40 ft/sec (From Parkin and Kermeen 1953)

regime on the body, namely an attached boundary layer in which these small, essentially stationary, bubbles grow, they conclude, by a process of air diffusion. Subsequently, these bubbles, when of sufficient size, would be "stripped off" to "feed" the downstream macroscopic cavitation seen by the eye. It will be noticed that at the location of the observed small bubbles the local pressure is actually above the fluid vapor pressure, hence, vaporous growth would be impossible there. Presumably, truly microscopic bubbles could grow further upstream near the minimum pressure point, but these were not observable with the photographic technique used. Parkin and Kermeen also stressed that travelling-bubble cavitation did not occur in their tests readily because the new facility had a "resorber" which prevented comparatively large freestream bubbles (the nuclei for the travelling bubbles) from being recirculated, and thus, that this type of cavitation had a true boundary-layer origin.

This work had a vital, energizing effect on cavitation research and the physical ideas presented were used as the basis for a number of theories of the scaling effect (e.g., van der Walle 1962, Holl and Kornhauser 1969, among others). These theories incorporated the idea of a microbubble stabilized on the surface of a body so that growth by gas diffusion could occur until some critical size was achieved when downstream transport into the flow would take place. Further refinements in bubble dynamics accounting for thermodynamic effects (Plessset and Zwick 1955) and growth by oscillating pressure fields, i.e., "rectified diffusion" (Hsieh and Plessset 1961), did not provide additional mechanisms sufficient to explain the large scale effect. Before turning to some of these data we mention two additional concepts dealing with inception on smooth surfaces.

The first of these, due to Daily and Johnson, pointed out that the turbulent fluctuations in fully-developed pipe flow can also lead to cavitation. (This observation has been expanded subsequently by Arndt and others to deal with jet cavitation, but this is not the subject of the present work.) In the meantime, Ripken and Killen were able to demonstrate in certain types of cavitation the importance of the undissolved gas, i.e., the microbubble "nuclei" within the flow. In addition, they published size

distributions of these freestream nuclei, the first, to our knowledge, to be measured in a flow facility. It seemed quite plain then, that these nuclei were the ones responsible for the travelling bubbles photographed by Knapp. That being so, it would appear that if these freestream microbubbles were diminished in number and size, travelling-bubble cavitation would be similarly diminished. One mechanism, whereby the larger freestream bubbles could be selectively removed from the low pressure region surrounding a body, was proposed by Johnson and Hsieh; in their concept bubbles migrate across streamlines under the action of the pressure field around the body. Indeed, they show, by calculation, that the population of larger bubbles near the position of minimum pressure can be reduced, and that from this "screening" effect a size-dependent effect on travelling-bubble growth with a given freestream nuclei distribution is found. Thus, a scale effect is produced based upon the concept of travelling cavitation bubbles originating from freestream microbubbles. At about the same time, Schiebe (1966) proposed a scheme of inception measurement based upon the idea of measuring the rate of these travelling-bubble cavitation events, a concept which has subsequently received much attention and development at the St. Anthony Falls Hydraulic Laboratory and elsewhere.

This early development of cavitation-inception observation, development of basic theory and phenomenological tests, may be said to have culminated in the round robin tests on a standard body sponsored by the International Towing Tank Conference in 1966. But before dealing with these findings, we need to look in more detail at the inception scaling effects that had already been reported. Of these, certainly the work by Parkin and Holl (1953) has been most influential in providing a source of information used by co-workers in formulating theories. There is a pronounced Reynolds-number effect on these bodies, and a "size" effect (or unit Reynolds-number effect) showing that additional parameters are important (Figure 3). An even larger size effect was produced in an inception study on hydrofoils, Parkin (1952), as seen in Figure 4. These effects were so large that it is easy to understand the intense effort to explain them by many laboratories and investigators. Despite many attempts,

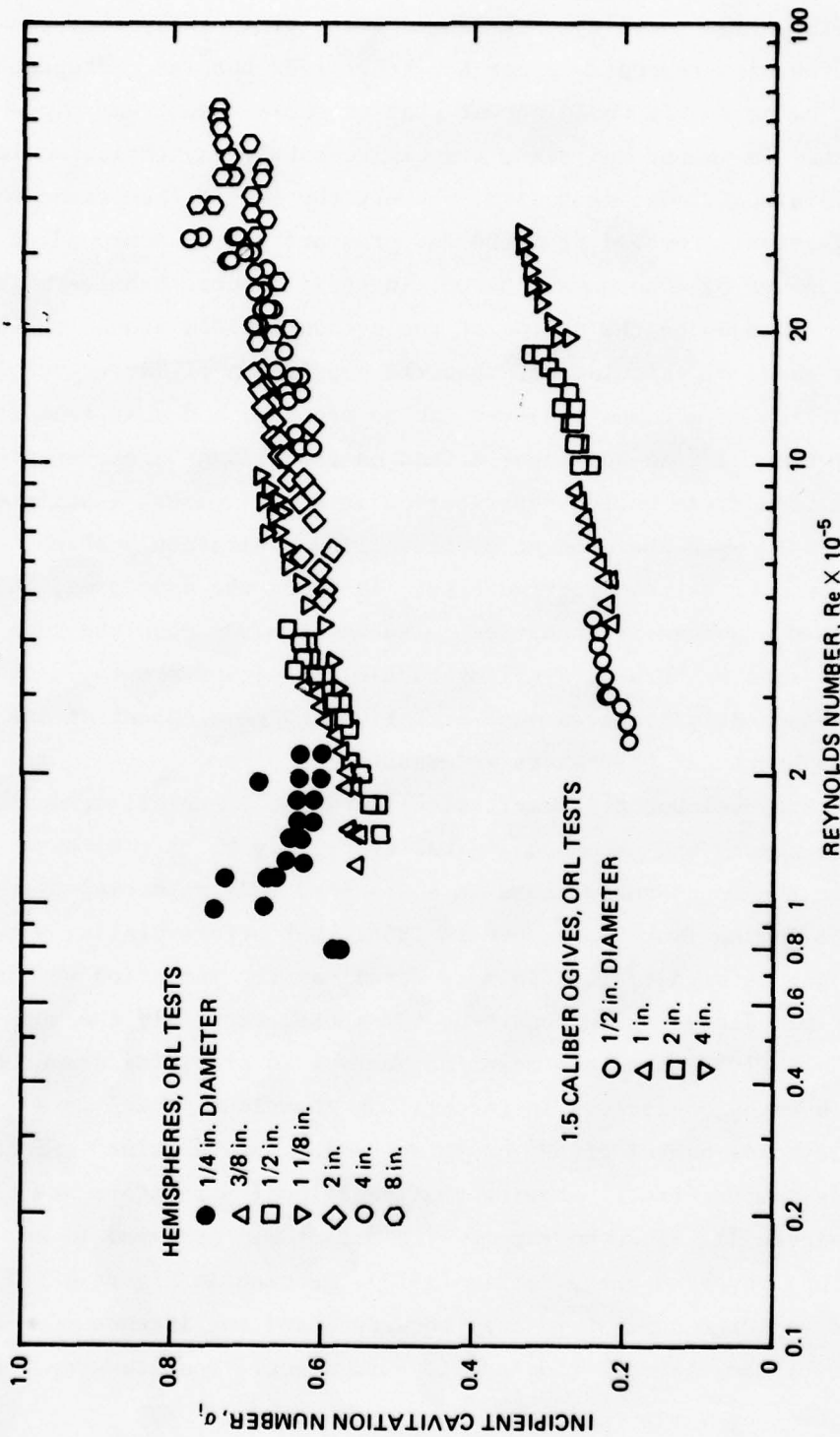


Figure 3 - Cavitation Index on Hemispherical and 1.5-Cal Ogive Bodies as a Function of Reynolds Number (From Parkin and Holl 1953: The point of disappearance of the cavitation is used as the index in this case and this is termed "desinent" cavitation by Holl.)

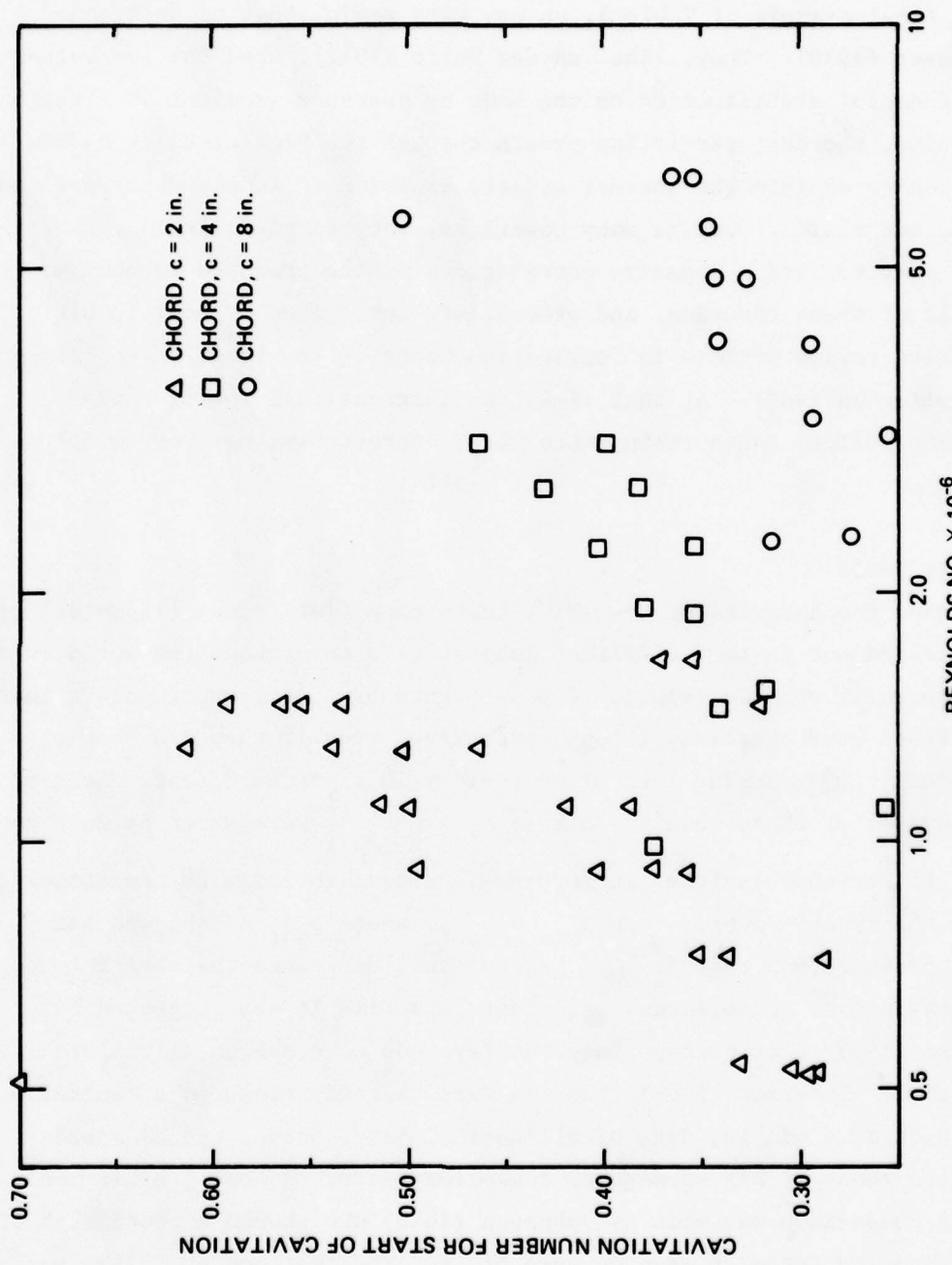


Figure 4 - Cavitation Index on a Series of Geometrically Similar Hydrofoils Showing a Size Effect  
(Parkin 1952)

no simple correlations with surface tension or "time of travel" have proved successful. And, as suggested, the subsequent theories based largely on Parkin and Kermeen's 1953 observations have had difficulties. As the final example of Table 1, we may cite again, that of Holl and Kornhauser (1970). They, like van der Walle (1962), used the conceptual idea of nuclei stabilization on the body by pressure gradient in a region of tension, thereby, permitting growth through the Plesset-Zwick bubble mechanics to explain the thermal effects experienced in hot water and some non-aqueous fluids. Unlike many coworkers, they carried out many experiments, only to find a negative correlation for the proposed mechanism.

All of these theories, and others, are summarized by Holl in his exhaustive review article in "Cavitation State of Knowledge," (Robertson and Wislicenus 1969). At that time, the International Towing Tank Conference (ITTC) round robin tests were, regrettably, not very widely known.

#### The ITTC Tests

Under the auspices of the ITTC, tests on a flat-faced ellipsoidal body were carried out in many different laboratories throughout the world, with the apparently chaotic results seen in Figure 5. There was no doubt that these tests were extremely thought-provoking, even if they did show a potentially embarrassing lack of uniformity in a standard test. Some of the oddities of these results, namely  $\sigma_i \gg -c_{p_{\min}}$  were shown by Holl to be due to attached cavities in more-or-less equilibrium with the dissolved air in the tunnel water. Then  $p_{\min} = p_{\dot{\text{sat}}}$ , where  $p_{\dot{\text{sat}}}$  is the gas saturation pressure, so that  $\sigma_i \approx p_{\dot{\text{sat}}} / q$  and as  $q$  decreases the cavitation index may become quite large. At about this time it was suggested by Johnsson (1969) that perhaps these differences were due to a laminar separation. Peterson (1969), had, in fact, already observed a laminar separation on a similar type of ellipsoidal body, but at tunnel speeds less than those of his subsequent inception tests. A most graphic and telling comparison was made by Johnsson (*ibid*) who showed a photograph of the cavitation actually seen on some of the ITTC test bodies. Then part

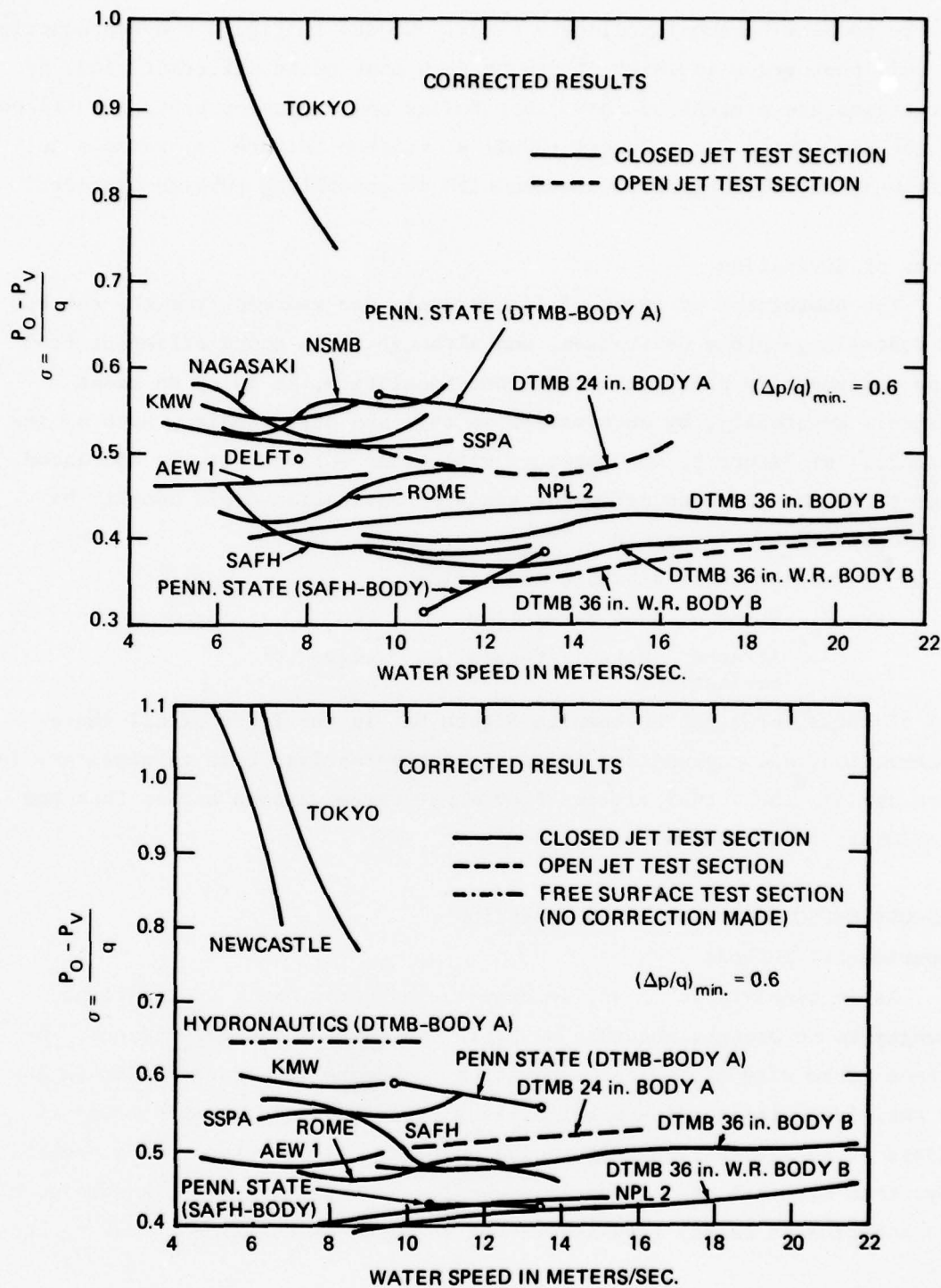


Figure 5 - Cavitation Inception Index versus Tunnel Speed for Two Dissolved Air Contents on a Flat-Faced Ellipsoidal Body for Various Test Facilities (Lindgren and Johnsson 1966, ITTC Tests)

of the problem became immediately clear. We see in Figure 6 a reproduction of this photograph in which it can be seen that quite different kinds of cavitation are present on those test bodies and a closeup photograph taken in the High Speed Water Tunnel (HSWT) at Caltech (Figure 7), reveals an attached, smooth form of cavitation with no travelling bubbles whatever!

#### Forms of Cavitation

The photograph of Figure 7 is certainly far removed from the concept of travelling-bubble cavitation, and although it is quite different from many contemporary photographs in other facilities, it is by no means unique. Eventually, by observation on this and other bodies, such as the hydrofoil of Figure 8, we, together with other workers, became convinced that three more-or-less different kinds of cavitation could usually be distinguished. These are:\*

1. Travelling-bubble cavitation.
2. Sheet or band cavitation.
3. Attached spots, "fingers" or "wedges" of cavitation.

All of these forms can be seen in Figure 6. In the light of all these observations and suggestions it seemed an appropriate time to consider, in more detail, the actual viscous flow about these various bodies that had previously been studied.

#### VISCOUS EFFECTS ON CAVITATION INCEPTION

##### Experimental Methods

As in aerodynamic flows, we expect, in hydrodynamic applications, changes to be brought about by viscosity in surface boundary layers. We expect to be wary of laminar separation in adverse pressure gradients and to anticipate laminar-to-turbulent-flow transition of attached boundary layers at sufficiently high Reynolds numbers. Also we know, in a general way, that although transition is a complex process, a precise knowledge of its location is rarely required except for drag calculations. But to know,

---

\*Vortex cavitation also occurs on lifting surfaces but is not included in the present discussion.



1. ROME



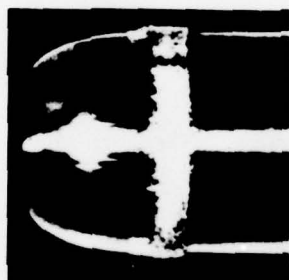
2. AEW



3. DELFT



4. NPL



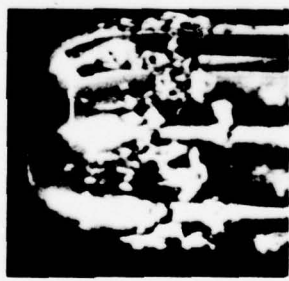
5. CAL. TECH.



6. CAL. TECH.



7. SSPA



8. SSPA



9. SSPA

Figure 6 - Incipient Cavitation on the ITTC Headform in Various Facilities (Johnsson 1969)

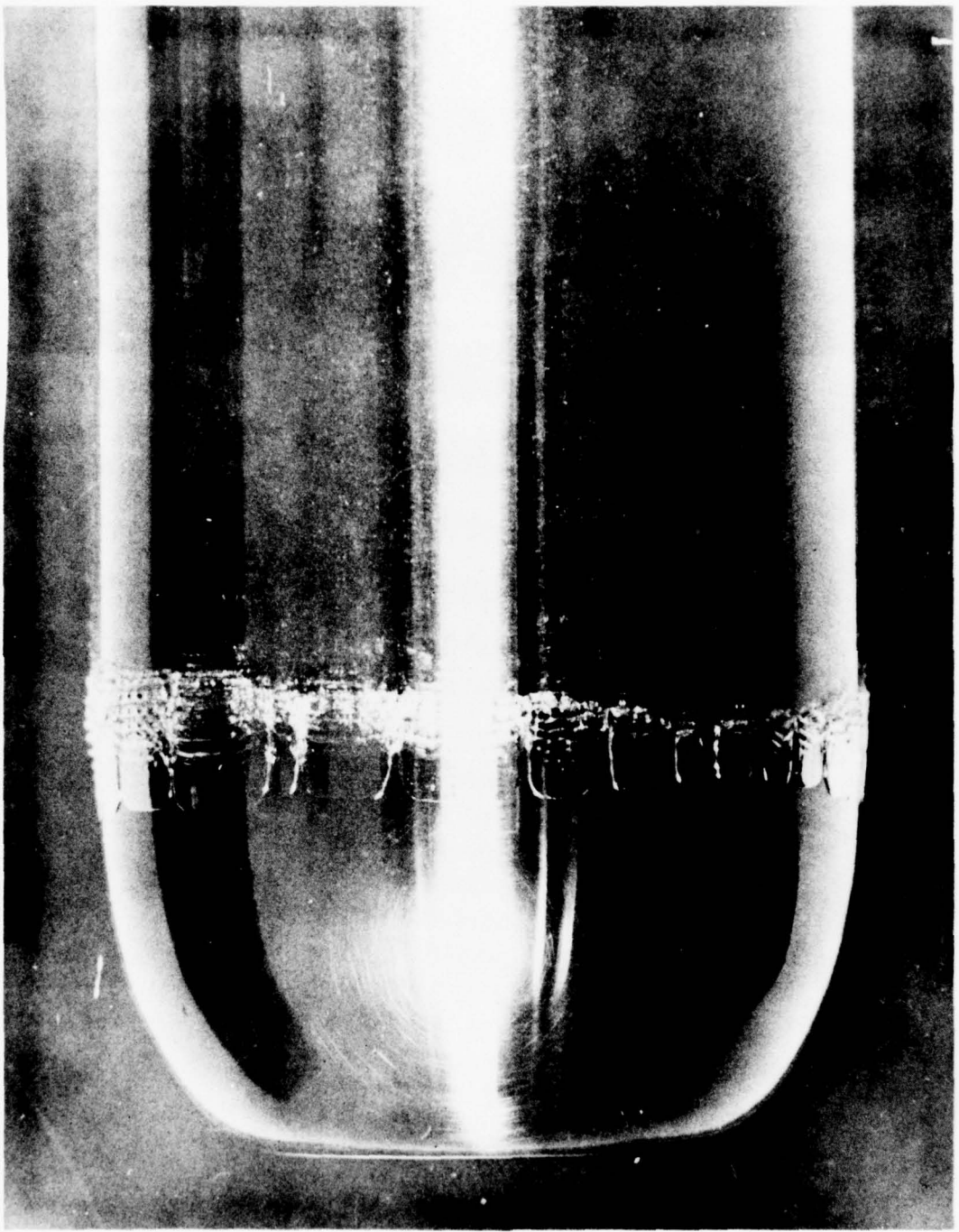
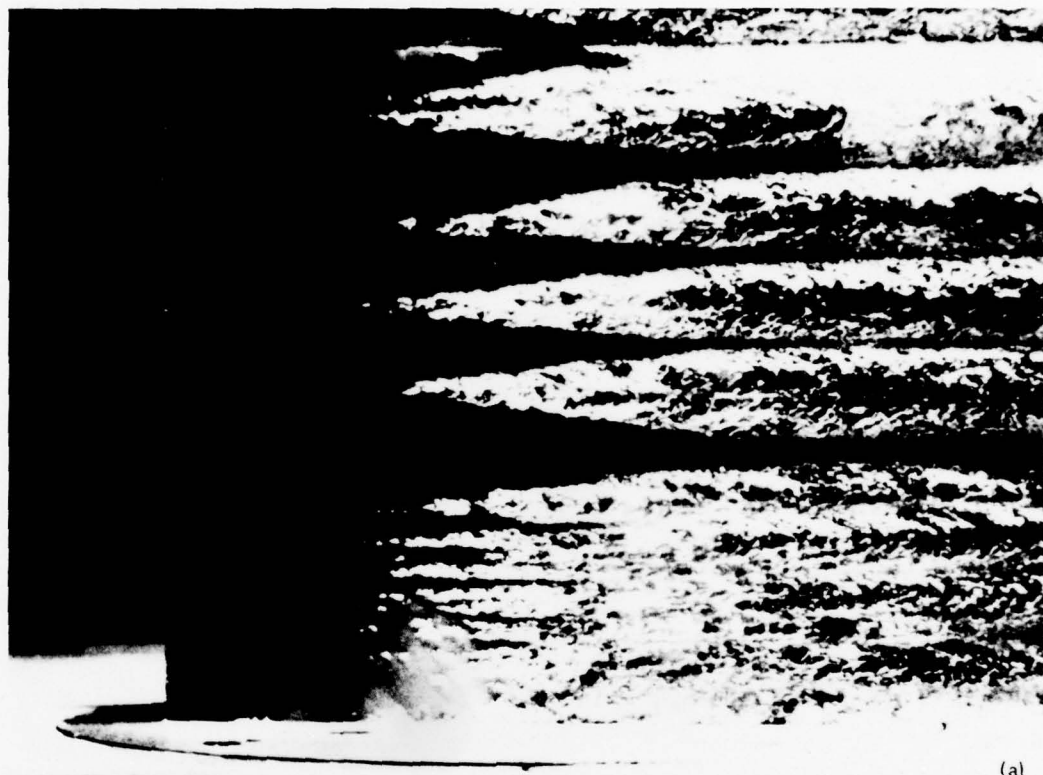


Figure 7 - Cavitation Inception on the ITTC Body--Caltech HSWT



(a)

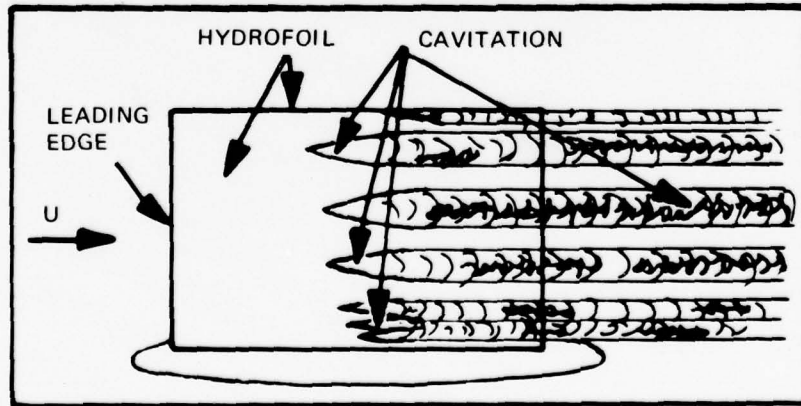


Figure 8 - A Form of Cavitation Inception on a Hydrofoil (Arakeri 1971)

in more detail, which of these features (as well as others not mentioned) is actually present in particular hydrodynamic experiments requires some means of boundary-layer flow visualization. Surface films of various types have traditionally been used in aerodynamic applications for this purpose and in hydrodynamic work oil films have been found useful for detection of laminar separation and transition (see, e.g., the review Acosta and Parkin 1975). But a much more sensitive method for water is schlieren photography. It is, of course, necessary in this method to provide a density contrast; this can be achieved by injection of another liquid or, more simply, by heating or cooling the surface layers. One sees then, in the usual schlieren setup the thermal boundary layer which is for water at room temperature about one-half the mechanical boundary layer thickness.

We were concerned at first about the effects of this heating or cooling on the boundary layers themselves. Fortunately, this problem had already been exhaustively treated by Wazzan et al. (1968), (see also Wazzan and Gazley 1977) to show that under the expected laboratory conditions the effect was negligible near a laminar separation but that some delay in a turbulent transition might be expected. (We shall return to this point later.) A schematic arrangement is shown in Figure 9; this is basically the same as that of Arakeri et al. (1973) but with an improved spark source. A photograph of the experimental arrangement in the Caltech Low Turbulence Water Tunnel (LTWT) may be seen in Figure 10.

#### Laminar Separation

The schlieren technique was surprisingly easy to apply. For example, Figure 11 shows a photograph of the flow past a 2-in. diameter hemisphere body at a flow speed of about 22 ft/sec, well within the range of experimental Reynolds numbers of the data of Figure 3. The clear laminar separation on this body is easily seen, together with the turbulent reattachment of the free shear layer further downstream. The results really exceeded our expectations for it could be quickly confirmed that a laminar separation was present on the hemispherical body up to the top speed of about 60 ft/sec in the HSWT at Caltech (a body Reynolds number of about

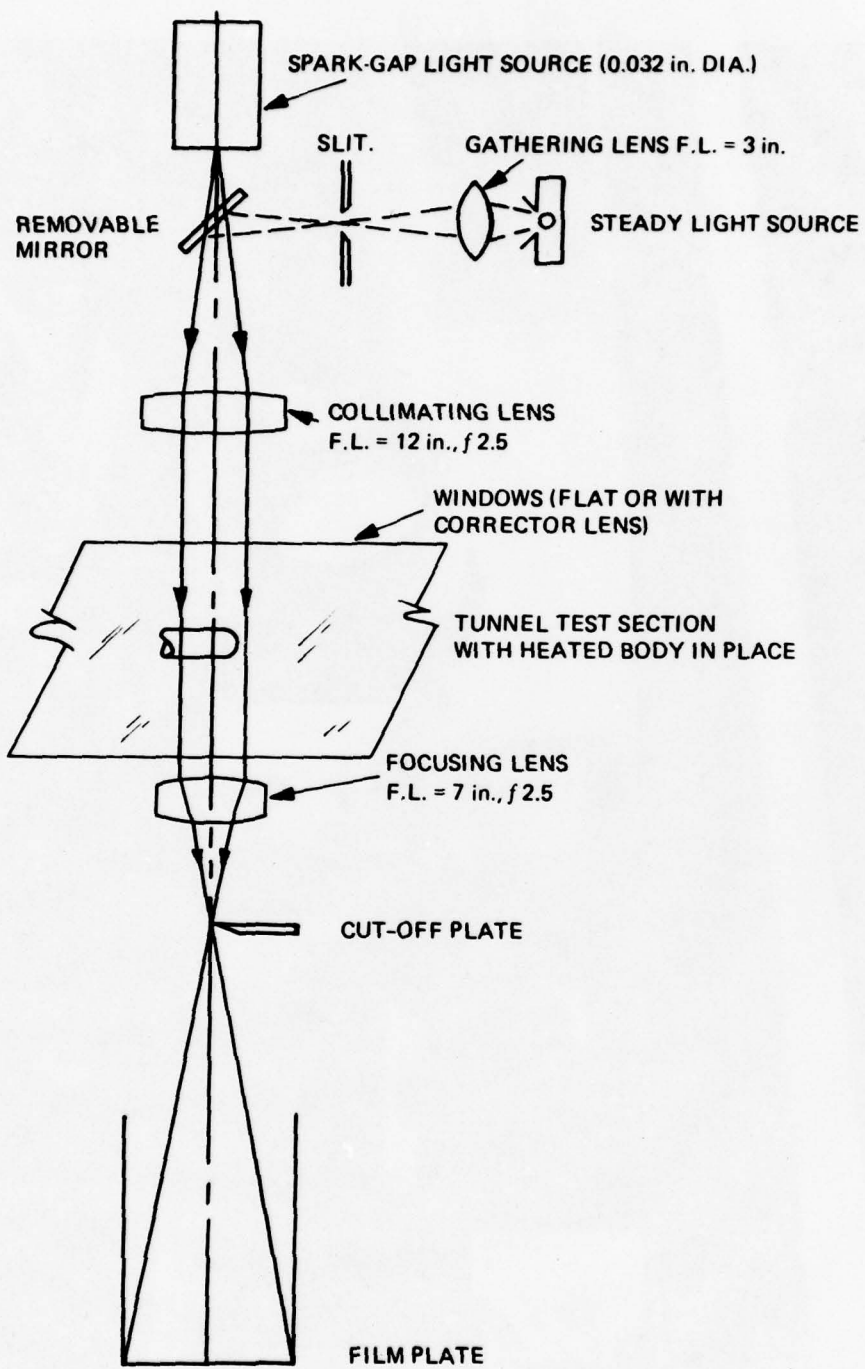


Figure 9 - Schlieren Flow Visualization System  
(Lindgren and Johnsson 1966)

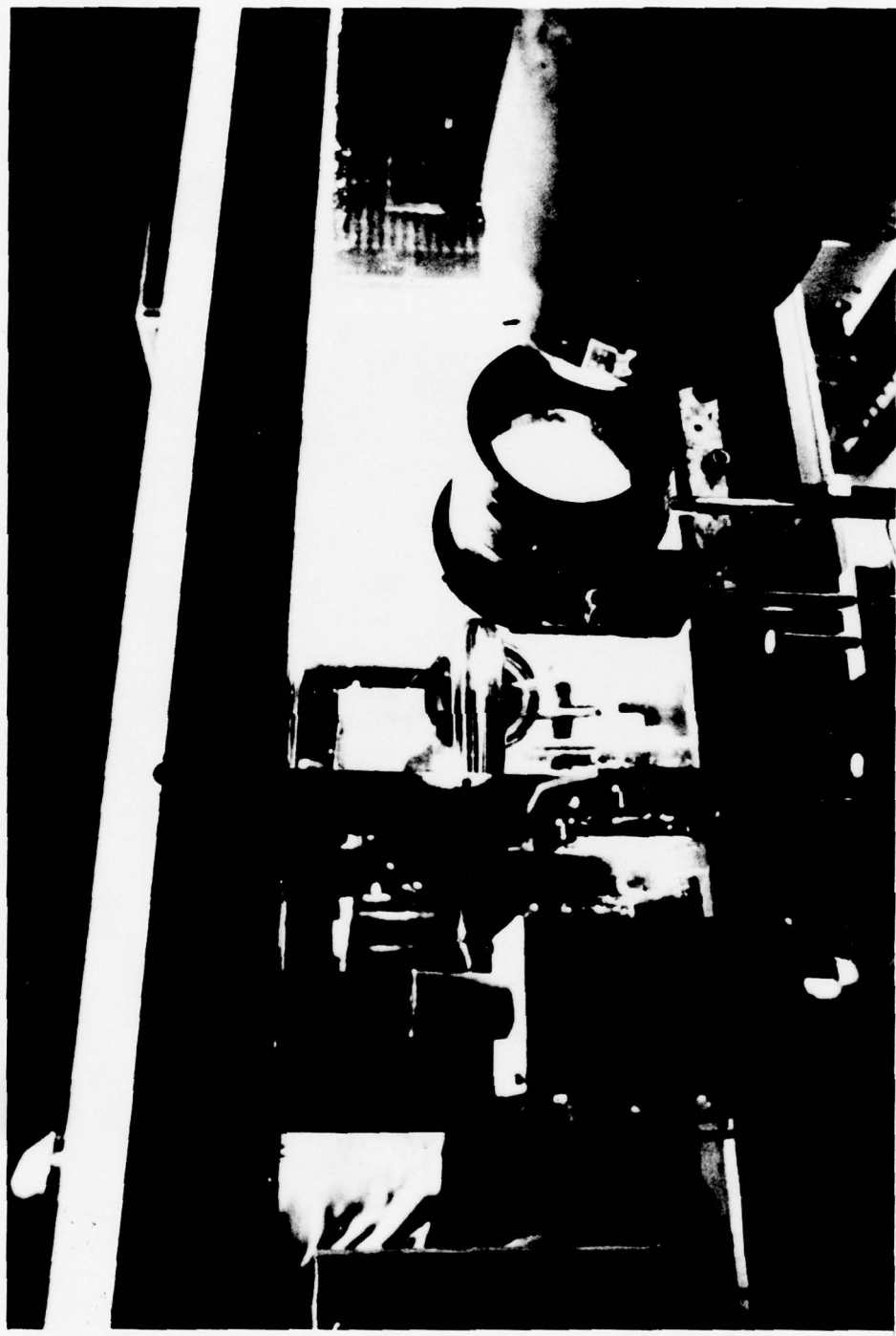


Figure 10 - The Spark Source, Steady Source, and Collecting Lens Setup in the Caltech LTWT  
(Lindgren and Johnsson 1966)

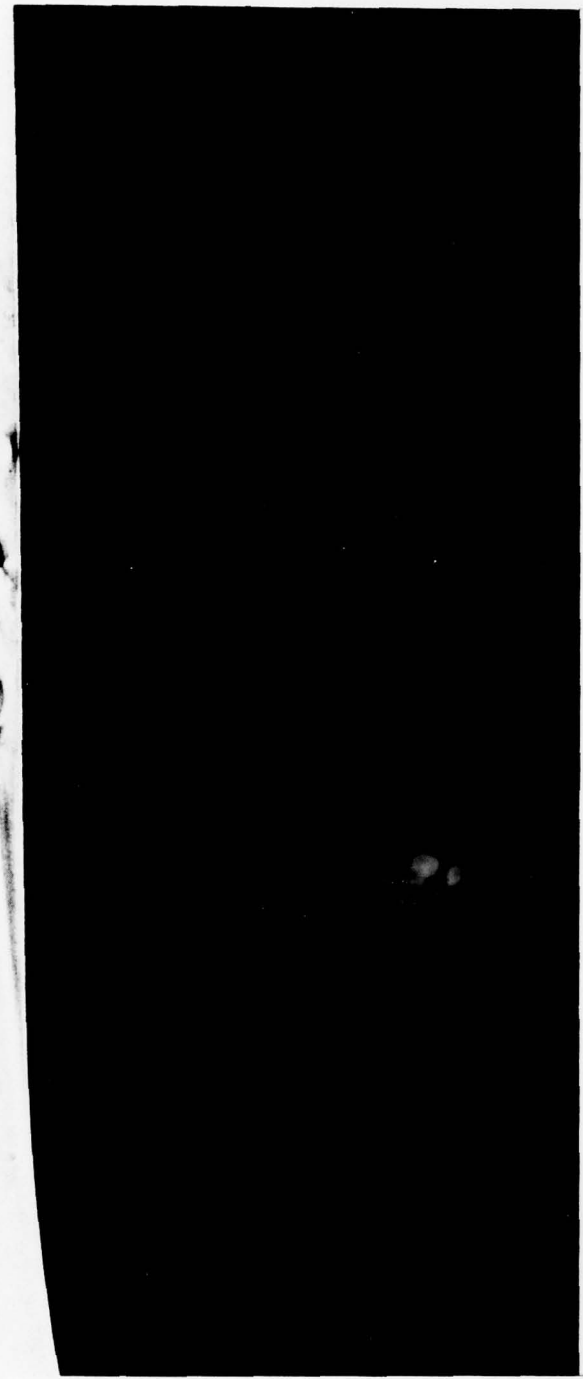


Figure 11 - A Two-Inch Diameter Hemisphere Showing Laminar Separation and Turbulent Reattachment  
at a Body Reynolds Number of  $2.6 \times 10^5$  (The height of the separation region is about  
0.01 inches, Gates et al. 1978)

$10^6$ ) and that laminar separations were present on the ITTC test body and the modified ellipsoidal head form previously tested by Peterson at the David W. Taylor Naval Ship Research and Development Center (see Arakeri and Acosta 1973, 1976).

At first, it was surprising to realize that laminar separation could exist on these well-known test bodies to comparatively high Reynolds numbers because of contrary assumptions found in some of the cavitation literature. Yet, even the simplest approximate laminar boundary-layer calculations\* showed that, on these bodies, a separation was to be expected. It then seemed evident that the presence or absence of this laminar separation would be extremely important in cavitation inception.

#### Inception Observations within the Laminar Separation

With the schlieren system in operation, it became possible to carry out simultaneous observations of inception and the thermal boundary layer. The hemisphere body proved to be a good candidate for this purpose. The development of cavitation on this body may be seen in Figure 12. Cavitation is seen to commence within the reattachment region of the laminar separation. Many small bubbles are seen within the recirculation region of the separation; these are presumably the same small bubbles seen in Parkin and Kermeen's photographs. Motion pictures were also taken of the flow in this region, at the same magnification of the schlieren photographs. From these, it was inescapable that these small bubbles were in the recirculation region of the separation, but it was not possible to establish a direct relation between these very small bubbles and the larger macroscopic cavitation patches seen further downstream.

With continued reduction in pressure, the macroscopic region of cavitation grows to eventually result in the smooth, clear viscous-cavitation separation seen in the last of Figure 12. This is a new type of separation phenomenon, somewhat related to separation in lubrication. (Arakeri (1975a) was able to make semi-empirical correlations for the location of this separation.) A similar sequence of events was found for cavitation

---

\*For example the axisymmetric version of Thwaites method, see "Laminar Boundary Layers," Oxford, Rosenhead (ed.) pp. 430-432.

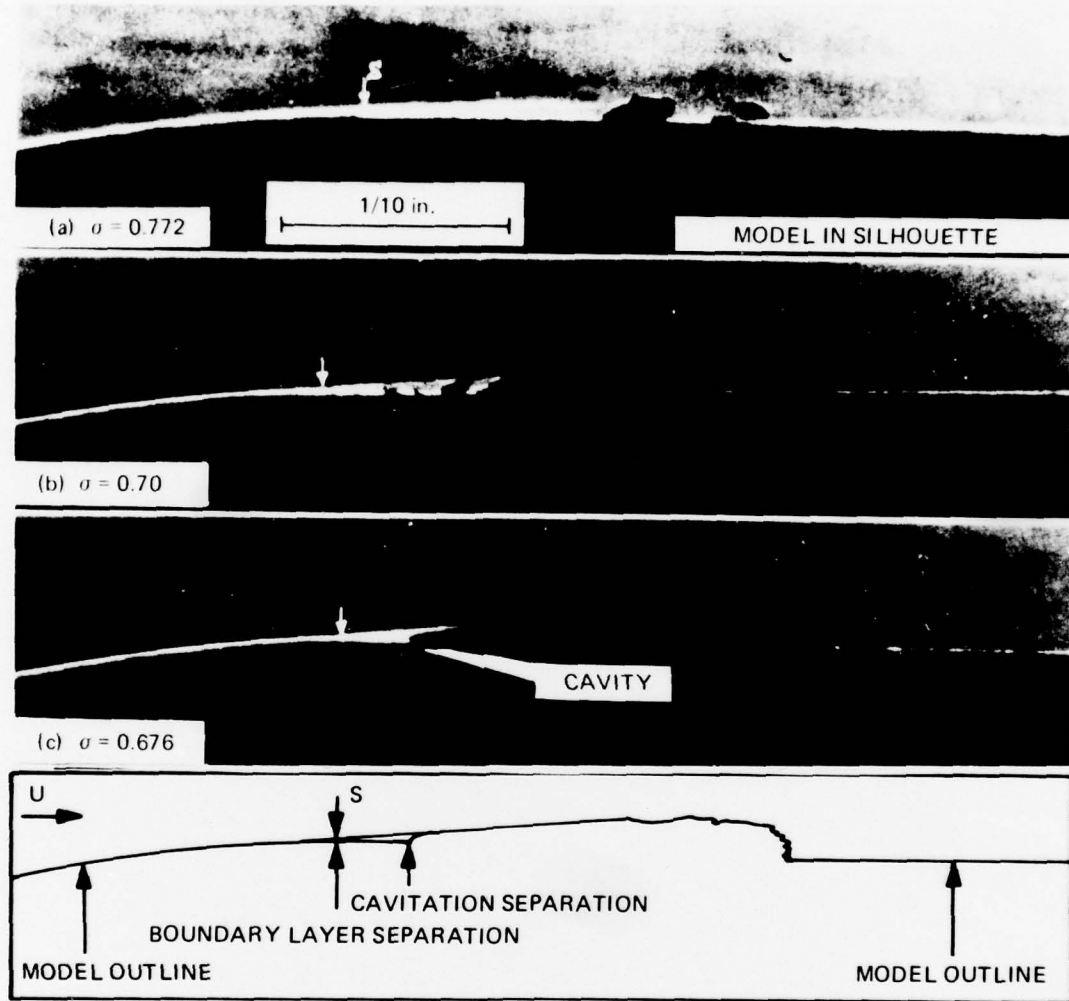


Figure 12 - The Form and Extent of Cavitation Originating Within the Viscous Separated Region of the Hemispherical Nose at Three Levels of Tunnel Pressure (The freestream speed is 40 ft/sec and the body Reynolds number is  $6 \times 10^5$ . The dark patches above the model outline are the cavitating areas. Arakeri and Acosta 1973)

development on the ITTC body. This body, however, has a much smaller laminar-separation region and in the Caltech HSWT the progress from initial inception to the macroscopic cavitation seen in Figure 7 is practically instantaneous. But, again, careful study shows that the terminus of the laminar region is the location of the most intense cavitation, and it is this location where cavitation is seen to disappear as pressure is raised.

We can see that a laminar-separation region has an important role in cavitation inception. At the very least, the static pressure there provides the reference pressure at which inception occurs. It would then seem most plausible that

$$\sigma_i \approx -c_{p_s} \quad (6)$$

or

$$\sigma_i \approx -c_{p_{reattach}} \quad (7)$$

i.e., we identify the inception index with the pressure coefficient at separation or reattachment, the latter being Reynolds number dependent. In fact, this suggestion had previously been made by Bailey (1970) based on hydrofoil tests. Here we exhibit tests on the two bodies, hemisphere and ITTC, made in the Caltech HSWT in Figures 13 and 14, respectively, in which it may be seen that the rule is better than

$$\sigma_i \approx -c_{p_{min}} \quad (8)$$

and that the inception index approaches  $-c_{p_s}$  as speed increases. But, there are differences in the two sets of results: namely,

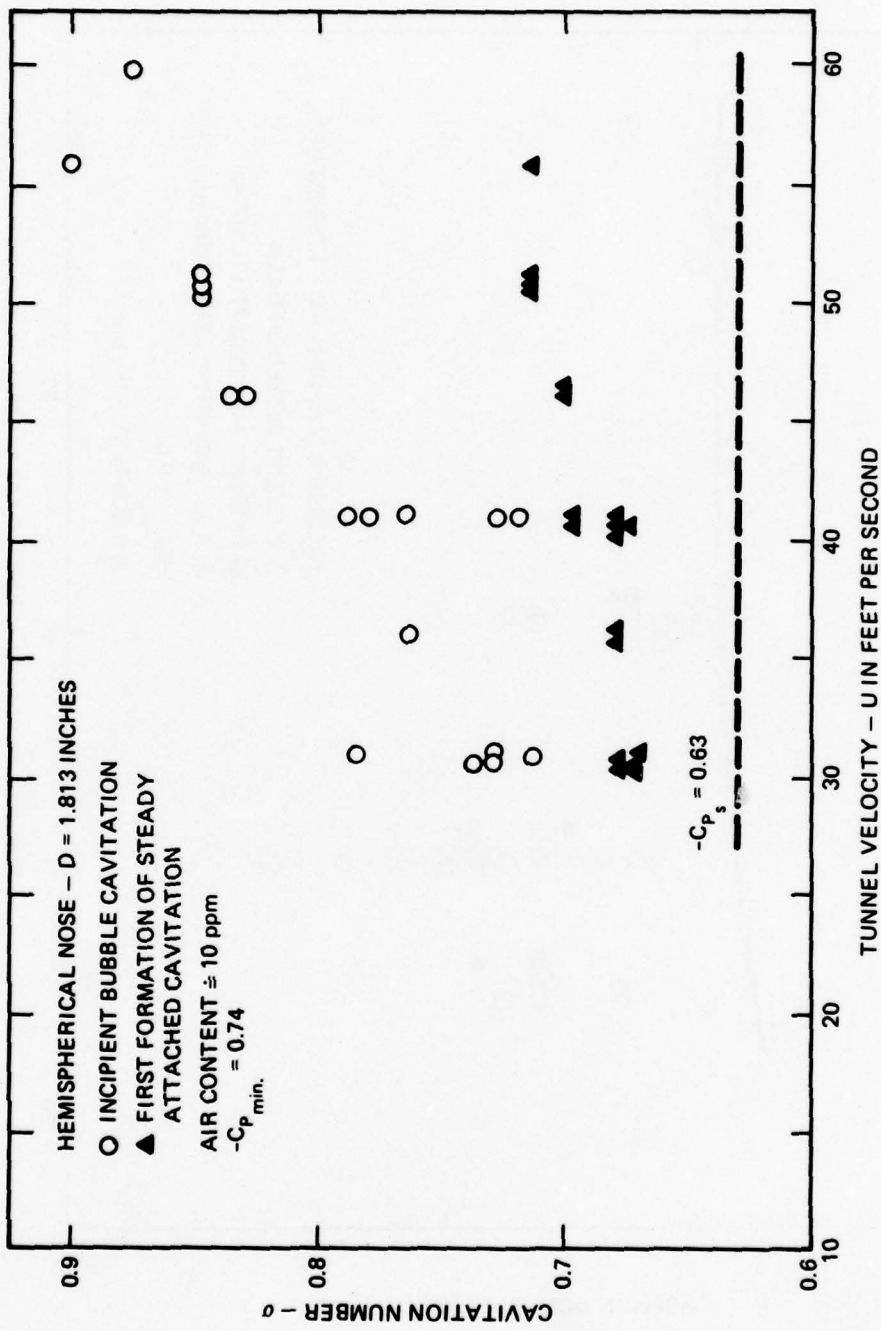


Figure 13 - Inception Observations on a Hemisphere-Nose Body in the Caltech HSWT  
(Arakeri et al. 1973)

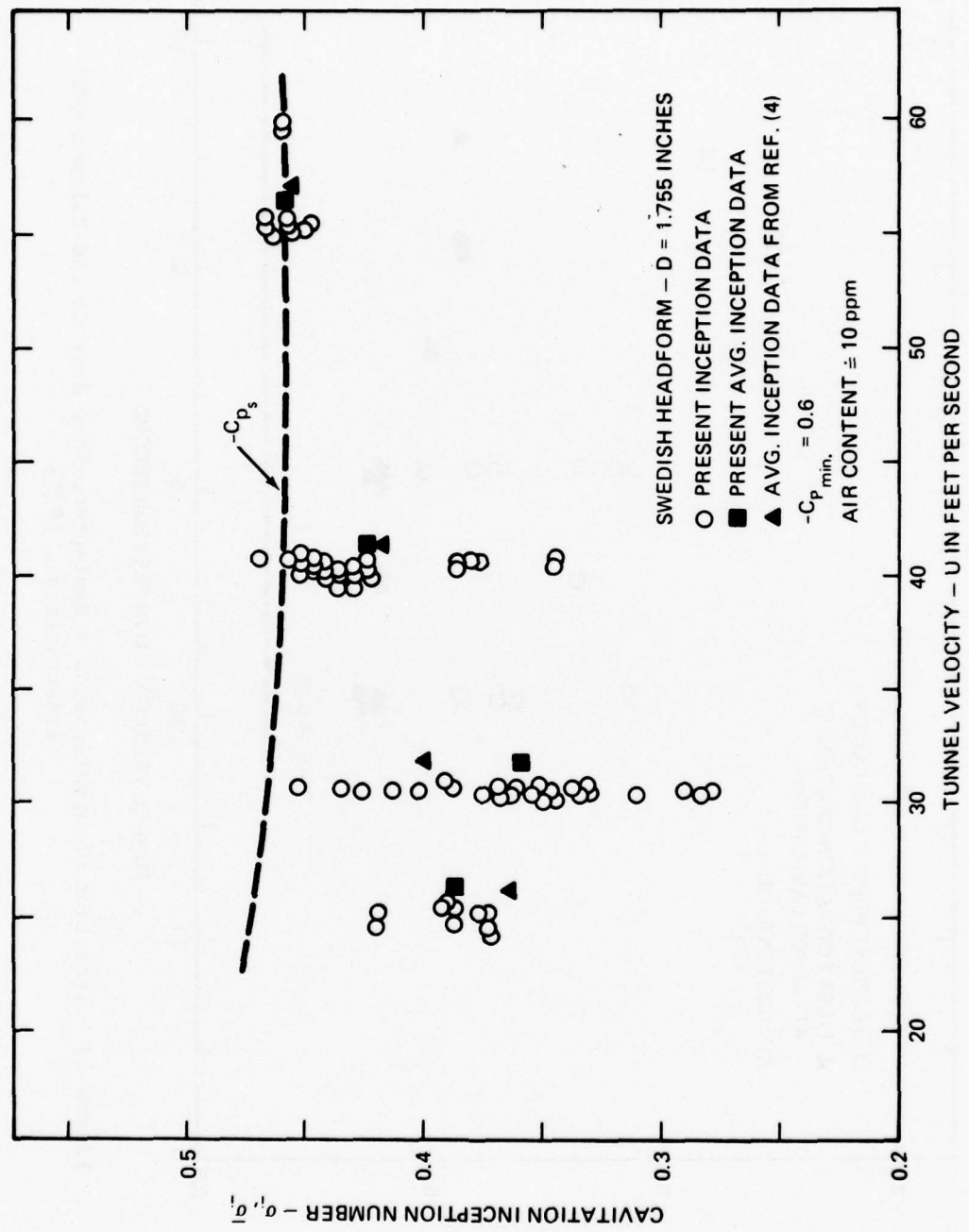


Figure 14 - Inception Observations on the ITTC (Swedish) Headform in the Caltech HSWT  
 (Arakeri et al. 1973)

$$\sigma_i \geq -c_{p_s} \text{ hemisphere body} \quad (9)$$

and

$$\sigma_i \leq -c_{p_s} \text{ ITTC body} \quad (10)$$

Although there is some improvement when the reattachment pressure coefficient is used,\* the two bodies are seen to behave quite differently. And the original observations of Parkin and Kermeen (namely that the local pressure exceeds vapor pressure yet the cavitation still occurs) on the hemisphere body are confirmed once again.

Before moving on to questions raised by these data, it is appropriate to point out that in this section we have been dealing with attached forms of cavitation which are seen to occur within a boundary layer separation. It seems clear that the sheets, or band forms of cavitation, are due to this separation. In the Caltech experiments so far reported, this type of cavitation occurs without travelling bubble cavitation. But we see, for example on the ITTC body in Figure 6, that other forms of cavitation also occur and it should not be supposed that the approximate correlation,  $\sigma_i \approx -c_{p_s}$ , is valid for them. Indeed, the great variability of the ITTC inception results of Figure 5 makes it plain that each of these forms of cavitation inception will have its own governing dynamics. Of course, one is left with the problem of determining, in a particular flow situation, the particular form of cavitation, so that the appropriate physical model may be used to determine the scaling procedure.

#### Conditions within the Separation

There is still the problem of explaining cavitation on the hemisphere body when the local pressure (in the separation region) exceeds vapor pressure. (We exclude gaseous cavitation here by the slowness of the diffusion process.) The implication is clear that there must be local,

---

\*See Arakeri (1973) for these measurements.

transient pressure fluctuations sufficiently strong to create liquid tensions sufficient for microbubble growth. From the data of Figure 13, for example, a fluctuation magnitude of about ten percent of the dynamic pressure would be required to establish cavitation on the hemisphere body. These fluctuations would be expected to occur at the reattachment of the separation region, as can readily be appreciated from Figure 15. Rather surprisingly, the literature is very scarce on this feature of real fluid flows. It was possible, however, to install a single point pressure transducer on the hemisphere body of Figure 15 (Arakeri 1975b). The results were most interesting and show that rms and peak fluctuations are certainly large enough in themselves to cause liquid tensions in the regions of observed inception. Later, these findings were confirmed, with even more dramatic and precise results on a larger body, by Huang and Hannan (1975). Some of their findings are shown in Figure 16, to demonstrate that the fluctuating pressure environment is sufficiently strong to make it very likely for cavitation to occur on these bodies at local pressures slightly exceeding the liquid vapor pressure.

From these findings then, it is tempting to account for these transient fluctuations by putting the inception index in the form

$$\sigma_i = -c_{p_{loc}} + c_{p_t} \quad (11)$$

where  $c_{p_{loc}}$  is a local pressure coefficient where inception is observed, and  $c_{p_t}$  is the fluctuating pressure-coefficient amplitude there. This type of representation indeed makes the hemisphere data much more plausible because the  $c_{p_{loc}}$ , measured near the end of the laminar separation bubble, (and perhaps the fluctuating component too) is strongly Reynolds number sensitive (Huang and Hannan ibid). This prescription ignores the physical state of the fluid, however, so that some caution should be exercised in seeking correlations based solely on Equation (11), and does not explain the contrary finding of Figure 14, namely that  $\sigma_i < -c_{p_s}$  or  $-c_{p_{reattach}}$ .

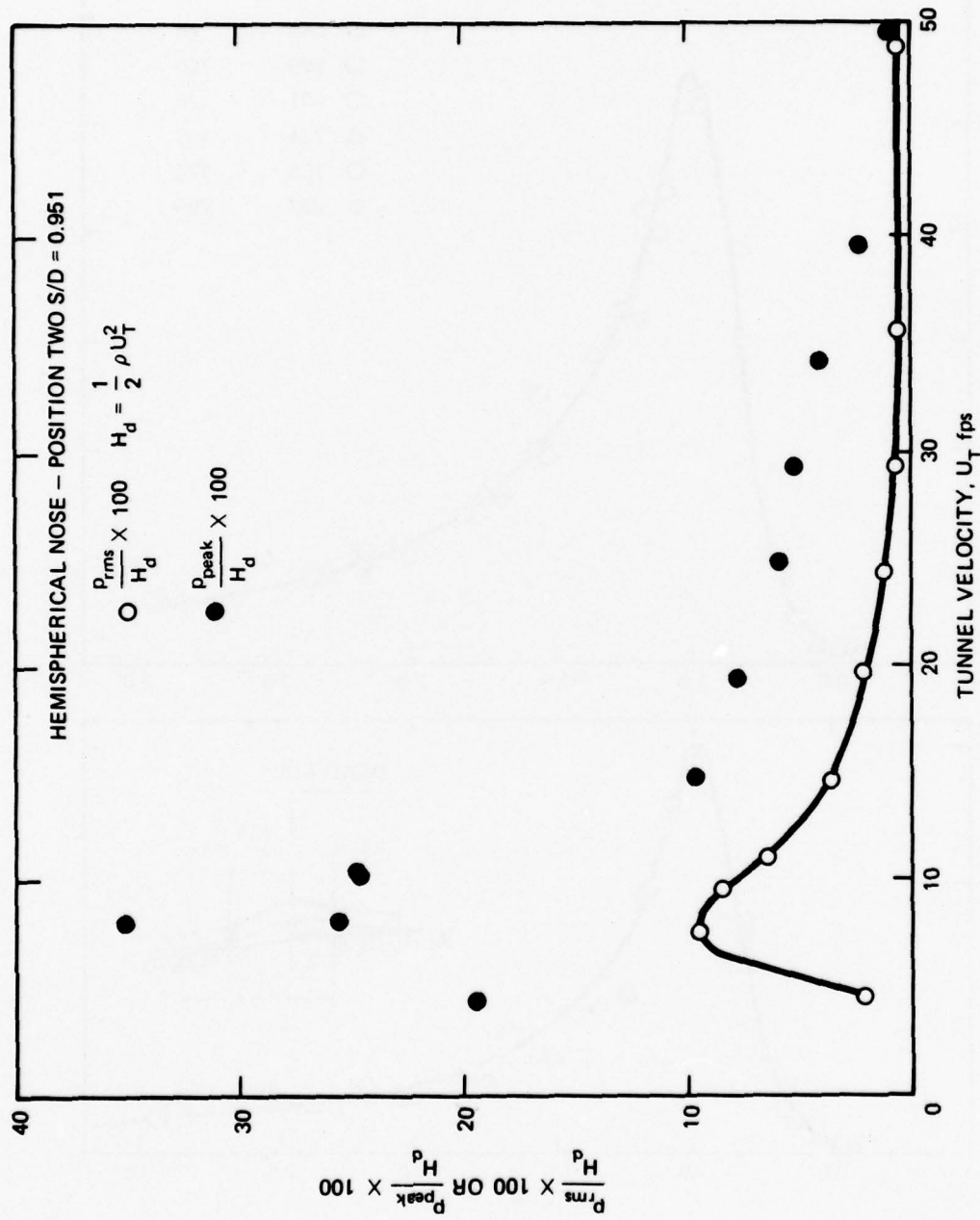


Figure 15 - Peak and RMS Pressure Fluctuations on a Two-Inch Hemispherical Body  
 (The transducer is located at an arc-diameter ratio of 0.95. The active diameter of the transducer was several times the disturbance wave length. Arakeri 1975b)

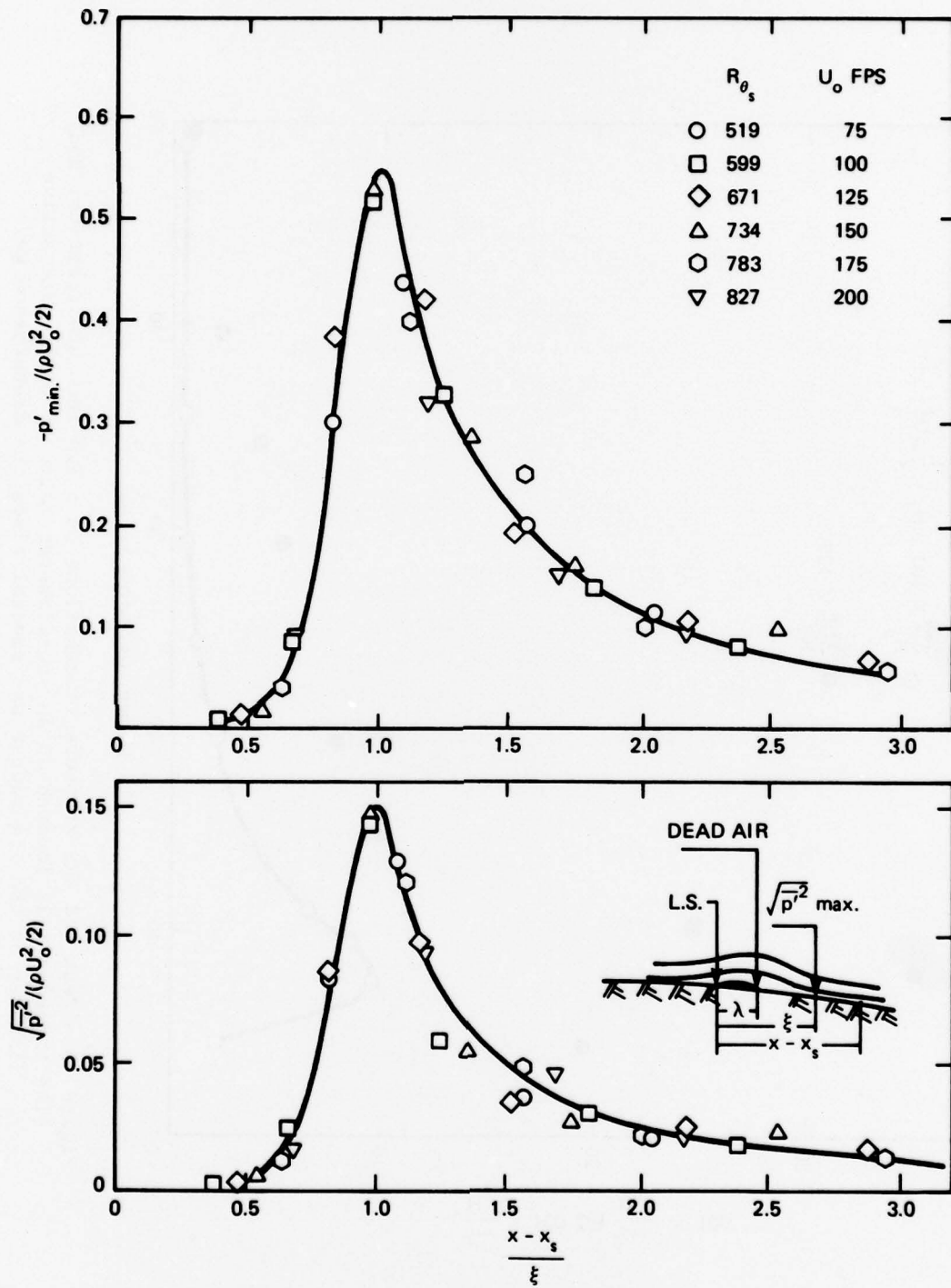


Figure 16 - Pressure Fluctuations (Negative Peak Upper and RMS Lower) on a Body of Revolution Downstream of a Laminar Separation Reattachment (Huang and Hannan 1975)

Nevertheless, there is considerable appeal of the idea that a more realistic appraisal of the actual features of the real viscous flow around bodies of interest may help considerably in improving our knowledge of cavitation inception and the development of better scaling laws. This, in turn, leads us to reflect on just what the locations of inception might be (and hence the value of  $c_{p_{loc}}$  there) and the strength of any unsteady fluctuations there--without, for the moment, worrying about how the cavitation might originate. With this in mind, we summarize some of these real fluid features that might influence inception on smooth bodies:

1. The laminar-separation reattachment region.
2. A "natural" transition.
3. Stimulated or "tripped" boundary layers.
4. Freestream effects, e.g., turbulence, particulates, polymer solutions.

We cannot deal extensively with these well-known fluid mechanics problems; much of the presently-known structure of laminar-separation bubbles may be found in Gaster (1966) and the principal new features here are the astoundingly large pressure fluctuations as already mentioned. There has been recent progress in determining the length of these separations, and of the turbulent transition process seen on the free shear layer of these flows (Van Ingen 1975). But it is a well-known fact that the steady, laminar flow on smooth bodies gives way to a turbulent flow at a sufficiently large Reynolds number and that, if this transition is completed upstream of a laminar separation, this separation will disappear. Flow transition may be stimulated by many methods if the Reynolds number is not high enough for a "natural" one--as it, indeed, has been done historically in naval hydrodynamics. And, if by this process, a prior laminar separation is foisted, one would expect major consequences for the cavitation inception process there. Other traditional, and some nontraditional, issues naturally arise when transition in laboratory facilities occurs. Of these, surely that of freestream turbulence has been one of the most recurring ones. In hydrodynamic applications, solute molecules and particulate suspensions may have profound effects on both laminar and turbulent

flow structure.\* Of these, the long chain 'polyox' polymer has received much attention in the hydrodynamic community for its astounding effect on turbulent drag and heat transfer reduction. It would be surprising, in a way, if there were not an equivalent effect for cavitation. We now take up some of the features briefly, but with primary reference to cavitation.

#### Transition and Cavitation

Here we need to have some idea of the location of "natural" transition of attached boundary layers to determine the "local" pressure needed for a cavitation-inception measurement. This is a basic "reference" problem in fluid mechanics that does not appear yet to be in a satisfactory state (Mack 1978). At best, there appear to be semi-empirical methods based upon the use of linear stability theory. In its present form, the concept, as explained in the comprehensive report by Wazzan, Okamura, and Smith (1968), is to calculate the factor by which certain disturbances in the laminar boundary layer may be amplified. As an empirical observation, transition may be said to occur when this factor reaches a certain level. The difficulties and objections to this approach are reviewed at length by Reshotko (1976) and later by Mack (*ibid*) and Van Ingen (*ibid*). These center on the fact that the ambient unsteady disturbances in the flow are largely unknown, and that the "receptiveness" of the boundary layer to these disturbances is not known either, a concept due to Morkovin (see Reshotko 1976). It does not necessarily follow that transition is due only to growing, unstable two-dimensional waves; this process may be circumvented by a roughness element, for example. Nevertheless, this method, the  $e^n$  method, as it is called, has value in comparing different flows in a fixed environment, and is in any case the most quantitative method now available. For example, simplified prediction schemes based on these stability methods can now readily account for transition of heated water boundary layers (Wazzan and Gazley 1978).

With the linear stability method of Smith, Wazzan, and coworkers, it is readily possible to calculate the transition location (or the start of

---

\*Suspended 'dust' particles may have some similar effects in gas flows.

transition) for a range of amplification levels. Values of the level chosen range from  $e^7$  (Arakeri 1975b) to  $e^{13}$  (Huang and Hannan 1975) with  $e^9$  as the original value chosen by Smith. Many such transition estimates have now been made, e.g., on bodies of interest in naval hydrodynamics (Kaups 1974 and Power 1977), but Arakeri (1973) was evidently among the first to apply this idea to cavitation inception. Calculations were made of the pressure coefficient at transition (using the amplification level of  $e^7$ ), and the results so obtained were compared with the desinent cavitation observations of Parkin and Holl (1953) on a 1.5-cal ogive. These results, reproduced in Figure 17, are extremely suggestive. Later, it was possible to measure surface pressure fluctuations at a point on this same body (Figure 18) to reveal large peak pressure fluctuations at the site of transition. The spectra of these same fluctuations were compared with the expectations of the linear stability calculations (Figure 19) to show, remarkably, that the most sensitive frequencies according to the theory were actually observed. So it was with some anticipation that spark schlieren photographs were taken of this body (Figure 20). These appeared to reveal cavitation inception at the observed position of what are interpreted to be boundary layer transition disturbances (Arakeri and Acosta 1974).

More recent work of McCarthy et al. (1976) has shown a similar favorable agreement of surface (hot film) fluctuation frequency response with the estimates made from linear stability calculations. Perhaps then the plausibility of cavitation inception correlations with the location of transition, i.e., a relation such as Equation (11), is heightened with this closer association of transition as a site of fairly large disturbances. Direct confirmation of transition-connected cavitation on small bodies having deeper minimum pressures present some experimental problems because of the small range of speed and pressure variables available for cavitation index and Reynolds number excursions. One such body that has proved useful in laboratory comparisons is the modified ellipsoidal flat faced head form similar to the ITTC body except with a deeper pressure minimum. It was used in cavitation studies first by Peterson (1969) and then later by

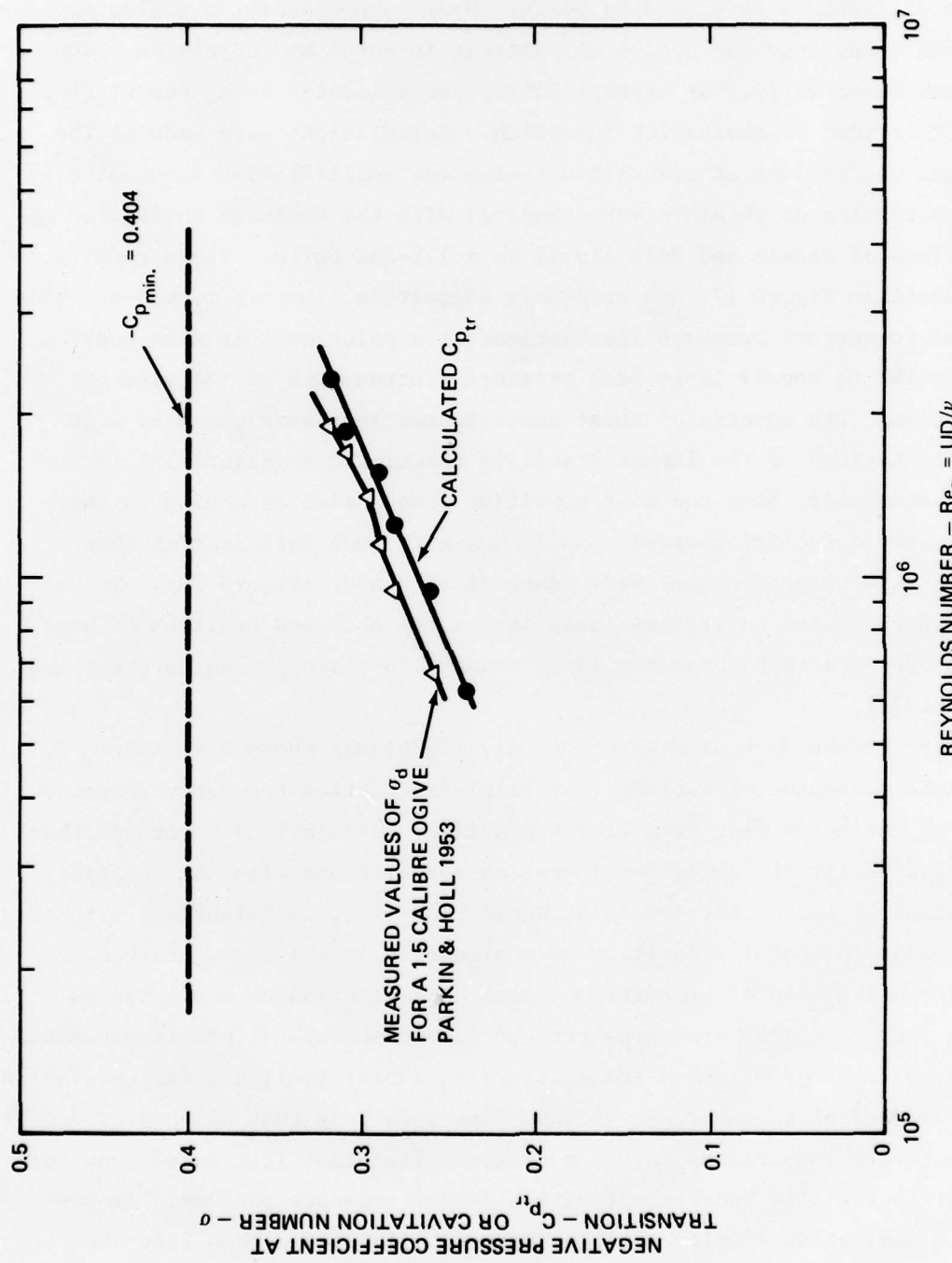


Figure 17 - Comparison of Desinent Cavitation Measurements with the  
 Negative of the Pressure Coefficient at the Site of Calculated  
 Point of Transition (Arakeri 1973)

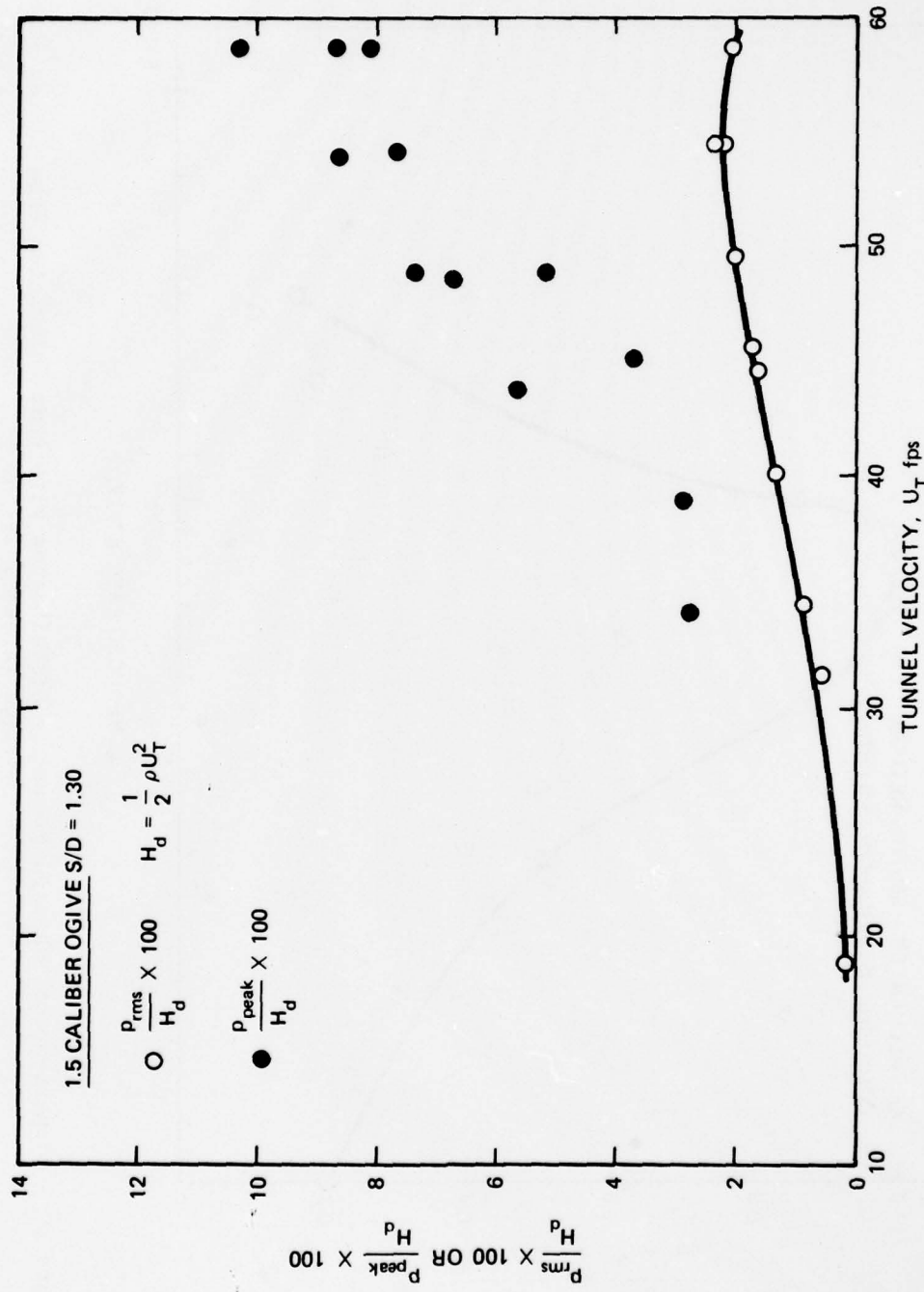


Figure 18 - Pressure Fluctuations on the Surface of a 1.5-Caliber Ogive at the Arc-Diameter Ratio of 1.3  
(Arakeri 1975b)

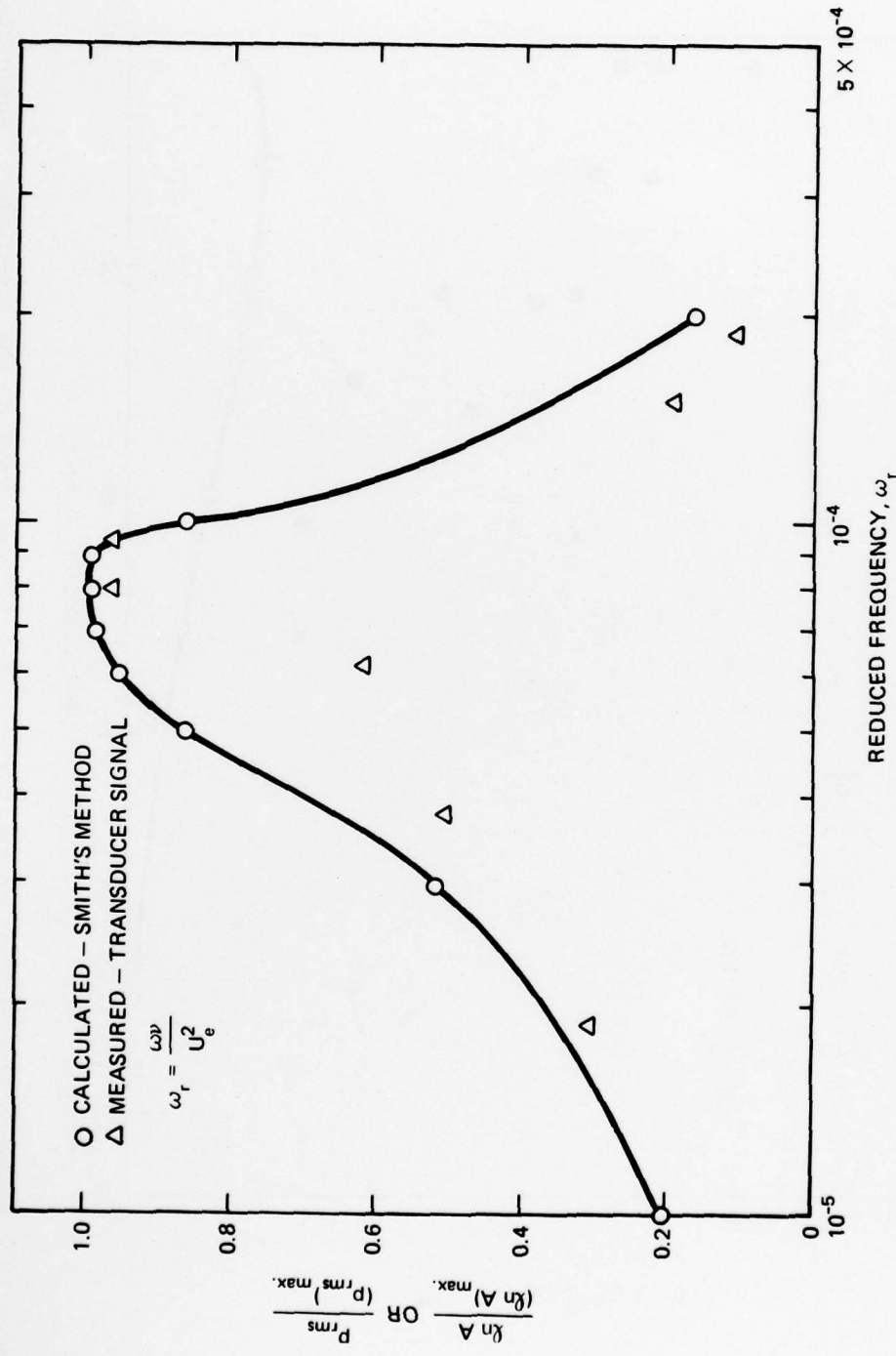


Figure 19 - Comparison of Measured Frequency Distribution with that Calculated from Linear Stability Results (Arakeri 1975b)

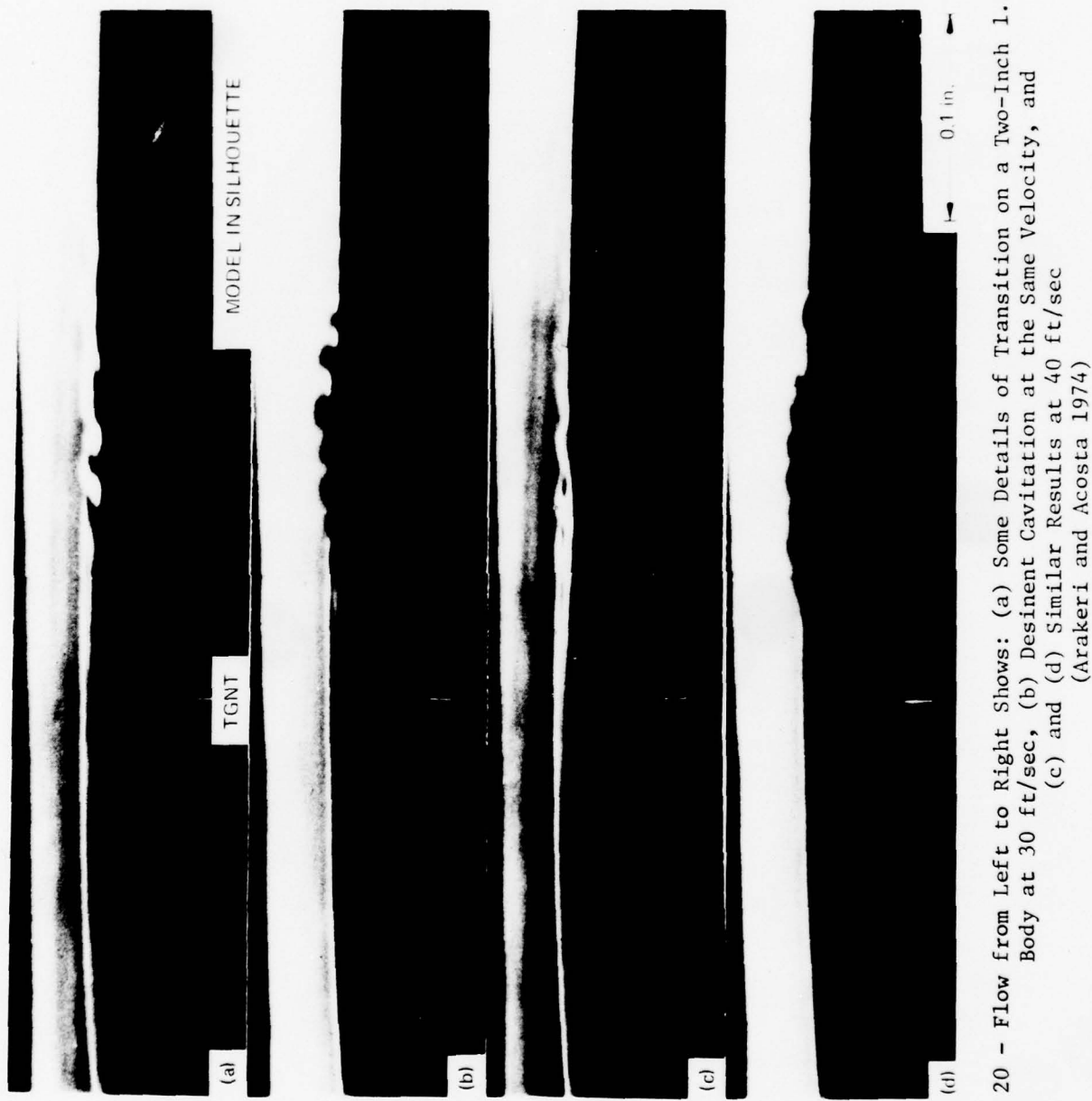


Figure 20 - Flow from Left to Right Shows: (a) Some Details of Transition on a Two-Inch 1.5-Cal Ogive Body at 30 ft/sec, (b) Desinent Cavitation at the Same Velocity, and (c) and (d) Similar Results at 40 ft/sec (Arakeri and Acosta 1974)

Brockett (1972). This body, termed the NSRDC body, like the ITTC body, possesses a laminar separation up to a critical Reynolds number based on a diameter of about  $0.46 \times 10^5$  at which both the  $e^n$  method ( $n = 7$ ) and observations show transition to occur, thereby forestalling the presence of separation.

For Reynolds numbers less than this critical one the appearance of cavitation on this body is very similar to that on the ITTC body, i.e., a smooth band cavity is seen (in the Caltech HSWT). At greater Reynolds numbers this band type gives way to patchy regions of foamy cavitation bubbles, intermittently spaced around the periphery with the smooth sheet cavity. Finally, at greater Reynolds numbers of say  $7 \times 10^5$ , spots or wedges of cavitation are seen. The inception index on one such body has been determined in two different facilities with quite different results (Arakeri and Acosta 1976). In the Caltech facility the correlation

$\sigma_i \approx c_{p_s}$  was found to be valid for Reynolds numbers less than the critical one.

A natural transition, precluding the separation, existed for Reynolds numbers greater than about  $5 \times 10^5$ . The observed inception index remained quite close to the pressure coefficient at the site of the predicted transition location (Figure 21) though there was hardly any change in the pressure coefficient from the separation value.

Spot or wedge cavitation was also observed to occur at the greatest values of Reynolds number originating from positions near  $c_{p_{min}}$ . These indices are quite different from the attached cavitation associated with the presumed location of transition.

However, more recent studies, by Huang and Santelli (1977), show that on one body not subject to a laminar separation, travelling-bubble inception was, in fact, observed at the estimated position of transition. From these observations, they deduce an inception index behavior of the form of Equation (11) with the local pressure coefficient being that of transition as in Figure 17 and with the unsteady term being about -0.06. This latter is, however, air content sensitive, which is a subject we shall return to later.

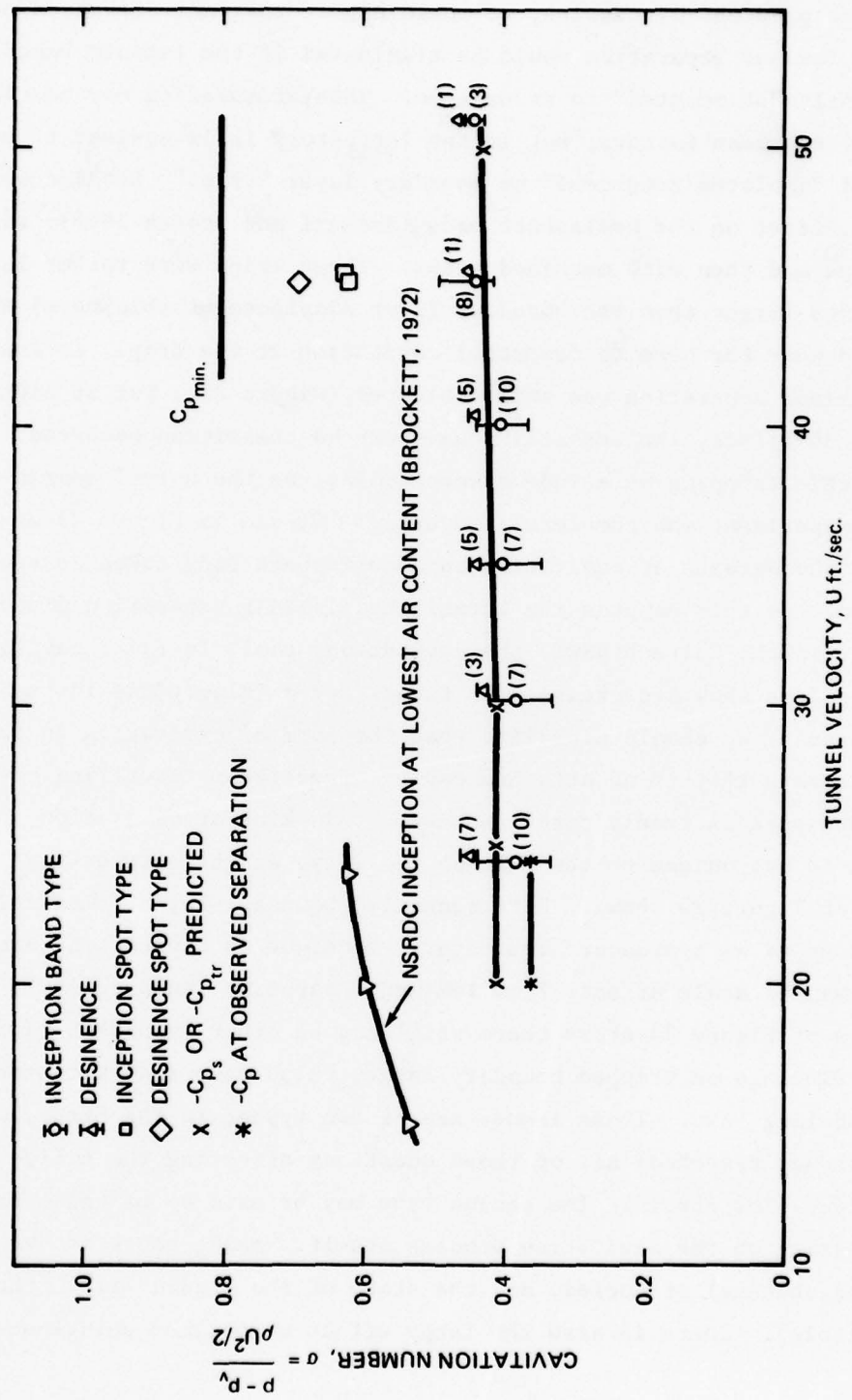


Figure 21 - Inception and Desinent Cavitation Index for the NSRDC Body in the Caltech HSWT at an Air Content of 10.4 ppm (The numbers in parentheses represent the number of data points and the height of the bars, the range of the data. Laminar separation was not observed greater than about 28 ft/sec.) (Arakeri and Acosta 1976)

### Stimulated Boundary Layers

From the previous discussion, we would expect that any effect on cavitation of a laminar separation would be eliminated if the laminar boundary is sufficiently "stimulated" to transition. This stimulation may be via a variety of freestream factors, but in the laboratory it is easiest to use a mechanical "isolated roughness" or boundary layer "trip." Studies were carried out, first on the hemisphere body (Arakeri and Acosta 1976), with trips of tape and then with machined steps. These trips were rather large (several times larger than the boundary layer displacement thickness) and were located near the nose to forestall cavitation at the trip. At low speeds a laminar separation was still observed (Figure 22), but at higher ones, about 30 ft/sec, the separation gave way as transition occurred. The results of this tripping were indeed spectacular, as the normal course of a cavitation experiment was completely reversed. We see in Figure 23 a sequence of photographs of cavitation on a hemisphere body taken as speed is increased. As this happens the established laminar separation disappears and with it, in the Caltech HSWT, the cavitation, too! In fact, cavitation inception indices show a decrease with tunnel speed (Figure 24) instead of the usual trend. We should emphasize that the form of cavitation in this tunnel was always that of an attached cavity; freestream travelling cavitation events were extremely rare. However, this kind of cavitation observation is not unique to the Caltech facility, as the interesting photograph of Figure 25 shows. More recently, boundary-layer stimulation has been proposed as a standard laboratory technique in cavitation testing to avoid unwanted scale effects from laminar separation (Kuiper 1978). As the findings of Figure 23 shows there still may be other important factors.

These findings on tripped boundary layers raise many issues concerning inception scaling laws. These issues are of two types; in the first, we have (as already sketched) all of those questions affecting the fully-wetted viscous flow itself. The second type may be said to be those having a direct bearing on the cavitation process itself. Among these is the presence (or absence) of nuclei, and the state of the liquid (i.e., thermodynamic factors). There is also the large effect of polymer solutions on

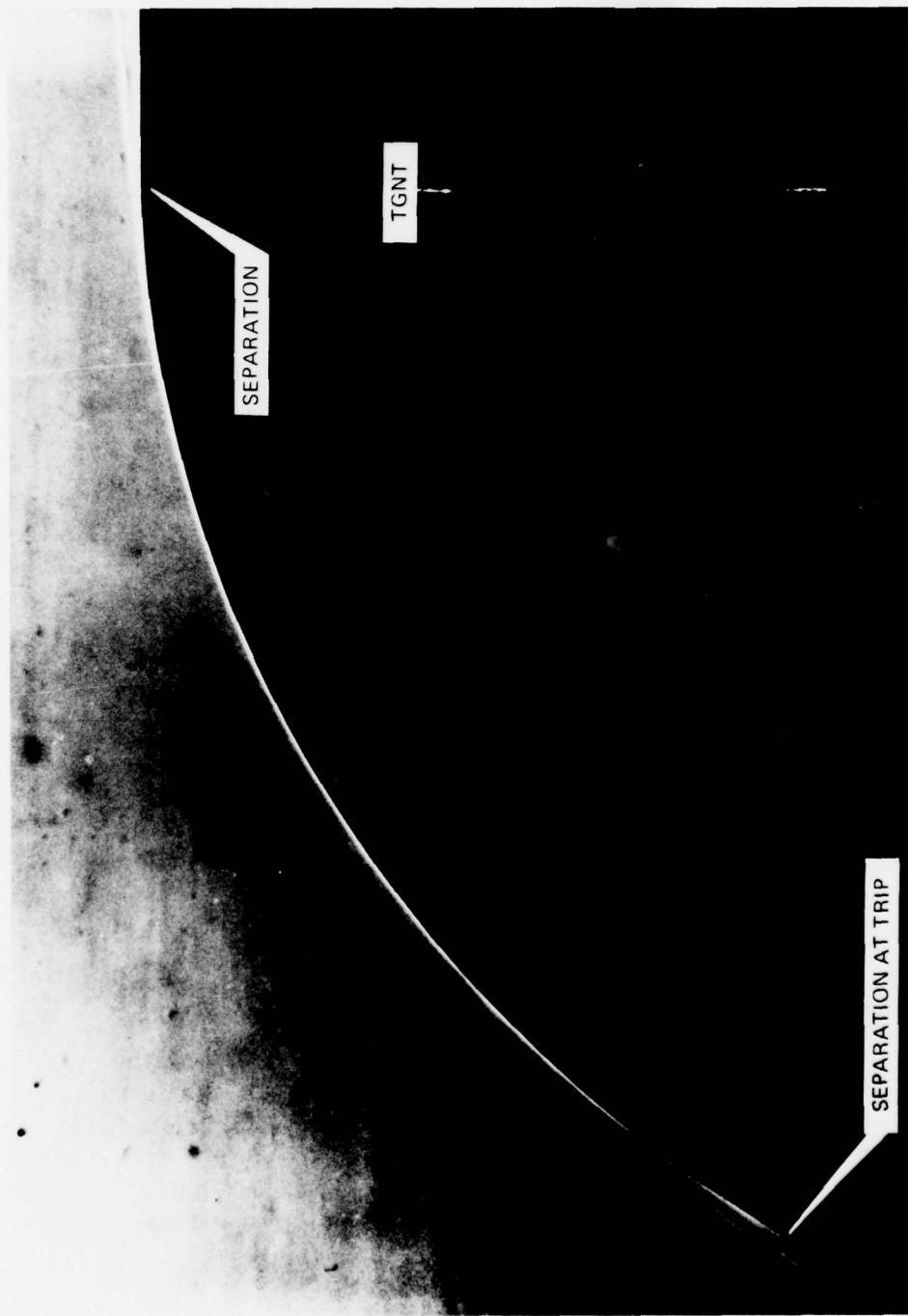


Figure 22 - A Tripped Boundary Layer on a Two-Inch Hemisphere Body at a Subcritical Reynolds Number (The trip is located 30 degrees from the nose and is 0.012 inches high, Arakeri and Acosta 1976)

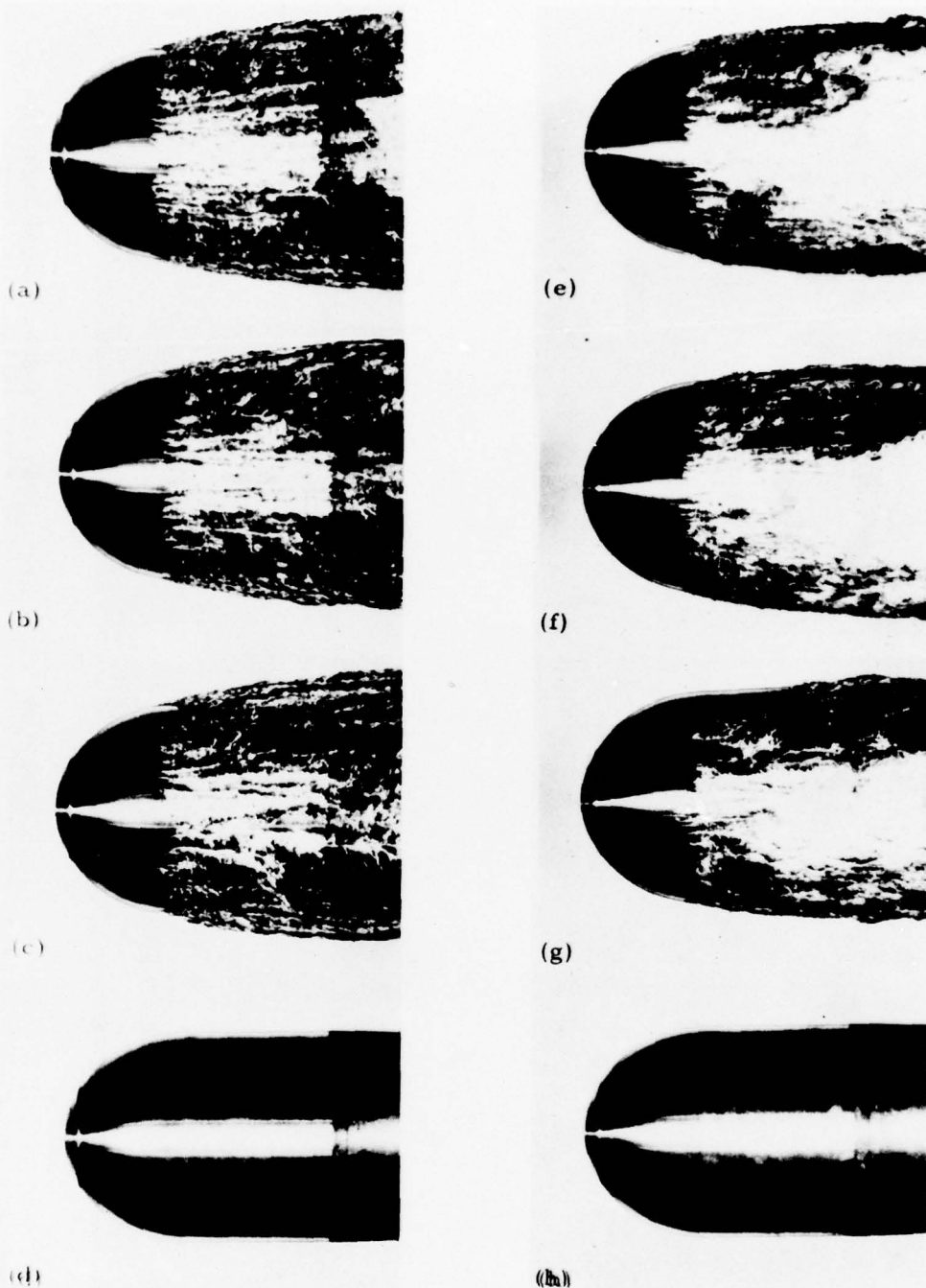


Figure 23 - A Two-Inch Hemisphere Body with Trips Showing the Disappearance of Cavitation as Tunnel Speed is Increased and the Cavitation Index Decreased  
 (The left side sequence has a trip height of 0.012 inches and the right side has a trip of 0.005 inches,  
 Arakeri and Acosta 1976)

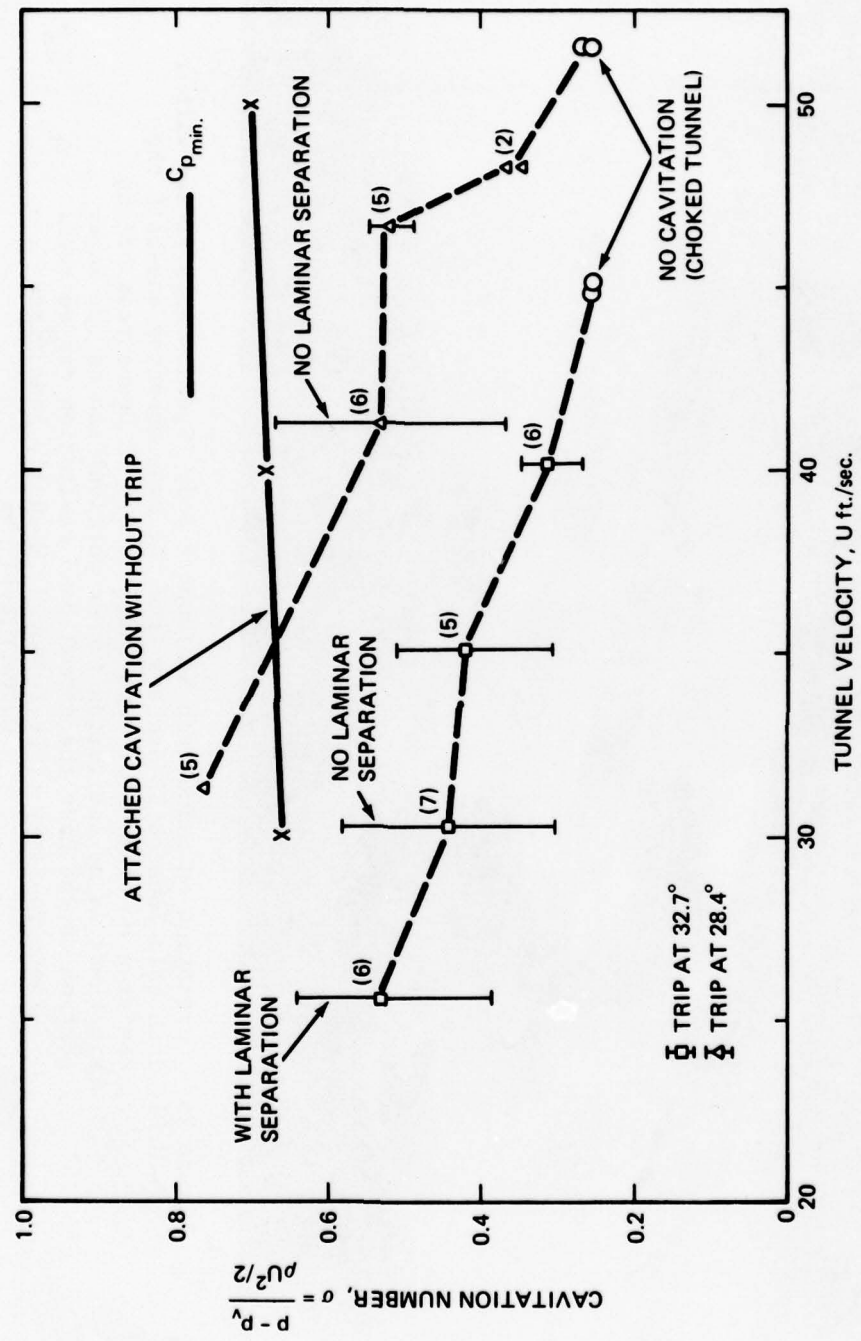


Figure 24 - Cavitation Inception Index versus Tunnel Speed for a 1.81-Inch Hemisphere Body with a 0.005-Inch Trip (The water tunnel is the Caltech HSWT: in every case inception occurs as an attached cavity. The numbers are the number of data points and the bars show the experimental range. Arakeri and Acosta 1976)

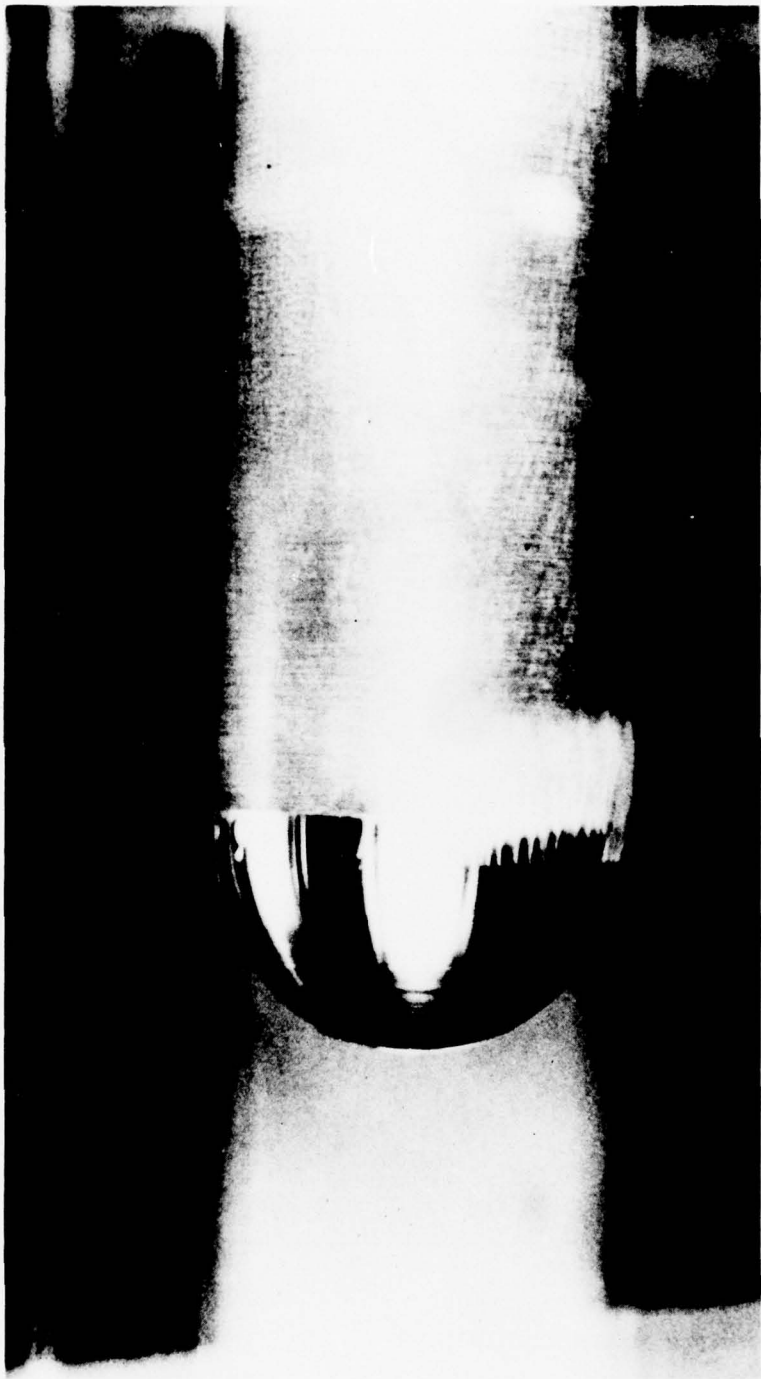


Figure 25 - Cavitation on a Two-Inch Hemisphere Body (Speed = 43.5 ft/sec with a 0.014-inch trip located 30 degrees from the nose spanning one-half the circumference. The cavitation index is 0.56. Downstream of the trip there is no cavitation (upper portion) and on the lower portion of the body the normal band cavitation can be seen.

Photo courtesy of Professor J. W. Holl, Penn State University.)

decreasing, perhaps by one-half, the cavitation inception index in jets and the flow over bodies reported by many workers (e.g., Ellis and coworkers, Holl, Arndt and coworkers, Hoyt, van der Meulen; see van der Meulen 1974, Gates 1977 for review). Despite the initial conclusions of Ellis (Ellis et al. 1970) that bubble mechanics were not a factor in this suppression, considerable uncertainty as to the basic cause of the effect remained.

#### The Polymer Effect in Cavitation

It is certainly fair to say that the presence of long-chain polymers in dilute liquid solutions has had a vitalizing effect on liquid fluid mechanics. The many reasons for this development are well covered by the extensive review of Hoyt (1972). But, as sketched in the foregoing discussion, there is an additional unique effect of polymer solutions on cavitation inception. Two kinds of flows have been extensively pursued, cavitation inception on bodies (as discussed herein) and in jets. The magnitude of the effect appears to be equivalent; we discuss only smooth body inception in the following sections.

It seems most natural in discussing these types of fluid to note the appearance of particular phenomena with a characteristic time ratio, such as the ratio of the time required for the fluid to move a certain length, to a characteristic polymer molecular relaxation time. In fact such a relation was used by Arndt (Arndt et al. 1976) to correlate such suppression results, and it appeared to work best if a relevant boundary layer length was used as the length parameter. At about the time of the 17th ATTC conference (Morgan 1974) it was suggested by several workers including J.W. Holl that, based on the appearance of the cavitation band at inception, the polymer seemed to cause the interface to become turbulent with the implication that transition had occurred. But this demonstration remained for van der Meulen (1976) to carry out. He showed, by careful and ingenious adaptation of a schlieren-holographic technique, that the polymer fluid appears to trigger a turbulent transition and that, on the hemispherical body (for example), this transition removed the laminar separation. Then one would have, presumably, a situation rather similar to that of a body

normally having a laminar separation, but with a tripped boundary layer, and equivalent effects might therefore be anticipated. Thus, as in Figures 23 and 24, a cavitation suppression effect should be expected from the polymer fluid if the main effect of the polymer is on the boundary layer. Indeed, the magnitude of van der Meulen's suppression effect are similar to, but not as great as, those of Figure 24.

van der Meulen further reasoned that a body not normally possessing a separation should not exhibit a large suppression effect. To this end, he adopted a body shape previously suggested for hydrodynamic cavitation research by Schiebe (Schiebe 1972); namely, a body having nearly the same minimum pressure coefficient as the hemisphere ( $c_{p_{min}} = -0.75$ ) but without a predicted laminar separation. van der Meulen's experiments showed little effect of the polymer injectant on the cavitation-inception behavior of this body. Furthermore, his holographic schlieren observations confirmed the predicted absence of separation. He was also able to show that the position of transition estimated from these observations agreed on the whole quite well with the linear stability calculations. Interestingly in his test facility, travelling-bubble cavitation was the predominant form of cavitation observed on this Schiebe body. In a followup report (van der Meulen 1978) he summarizes his opinions about the hemisphere and Schiebe bodies thusly, "Since the influence of polymer additives is to suppress laminar boundary-layer separation on the hemispherical nose, the strong pressure fluctuations occurring at the position of transition and reattachment of the separated shear layers; and being the principal mechanism for cavitation inception, are eliminated and cavitation inception will start at much lower pressures."

Much the same conclusions had been reached at about the same time by Gates (Gates 1977, Gates et al. 1978) on the mechanism of polymer effect. Both Gates and van der Meulen injected polymer solutions at the stagnation point. Gates was able to observe a significant polymer effect at extremely low injectant rates on both the hemispherical body (Figure 26) and the Schiebe body (Figure 27). In these photographs, the injectant rate is

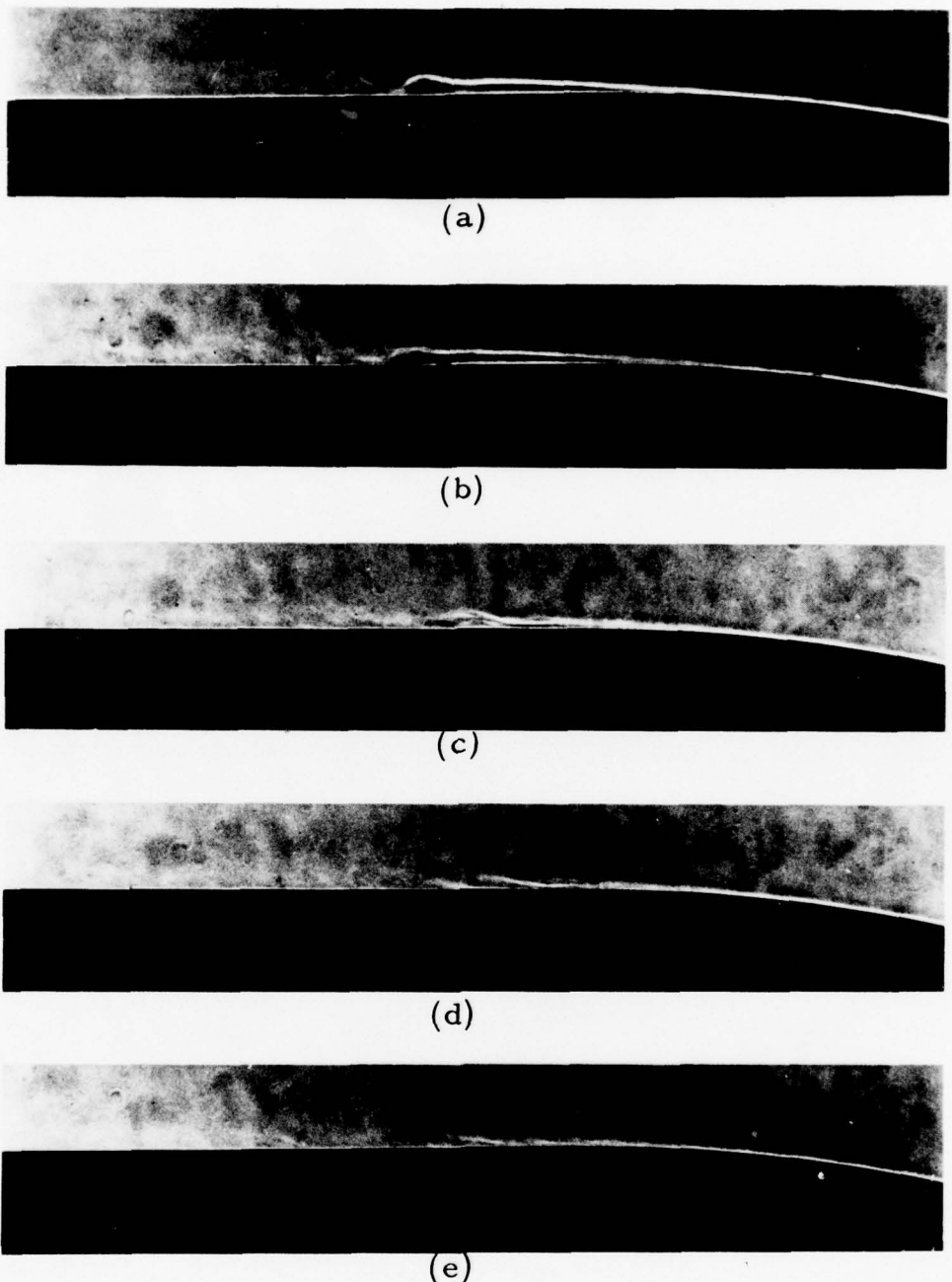


Figure 26 - Flow Past the Hemisphere Body with Injection of 100 wppm Polyox at a Reynolds Number of  $3.9 \times 10^5$  (The dimensionless injectant rates are, respectively: (a) no injection, (b)  $0.5 \times 10^{-6}$ , (c)  $1.1 \times 10^{-6}$ , (d)  $1.7 \times 10^{-6}$ , and (e)  $2.9 \times 10^{-6}$ , Gates and Acosta 1978)



(a)



(b)



(c)



(d)

Figure 27 - Flow Past the Schiebe Body at a Reynolds Number of  $4.2 \times 10^6$  with Injection of 500 wppm Polyox (The dimensionless injection parameters are, respectively: (a) zero, (b)  $2.3 \times 10^{-6}$ , (c)  $1.5 \times 10^{-5}$ , and (d)  $2.9 \times 10^{-5}$ . The photographs are each 0.2 body diameters in length centered on arc length ratios of 0.82, 0.75, 0.6, 0.53, respectively, Gates and Acosta 1978)

normalized to give the weight fraction within the boundary layer displacement thickness. It is evident that the very small concentration of only 2.9 ppm is sufficient to remove the laminar separation on the hemisphere, and significant forward movement of transition on the Schiebe body is accomplished, with somewhat larger concentrations. The main thrust of van der Meulen's findings, then, appear to be confirmed, and the cavitation inception inhibition on the hemisphere is traced to an overall viscous effect.

#### Turbulence Levels

We now, of necessity, touch briefly upon this ubiquitous standard problem in experimental fluid mechanics; namely, the influence of free-stream turbulence on flow past bodies. But, with the restricted emphasis herein on cavitation inception, our concern is primarily to determine if the stimulated transition causes a laminar separation to disappear or if there is any direct effect on cavitation inception of bodies not having such a separation. There are, of course, semi-empirical rules for the turbulence effect (e.g., Hall and Gibbings 1972, Van Driest and Blumer 1963) and the turbulence-modified amplification method of Mack (1978). But, as Reshotko (1976) has made clear in his review, the coupling between these freestream disturbances and boundary layer developments is unclear--particularly for large disturbances that may bypass the linear growth process. Thus, as in many areas of naval hydrodynamics, recourse must still be made to the laboratory to study particular experimental situations.

It has not been customary in much hydrodynamic work to quantify turbulence levels--let alone their power spectra--although a few such data on several water tunnels are now becoming available through the ITTC reports (12th ITTC Cavitation Committee). Thus, it is no surprise that there is no account of the effect of freestream turbulence on flow past bodies of interest in naval hydrodynamic applications. One problem in large hydrodynamic facilities has been the expense of the control of this real fluid feature. For this purpose a water tunnel having a low level of freestream turbulence to begin with is essential. The key features of one such research facility are shown in Figure 28. Some features, particularly

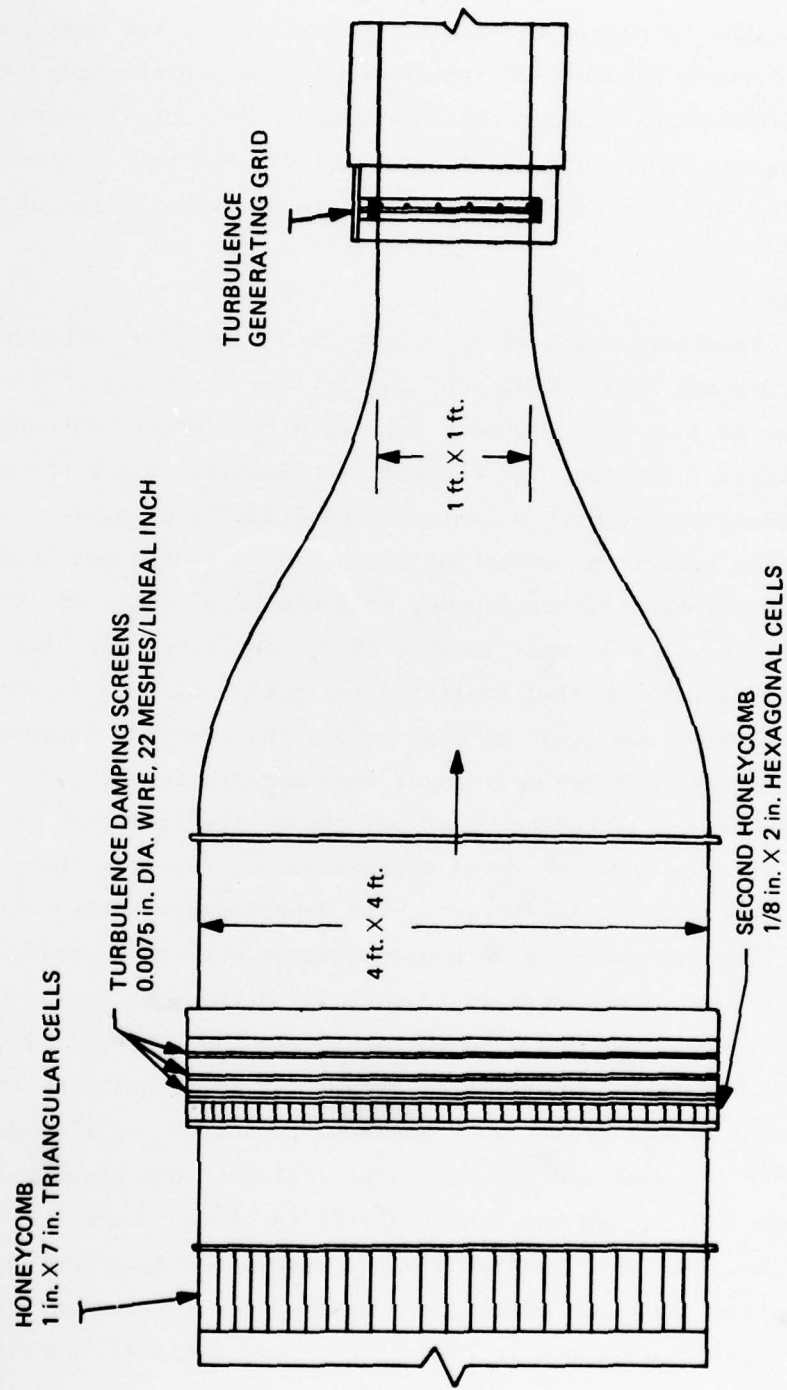


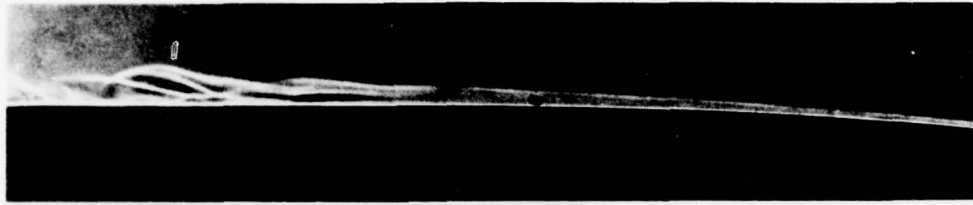
Figure 28 - Caltech Low Turbulence Water Tunnel (Gates 1977)

convenient for this kind of work, are the large (16:1) contraction ratio, the vaned elbows on each leg, the ready insertion of honeycomb straighteners and damping screens and, finally, the insertion of turbulence-generating grids at the entrance of the working section (see Gates 1973 for a full description). It was possible, thereby, to vary the freestream level by nearly a factor of 100 from a low value of about 0.05 percent. (Unfortunately, it was not possible to carry out cavitation experiments over the same range.)

It was anticipated that these turbulence levels would have a profound effect on bodies near transition but normally having a separation, such as the DTNSRDC body. We see, in Figure 29, that a turbulence level of about one percent is sufficient for transition to occur upstream of the separation on this body. A similar upstream progression of the site of transition at fixed body Reynolds number with increasing turbulence level was also observed on the Schiebe body (not shown). Indeed, the observations of transition location together with those of van der Meulen agree fairly well with the amplification computations of Wazzan and Gazley, Figure 30. Similar observations on the hemisphere body were surprising however, as the laminar separation appeared to be totally immune to the turbulence level! This unexpected result is traced (Gates 1977) to significant differences in the sensitive critical frequency of the respective boundary layers on these bodies (deduced from linear stability theory), the highest frequency being for the hemisphere body, DTNSRDC next, and then Schiebe body. Because of this difference in frequency and reasoning from typical grid turbulence spectra, it is argued that there is nearly two orders of magnitude more disturbance energy available for boundary stimulation on the DTNSRDC body than on the hemisphere. This seems a plausible explanation and shows the desirability of providing freestream spectral data in addition to intensity levels in future hydrodynamic work.



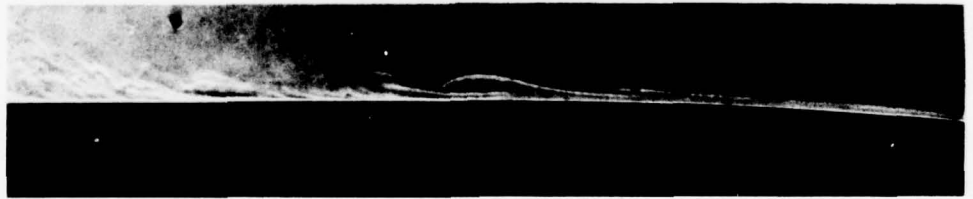
(a)



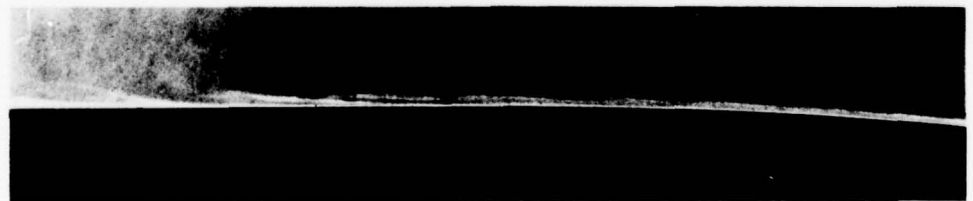
(b)



(c)



(d)



(e)

Figure 29 - The Effect of Freestream Turbulence on the Flow Past the NSRDC Body  
(The flow is from right to left at a body Reynolds number of  $1.6 \times 10^5$ . The turbulence intensity is: (a) 0.05 percent, (b) 0.65, (c) 1.1, (d) 2.3, and (e) 3.6 percent, Gates 1977)

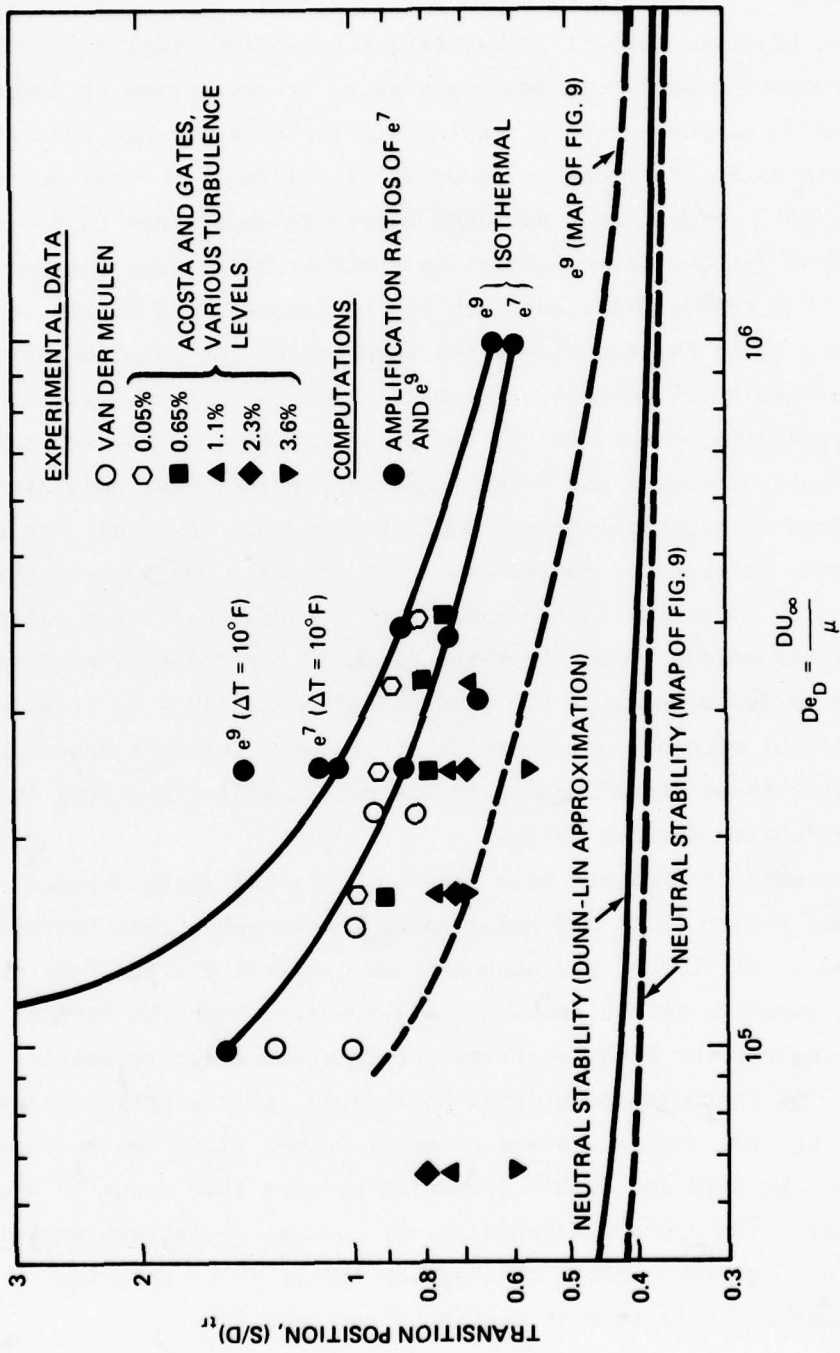


Figure 30 - Comparison of Observed Transition Locations with Values Predicted by the Amplification Method (Wazzan and Gazley 1978)

## CAVITATION NUCLEI, BUBBLE MECHANICS AND SCALING

### Nuclei and Their Measurements

Possibly, no other subject in cavitation inception research has proved to be so exacerbating as the nucleation sources of cavitation or "nuclei." The many theories proposing their nature, size, and occurrence are all extensively reviewed in the books by Knapp et al. (1970) and Robertson and Wislicenus (1969). Significant advances have been made since that time in the detection of (rather large) nuclei on a number of fronts; these are reviewed first by Morgan (1972), and then later by Acosta and Parkin (1975) and do not need to be further elaborated here except for some recent findings and some conceptual notions. The basic idea is rather simple; there must be some practical mechanism for the phase change to occur in engineering applications, otherwise the large tensions predicted for pure liquids far removed from the critical point, would be commonly observed. As explained in these references, nuclei can exist as small gas-vapor bubbles (perhaps with the interface contaminated with a surfactant) or a solid particle. It has become common to think of solid particles as good candidates for the nuclei because of the theoretical possibility of stabilizing a gas pocket within a solid particle. Indeed, Keller's recent work makes a case for these "pore" nuclei in his own facility in a very influential publication (Keller 1973).

The measurement techniques have been both optical (single point scattering, see Keller 1973) and holographic photography, (see Peterson 1972, Peterson et al. 1975), and acoustic and indirect via the Coulter counter. The acoustic method measures only bubbles; both the Coulter counter and single point light scattering techniques react to bubbles and particulates. As in photomicrography, holographic photography is limited in resolution but the entire cross-section of tunnel fluid can be examined at leisure for the form and number of nuclei greater than about 10 micrometers diameter. (We are now discussing, of course, freestream nuclei; it is also possible for the surface of the body itself to be the site of nucleation, just as it is in most boiling situations.)

From various sources, we summarize (Figures 31 and 32) the number of density distributions down to about 10 micrometers diameter. It is clear that these concentrations can vary by several orders of magnitude; several different types are probably represented on these figures. The scattering data contain, undoubtedly, both solid particles and microbubbles, although for the larger sizes it is clear from the reports (Arndt and Keller 1976 and Keller and Weitendorf 1976) that air bubbles are the main contributor. Gavrilov (1970) and Medwin (1977) measure microbubbles acoustically. Both particulates and bubbles are seen in the holographic studies of Peterson (1972), Peterson et al. (1975), Gates and Bacon (1977), and Katz (1978). From the latter we present an example showing how it is possible to readily detect particulates in the holographic reconstruction process (Figure 33). We could add to these plots additional data from the St. Anthony Falls Hydraulic Laboratory (e.g., Schiebe 1969), of ocean particulates measured by the Coulter counter (Peterson 1974) and similar measurements by the Naval Ocean Systems Center.\* These findings all fall within the bands of data of Figure 31, and they all have about the same functional behavior for the small sizes (even to less than one micrometer for the particulates). This apparent uniformity seems quite remarkable.

Now that microbubble and particulate nuclei distributions are beginning to appear more frequently in the hydrodynamic literature, one may well ask just how these data are to be used quantitatively in cavitation inception studies and in flows with more fully developed cavitation. The several orders of magnitude difference in number density seen in Figure 31 suggest that there may be some considerable differences to be expected in cavitation. We have in fact seen such differences appearing on inception forms already in Figure 6; it seems certain that many of the differences seen there are due to the nuclei content. It is also clear that the Caltech HSWT has a very low bubble nuclei population (Figure 32), and that the numerous particulates of that facility do not serve as nuclei. Other investigators have shown the vital importance of microbubble supply (but unquantified) in the unsteady flows of model propeller wakes (e.g., Albrecht and Bjorheden 1975, Noordzij 1976). There are other interactions

---

\*T.G. Lang, private communication.

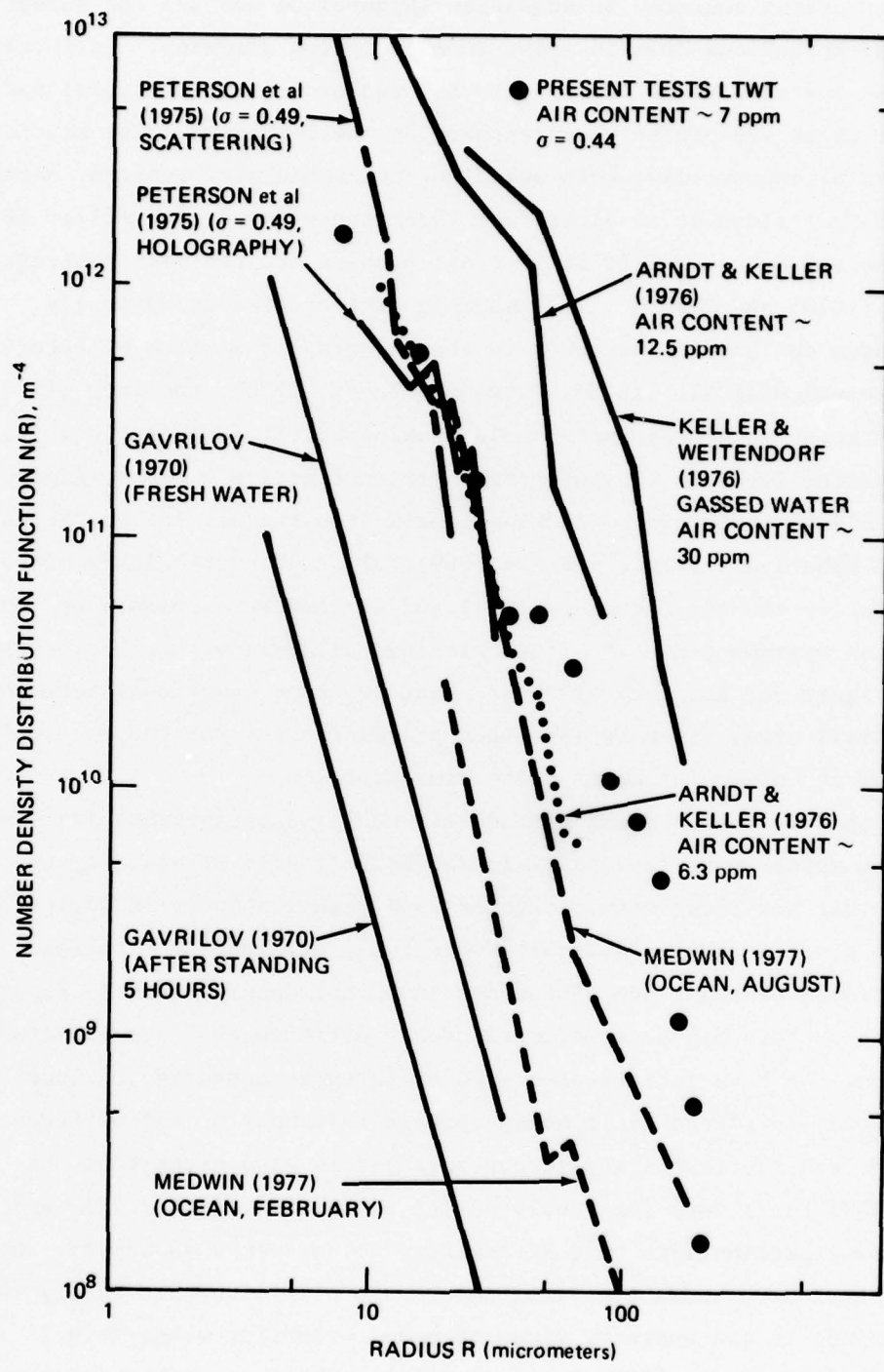


Figure 31 - Freestream Nuclei Number Density Distributions from Various Sources (Gates and Acosta 1978)

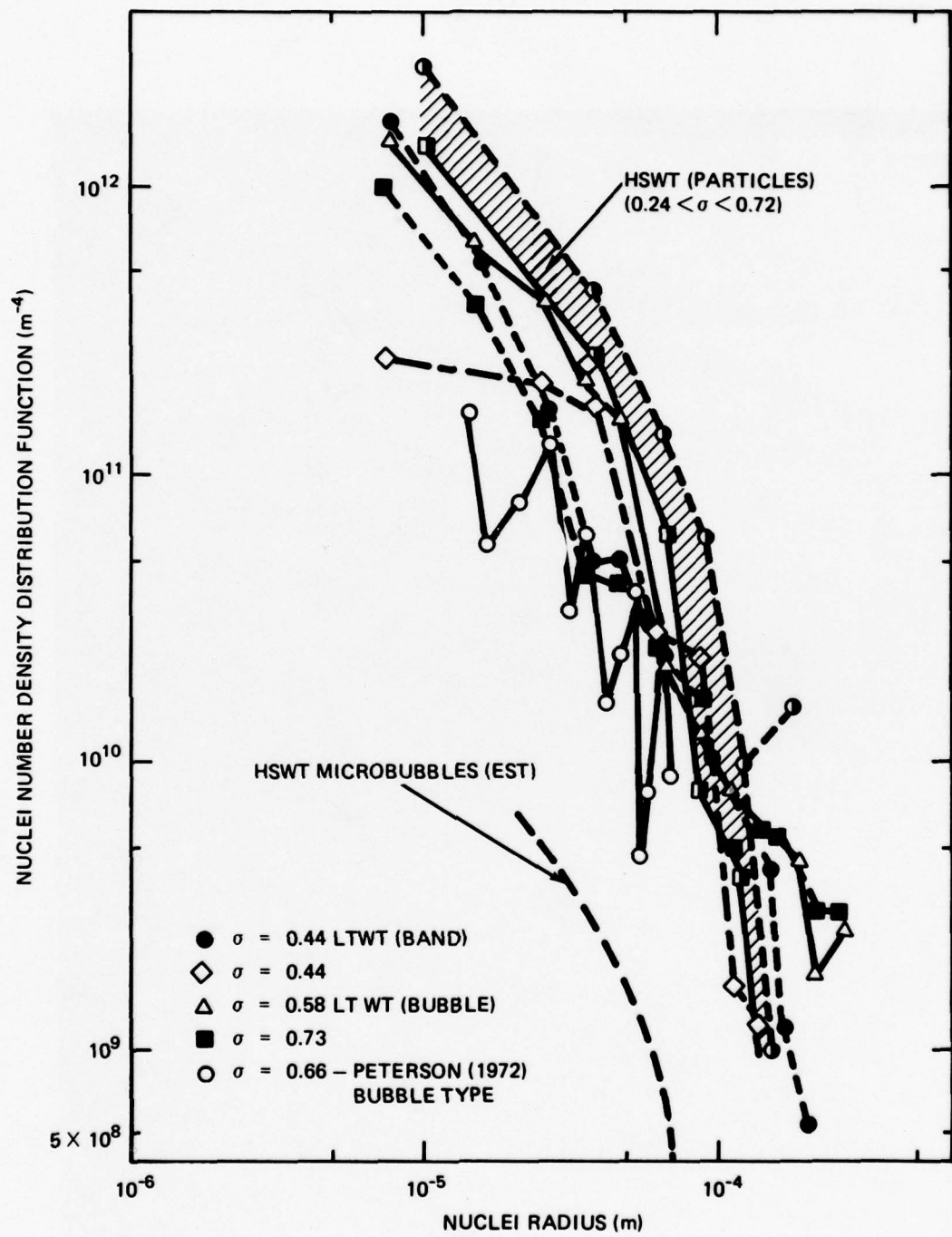


Figure 32 - Nuclei Distributions Measured by Holography in the Caltech LTWT (All Microbubbles) and HSWT (Essentially All Solid Particles) (Gates and Acosta 1978)

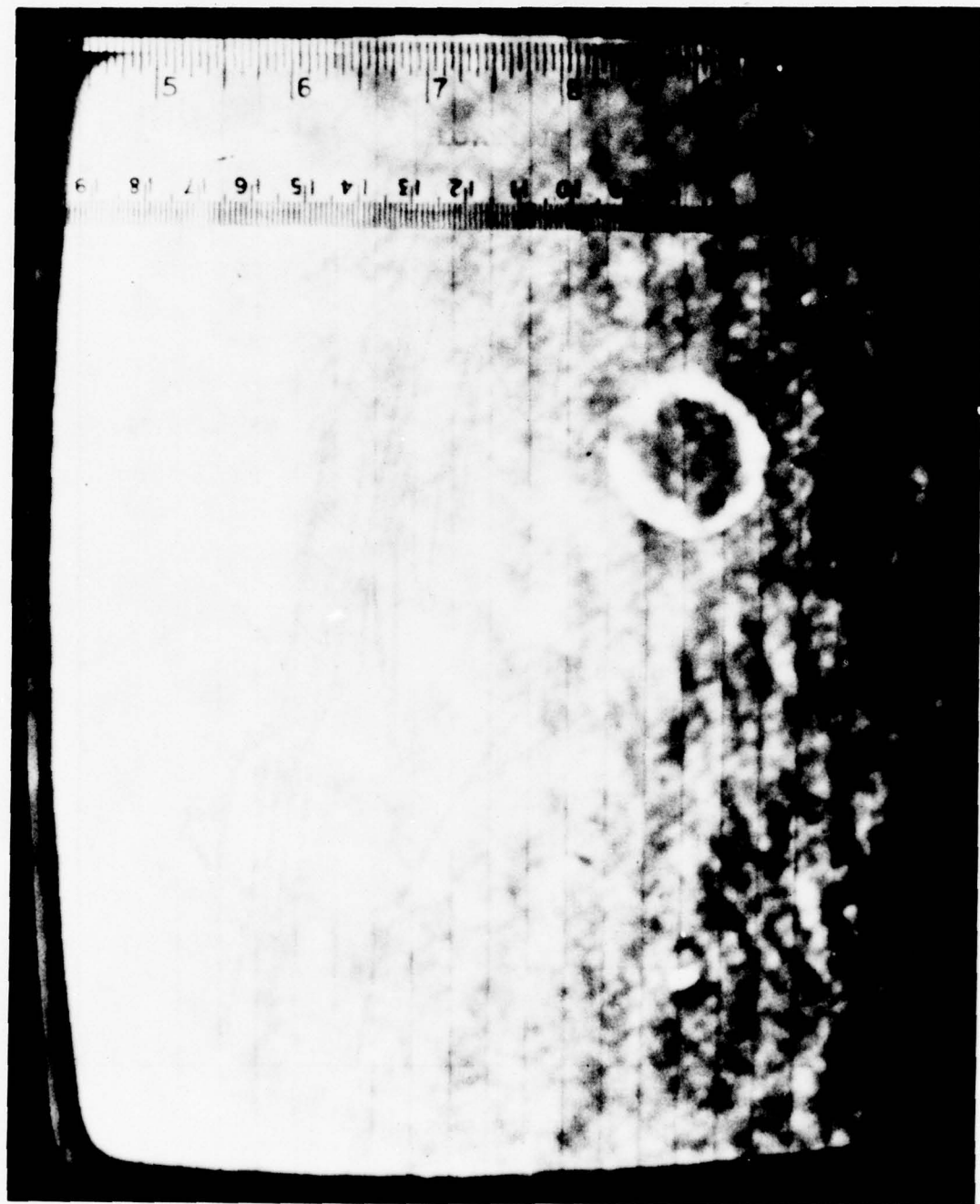


Figure 33 - TV Monitor Showing Holographic Reconstruction of a 20-Micrometer Particle and 200-Micrometer Bubble (Katz 1978)

between bodies, such as between a ship hull and unsteady propeller cavitation, where the nuclei content affects the gas void fraction of the medium directly, a different kind of problem to which we now, momentarily, defer.

To make full use of the nuclei distribution information, we need an appropriate physical understanding of just how the nuclei themselves lead to cavitation in the flows of interest. (Direct observation of this process is still lacking.) And of course, one would like to predict from laboratory tests (given full control over all laboratory variables) what cavitation inception indices and forms might be on previously untried prototype bodies and conditions. We think this is still not quite possible except for a certain kind of cavitation, namely travelling-bubble cavitation. To appreciate the mechanism of this form of bubble growth, we digress briefly to review the key features of bubble mechanics.

#### Some Bubble Mechanics

We lean heavily, here, on the monograph of Knapp et al. We are concerned with the growth of a small bubble of initial radius,  $R_0$ , immersed in a pressure field,  $p_\infty(t)$ , i.e., the pressure far away is time dependent. The vapor pressure,  $p_v$ , depends on the temperature of the bubble wall,  $T(R)$ , and there may be a gas partial pressure,  $p_g$ . We need the equation for the motion of the bubble radius,  $R(t)$ , which is (from Knapp et al. (1970))

$$R\ddot{R} + \frac{3}{2} \dot{R}^2 = \frac{1}{\rho} \left[ p_{cav} - 4\mu \frac{\dot{R}}{R} - \frac{2\sigma_s}{R} - p_\infty \right] \quad (12)$$

where  $\rho$  is the liquid density,  $\mu$  the viscosity, and  $\sigma_s$  the surface tension and

$$p_{cav} = p_v(T(R)) + p_g \quad (13)$$

The partial pressure of the gas may be expressed as

$$p_g = \frac{K(T)}{R^3} \quad (14)$$

where  $K$ , proportional to the mass of gas within the bubble, may depend upon the temperature. At equilibrium, the bubble radius,  $R$ , is stationary, say  $R = R_0$ . Then Equation (12) is

$$0 = - (p_\infty - p_v) - \frac{2\sigma_s}{R_0} + \frac{K}{R_0^3} \quad (15)$$

Now we may ask whether or not this equilibrium is stable. To answer this question we put, in the usual way,

$$R = R_0 (1+\varepsilon(t)) \quad (16)$$

where  $\varepsilon(t)$  is supposed to be a small number, and linearize Equation (12) to get

$$\ddot{\varepsilon} + \frac{4v\dot{\varepsilon}}{R_0^2} + \frac{1}{\rho R_0^2} \left( \frac{3K}{R_0^3} - \frac{2\sigma_s}{R_0} \right) \varepsilon = - \frac{p_\infty - p_v}{\rho} - \frac{2\sigma_s}{\rho R_0} + \frac{K}{\rho R_0^3} \quad (17)$$

But, the right hand side is identically zero. We have now the equation of a single degree of freedom oscillator and we expect that

$$\varepsilon = \varepsilon_0 e^{j\Omega t} \quad (18)$$

$\Omega$  being the frequency. We readily find that

$$\Omega = \frac{2v_j}{R_0^2} \pm \sqrt{k_s - \frac{4v^2}{R_0^4}}, \quad v = \mu/\rho \quad (19)$$

where the spring constant,  $k_s$ , is given by

$$k_s \equiv \left( \frac{3K}{R_o^3} - \frac{2\sigma_s}{R_o} \right) \frac{1}{\rho R_o^2} \quad (20)$$

Periodic motion occurs for  $k_s > 4v^2/R_o^4$ , no oscillations take place when  $k_s = 4v^2/R_o^4$ , and exponential growth occurs for  $k_s < 4v^2/R_o^4$ . The "damped" case is not really one of great interest for we find that with water at one atmosphere of pressure difference the cut-off radius below which the bubbles do not oscillate is about  $1.4 \times 10^{-8}$  in. This is such a small number that the viscous effect may be neglected for our purposes. Likewise the compressibility damping effect may also be neglected (Clay and Medwin 1977, Chapter 6). The natural frequency then is closely equal to

$$\Omega_o = \left\{ \frac{3}{\rho R_o^2} \left( p_\infty - p_v + \frac{4\sigma_s}{3R_o} \right) \right\}^{1/2} \quad (21)$$

on eliminating  $k_s$  and  $K$ . We see immediately that this frequency vanishes when

$$p_\infty - p_v = - \frac{4\sigma_s}{3R_o} \quad (22)$$

These conditions may be termed the critical ones and the value of  $R_o$ , so found for a given gas content of bubble (or value of  $K$ ) the critical radius,  $R_{crit}$ . Figure 34 shows plots of these equilibrium radii and the locus of points (Equation (22)) separating stable and unstable regions. Some of the numbers from Equations (21) and (22) are interesting, and for reference we summarize a few in Table 2.

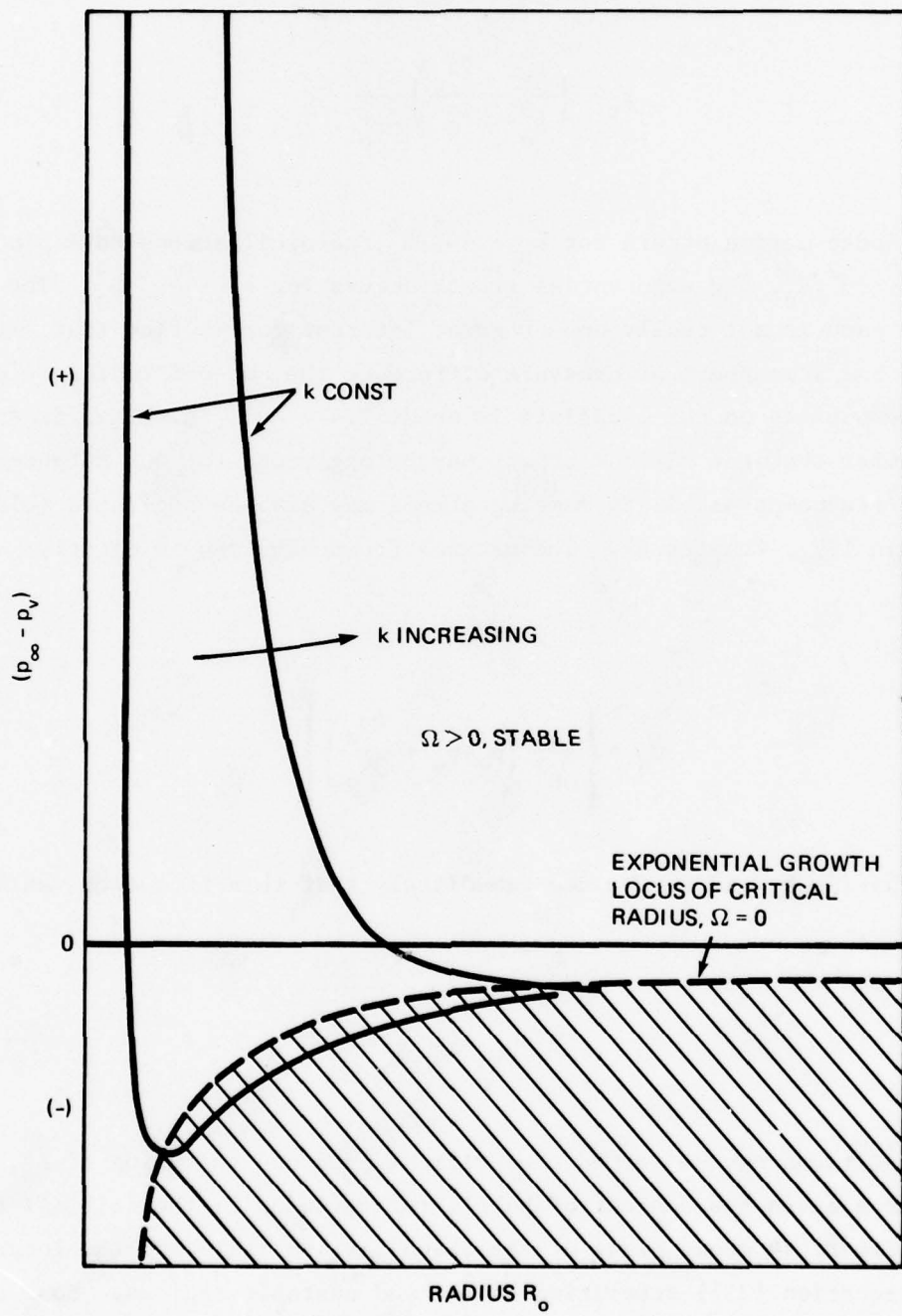


Figure 34 – Equilibrium Radius for Constant Gas Content K (Arbitrary Units)  
Showing Stable and Unstable Regions (Adapted from Knapp et al. (1970))

TABLE 2 - SOME VALUES OF NATURAL FREQUENCY AND CRITICAL RADIUS FOR BUBBLES

$R_o$	$\Omega_o$ ( $p_\infty - p_v = 0.1$ atm)	$(p_\infty - p_v)_{crit}$
$10^{-6}$ m	$2 \times 10^6$ Hz	1.21 atm
$10^{-5}$ m	$1 \times 10^5$ Hz	0.12 atm
$10^{-4}$ m	$1 \times 10^4$ Hz	0.01 atm

Before continuing on to consider how these results might be used in interpreting cavitation inception, we pause briefly to consider the vapor pressure term,  $p_v$ , and how it may be expected to change during bubble growth. The basic idea is that bubble growth implies evaporation of liquid and, hence, cooling of the bubble wall. This cooling depresses the vapor pressure and, hence, tends to reduce the pressure difference available for growth. Rough ideas of the magnitude of the "thermal effect" are easily obtained following physical arguments due to Plesset (1949). The pressure difference terms, on the right hand side of Equation (12), are split up as follows (see also Holl and Kornhauser 1970)

$$p_v(T) - p_\infty(t) = p_v(T_\infty) - p_\infty(t=0) + p_\infty(t=0) - p_\infty(t) + p_v(T) - p_v(T_\infty) \quad (23)$$

where  $(\infty)$  means far from the body, and  $T$  is the temperature of the liquid at the bubble wall. The vapor pressure difference is estimated from the Clausius-Clapeyron equation to be

$$p_v(T) - p_v(T_\infty) = \frac{\zeta}{T_\infty} \rho_v(T - T_\infty) \quad (24)$$

where  $\rho_v$  is the density of the vapor and  $\zeta$  is the latent heat. The heat flow supporting the evaporation is (approximately)

$$\dot{q} = - \frac{4\pi R^2 k_c (T_\infty - T)}{\delta} \quad (25)$$

$k_c$ , here, being the conductivity, and  $\delta$  a heat diffusion distance. This heat flux balances the evaporation requirement

$$\zeta \frac{d}{dt} \left( \frac{4}{3} \pi R^3 \rho_v \right) \quad (26)$$

and Plesset assumes  $\delta = \sqrt{\alpha t}$ ,  $\alpha$  being the thermal diffusivity. Bringing these together we have

$$\frac{p_v(T) - p_v(T_\infty)}{\rho} = - \left( \frac{\rho_v}{\rho} \right)^2 \frac{\zeta^2}{T_\infty} \frac{\rho}{k_c} R \sqrt{\alpha t}$$

The other pressure differences are expressed in terms of the conventional cavitation number and pressure coefficient. To express the scale of the problem let  $t = t^* L/U_o$ , where  $t^*$  is a dimensionless time, and  $L$  and  $U_o$  are a reference length and speed, respectively. We may then write the right hand side of Equation (12) (neglecting, now, the viscous term) as

$$RHS = - \frac{U_o^2}{2} (\sigma + c_p(t)) - \frac{1}{\rho} \left( \frac{2\sigma_s}{R} - \frac{K}{R^3} \right) - \left( \frac{\rho_v}{\rho} \right)^2 \frac{\zeta^2}{T_\infty} \frac{\rho}{k_c} R \sqrt{\alpha t} \quad (27)$$

Two interesting, limiting cases are immediately evident: first, neglecting the thermal effect entirely, we estimate the asymptotic growth rate for an imposed constant value of  $(\sigma + c_p)$ . Then for  $R \gg R_o$  we have the limiting "inertial" growth rate

$$\dot{R}_i = U_o \left( - \frac{1}{3} (\sigma + c_p) \right)^{\frac{1}{2}} \quad (28)$$

a constant. Second, we may now imagine that the thermal effect is large, so that the bubble growth is slow. Then, the inertial terms on the left hand side of Equation (12) may be imagined to be small. Again, for  $R \gg R_o$  bubble growth is then in thermal equilibrium with a rate

$$\dot{R}_{th} = -\frac{U_o^2}{2} (\sigma + c_p) \cdot \frac{1}{\left(\frac{\rho_v}{\rho}\right)^2 \frac{\zeta^2}{T_\infty} \frac{\rho}{k_c} \sqrt{\alpha t}} \quad (29)$$

These rates can be quite different. In the first case we say that we have "cavitation," and in the second, "boiling" is said to occur. The ratio of the two rates may be expressed as

$$\frac{\dot{R}_i}{\dot{R}_{th}} = \frac{2}{\sqrt{3}} \sqrt{\frac{t^*}{-(\sigma + c_p)}} \left(\frac{\rho_v}{\rho}\right)^2 \frac{\zeta^2}{c_p T_\infty} \sqrt{\frac{L U_o}{\alpha}} \cdot \frac{1}{U_o^2} \quad (30)$$

and for boiling to occur, the thermally controlled rate must be much less than the inertial one, i.e.,

$$\frac{\dot{R}_i}{\dot{R}_{th}} \gg 1 \quad (31)$$

This has led Brennen (1973) to identify the dimensional group of terms

$$\sum \equiv \left(\frac{\rho_v}{\rho}\right)^2 \frac{\zeta^2}{c_p T_\infty} \cdot \frac{1}{\sqrt{\alpha}} \quad (32)$$

as the "thermal parameter" of importance and thence, if

$$\sum \gg \frac{\sqrt{3}}{2} \sqrt{\frac{-(\sigma + c_p)}{t^*} \cdot \frac{U_o^3}{L}} \quad (33)$$

boiling occurs. For many applications in naval hydrodynamics, we may imagine that the term  $-(\sigma + c_p)/t^* \approx 1$  so that Brennen's  $\sum$  function can be made dimensionless with the result that if the term

$$\sum_T \equiv \left( \frac{\rho_v}{\rho} \right)^2 \left( \frac{\zeta}{c_p T_\infty} \right)^2 \gg \frac{U_o^2}{c_p T_\infty} \cdot \frac{1}{\sqrt{\frac{U_o L}{\alpha}}} \equiv \frac{E_k}{\sqrt{P_e}} \quad (34)$$

boiling is said to occur. In this group of terms,  $E_k$  is the Eckert number, and  $P_e$  is the usual Peclet number, both familiar in heat transfer. An example, here, may illustrate the point. We consider water with reference speed of 10 m/sec and reference length of 3 cm to form Table 3.

TABLE 3 - COMPARISON OF THERMAL PARAMETERS FOR WATER  
 $U_o = 10$  m/s,  $L = 3$  cm

$T = 20^\circ C$	$260^\circ C$	$360^\circ C$
$\Sigma_T = 1.4 \times 10^{-9}$	$7 \times 10^{-4}$	$5 \times 10^{-3}$
$E_k / \sqrt{P_e} = 1.5 \times 10^{-6}$	$1.5 \times 10^{-6}$	$1.5 \times 10^{-6}$
→ Cavitation	Boiling	Boiling

We see then, that these thermal effects are not important for hydrodynamics, but may be for power machinery. Brennen (1973) includes comparisons with many other fluids, and concludes, interestingly, that liquid hydrogen almost always boils rather than cavitates.

### Scaling Ideas

With these results from bubble mechanics in hand the main features of travelling-bubble-inception scaling scenarios become apparent: A microbubble, or nucleus of some size, may be imagined to be swept through the low pressure region of a flow. The small nuclei have a very high natural frequency and so react quasi-statically to the imposed pressure change. It may happen that the critical pressure difference is exceeded for a certain freestream microbubble; then it follows that there will be a period of exponential growth which, if of sufficient duration, will ensure a visible macroscopic bubble. Indeed many workers (e.g., Johnson and Hsieh 1966, Schiebe 1972, Silberman 1975) are concerned only with that portion of the fluid flow at below the critical pressure, since the subsequent bubble growth is so rapid. There is an additional possibility that turbulent pressure fluctuations in transition locations may actually excite nuclei there to unstable growth by resonance. In any case, from such arguments it is evident that the number of travelling-bubble cavitation "events" will be proportional to the number of microbubbles that can grow exponentially or explosively; this then, depends upon the nuclei density distribution, the pressure difference ( $p_{\infty} - p_v$ ), and the particular body.

Inception for travelling-bubble cavitation, then, is determined by the rate of such events for a particular body. This concept of "event counting" as previously mentioned has been followed vigorously by the St. Anthony Falls Hydraulic Laboratory (e.g., Silberman 1975, Schiebe 1972). In fact, these authors turn the process around to infer the number density distribution,  $N(R)$ , by the number of such events on "standard" bodies. Apart from this, their measurements of events show impressive correlation with their acoustically determined nuclei distributions. These facilities contain many nuclei at the 100 micrometer level so that only a slight pressure difference ( $p_{\infty} - p_v$ ) is needed to establish criticality (see, e.g., Table 2). But travelling-bubble cavitation is rare in the Caltech HSWT, and tensions of up to 1/2 atmosphere are readily sustained in flows past bodies at minimum pressure points. From this we conclude that freestream

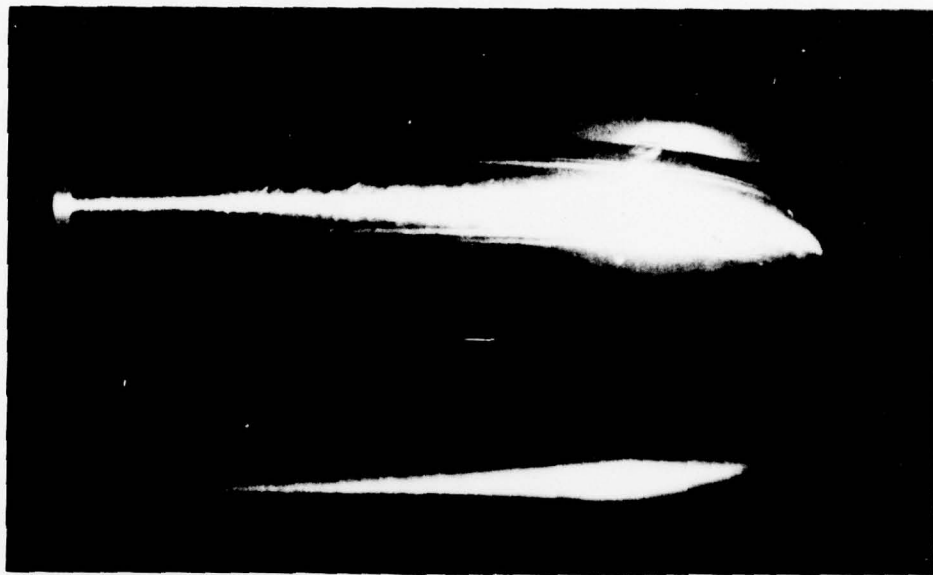
nuclei, larger than about 5 micrometers diameter, are not very abundant in this facility, a conclusion supported by the data of Figure 32. Furthermore, it points out that the range of sizes important in cavitation testing work should extend downwards at least that far.

There is, then, a direct influence of the nuclei density distribution on the rate of travelling-bubble cavitation events; when there are very few freestream nuclei, these events will of course be correspondingly few. And, as we have seen, appreciable tensions can be readily achieved, even in comparatively "dirty" tunnel water. From the physical evidence of tests in several tunnels, attached forms of cavitation may occur at inception even in the absence of laminar separation. Again, we return to the Caltech facilities in Figure 35 to show these different types of inception on identical test bodies. Not surprisingly, it was found that the inception indices differ markedly with travelling-bubble cavitation, showing the higher values (although still considerably below  $|-c_{p_{\min}}|$ ). In fact, in the HSWT there was a closer correlation with  $-c_{p_{\text{tr}}}$  than any other parameter (Gates and Acosta *ibid*). That attached forms of cavitation can sometimes occur first even on nonseparating bodies shows how difficult it is to have a single universal threshold measure of inception.

We can now recognize that a single kind of phenomenon that can lead to a uniform scaling law in cavitation inception does not occur. It is worthwhile, however, to draw together, in Table 4, the following "expectations" or trends in inception as we now understand it based on water tunnel tests (from Arakeri and Acosta 1979). It would be extremely valuable to extend these observations and even trends to prototype Reynolds numbers; this, however, must await a future day.

#### FULLY DEVELOPED CAVITATION IN INTERNAL FLOWS

We now leave inception to consider more developed states of cavitation. This is a subject for which vast literature exists. Our present purpose is, however, a more modest one; namely to consider developed



SCHIEBE BODY, LTWT, 24 ft./sec.  
D = 2 inches,  $\sigma$  = 0.52  
POLYOX INJECTION



SCHIEBE BODY, HSWT, 46 ft./sec.  
D = 2.0 inches,  $\sigma$  = 0.41, S/D = 0.47

Figure 35 - Cavitation on the Same (Schiebe) Body in the Caltech LTWT and the Caltech HSWT (Gates and Acosta 1978)

TABLE 4 - TYPES OF CAVITATION INCEPTION PHENOMENA

Nuclei Supply	Type of Flow on Body	Expected Inception Forms
CPIOUS	No Separation	Travelling bubble from $c_p$ (e.g., Silberman 1975). Event counting. $\sigma \leq -c_p p_{\min}$
CPIOUS	Laminar Separation	Mixed travelling-bubble and band cavity (sometimes fore stalled by myriads of bubbles)
FEW	No Separation	Attached cavities, $\sigma \approx -c_p p_{tr}$ (Arakeri et al.), wedges, fingers, patches often seen up to position of $c_p p_{\min}$
INTERMEDIATE	No Separation	Travelling-bubble cavitation/ attached forms, (e.g., Huang and Santelli 1977) $\sigma \approx -c_p p_{tr}$
INTERMEDIATE AND FEW	Laminar Separation	Band and sheet cavities. Glassy leading edges $\sigma \approx -(c_{p_s} + \Delta c_p(t))$ (e.g., Huang and Peterson 1976).

NOTE: Desinent cavitation and gaseous inception are not included.

cavitation in internal flows. These are the flows that take place in water tunnels, fluid machinery, and the duct flows of various types that arise in large hydraulic systems and the propulsion systems of ships (see, e.g., Narita and Kunitake 1977, Yamaguchi 1977). As in cavitation inception, different forms of developed cavitation occur, and for internal flows it is convenient to lump them into three types, as in Table 5:

TABLE 5 - TYPES OF INTERNAL FLOW CAVITATION

1. Attached two- and three-dimensional surface cavities.
2. Tip-vortex and tip-clearance flow cavitation.
3. "Bubbly" cavitation and two-phase flow.

Although all of these forms are commonly seen in water tunnel tests, type 2 is most often associated with flow in fluid machines, such as a propeller or pump. Often the tip-clearance flow in a pump is sufficiently strong to cause a significant "backflow" resulting, thereby, in a very complex inflow to the pump.

Attached cavity flows have, of course, received much attention because of the powerful analytic tools that can be brought to bear, as well as the intrinsic importance of these flows (see, e.g., Wu 1972). These same techniques may be used to explain tunnel-caused effects in steady flow which may be termed "wall effects" (see, e.g., the review by Baker 1977). When the void fraction of liquid-gas-vapor flows is appreciable it is customary to call these "two-phase flows" (see, e.g., the text by Wallis). Indeed, much effort has been, and is being, expended on this subject as it is a key issue in the understanding of the thermo-hydraulics processes in nuclear power plants. But many cavitating flows in naval hydrodynamics consist of dispersed cavitation bubbles in which the void fraction is well below one percent and these flows we may term bubbly cavitation. This kind of cavitation is common, even dominant, in cavitating pumps and, as we have seen, is also a highly visible feature of some water-tunnel flows.

A special feature of internal flows with cavitation is the coupling of the fluid motion in various parts of a system by the displacement of a changing volume of cavitation. This unsteadiness may arise deliberately as a part of a test procedure (e.g., a study of propeller-wake interaction), or it may happen that the cavitation itself is inherently unsteady. (Partial cavitation of about three-quarters chord length provides such an example.) Because of the coupling of the flow with unsteady cavitation, there is an interaction between the internal flow circuit and the basic flow past the cavitating body itself. This interaction may, in fact, so control the whole process that the original basic flow may be entirely masked (as for example in an unsteady hydrofoil test). The confining effect of a tunnel has been in fact a serious deterrent to measurement of unsteady forces on cavitating hydrofoils in the past. We need ways, then, to correct for the "unsteady" internal effect, as well as for the better-understood steady wall effect.

It may happen that, because of cavitation and circuit-cavitation interactions, an inherently steady or stable cavitation flow may exhibit self-excited oscillations. Such oscillations occur frequently in pump applications or in more complex systems, such as pump-fed liquid fueled rocket. This is the basis of the notorious "Pogo" longitudinal oscillations of large liquid booster rockets. In fact, some of these Pogo oscillations have reached acceleration levels of 50 g's\* and it is customary for all liquid fueled rockets to suffer some extent of this instability. Cavitating pumps are usually thought of primarily in connection with space applications. However, the types of designs and performance demands of modern high-speed naval craft, such as the PHM hydrofoil and surface effect ship propulsion systems, are very similar to those for large booster propulsion. But it is not necessary to go so far afield to find situations where unsteady cavitation-system coupling presents a problem of interpretation. A good example is afforded by the unsteady hull pressure-propeller cavitation measurements of Keller and Weitendorf (1970). In their tests, the pressure at several points on a wall adjacent to a cavitating propeller was measured in a closed tunnel as a function of

---

\*Dr. S. Rubin, Aerospace Corp.

undissolved void fraction ( $10^{-7}$  to  $10^{-4}$ ). The pressure was found to vary strongly with both frequency and void fraction when operating in a non-uniform wake except at very high void fractions ( $10^{-4}$ ) where the results appeared to be independent of frequency. These interesting observations show, again, the importance of the presence of microbubbles on the extent of cavitation, and they raise the question of tunnel interaction through the confining effect of the surrounding walls on a dynamic experiment.

We turn, now, to the immediate objectives of the present section. We first touch upon the available analytic methods that can be used to estimate these interaction effects for the types of cavitation mentioned, and we then discuss some recent experimental work aimed at characterizing unsteady flows through cavitating pumps.

#### Analytic Methods for Internal Cavitation

We refer now, briefly, to Table 5 for the types of cavitation to be considered. We are concerned here, primarily, with unsteady problems. It is clear from previous experience that attached unsteady cavities can be dealt with on the basis of linearized potential flow (Wu 1972). There are, however, still difficult problems for the proper formulation of unsteady, growing, attached cavities with realistic geometries. The tip vortex flow is also complex; dynamic treatment of these flows appear to be lacking. Pumps and propellers reveal attached cavities, as well as bubbly tip-clearance flows and inflows. The global properties of a volume of such bubble flow can be established with bubble mechanics for unsteady pressure fluctuations. But the concentration of bubbles in such flows must be small, otherwise the full two-phase fluid dynamic equations for the mixture of cavitating bubbles and liquid must be used. These equations are evidently not yet well developed analytically.\*

In the following sections, we sketch a sample problem intended to illustrate some of these dynamic features for a pump.

---

\*Private communication with Prof. L. van Wijngaarden.

### The Coupling Problem for a Pump

We sketch the blades of an axial inducer together with the types of cavitation in Figure 36. We imagine that the upstream pressure and inlet velocity are fluctuating. We anticipate that the outlet quantities of the pump will similarly fluctuate. There is upstream structure and downstream structure to input and receive the unsteady flow through the pump. Our coupling problem here is to provide the effect due to the insertion of the pump or other cavitating device on these up and downstream flows. It is natural, then, to think of the pump as having a "transfer function" whereby periodic input disturbances are connected to output ones. An extended system can then be treated by connecting its various transfer functions appropriately. In what follows, some components of such a transfer function are estimated from the standard reference problem in turbomachinery analysis, the flow through a cavitating cascade. The flow model is that of an attached blade cavity with a fluctuating axial inlet flow velocity. The cavity is assumed to be at constant pressure; its boundaries and volume change in some relationship to the inlet flow perturbations. To focus on the effects of cavitation, the wetted part of the cascade is taken to be infinitely long. This representation, at first sight, highly artificial, is actually a good one for the partial cavitation within the inducer portions of cavitating pumps. A sketch of the cascade is given in Figure 37a and linearized boundary conditions in Figure 37b. This linearized boundary value problem implicit in Figure 37b is capable of formal solution in an auxiliary plane where the entire blade and cavity geometry appears on the real axis by the methods outlined in Wu's review. We need not concern ourselves herein with these details except for several basic features of the solution. There must be a fluctuating pressure gradient approaching the cascade because of the fluctuating inflow velocity. There will be a similar fluctuating downstream pressure gradient, possibly with a different amplitude and phase, because of the changing cavity volume. We can anticipate that the actual pressure will be of the form

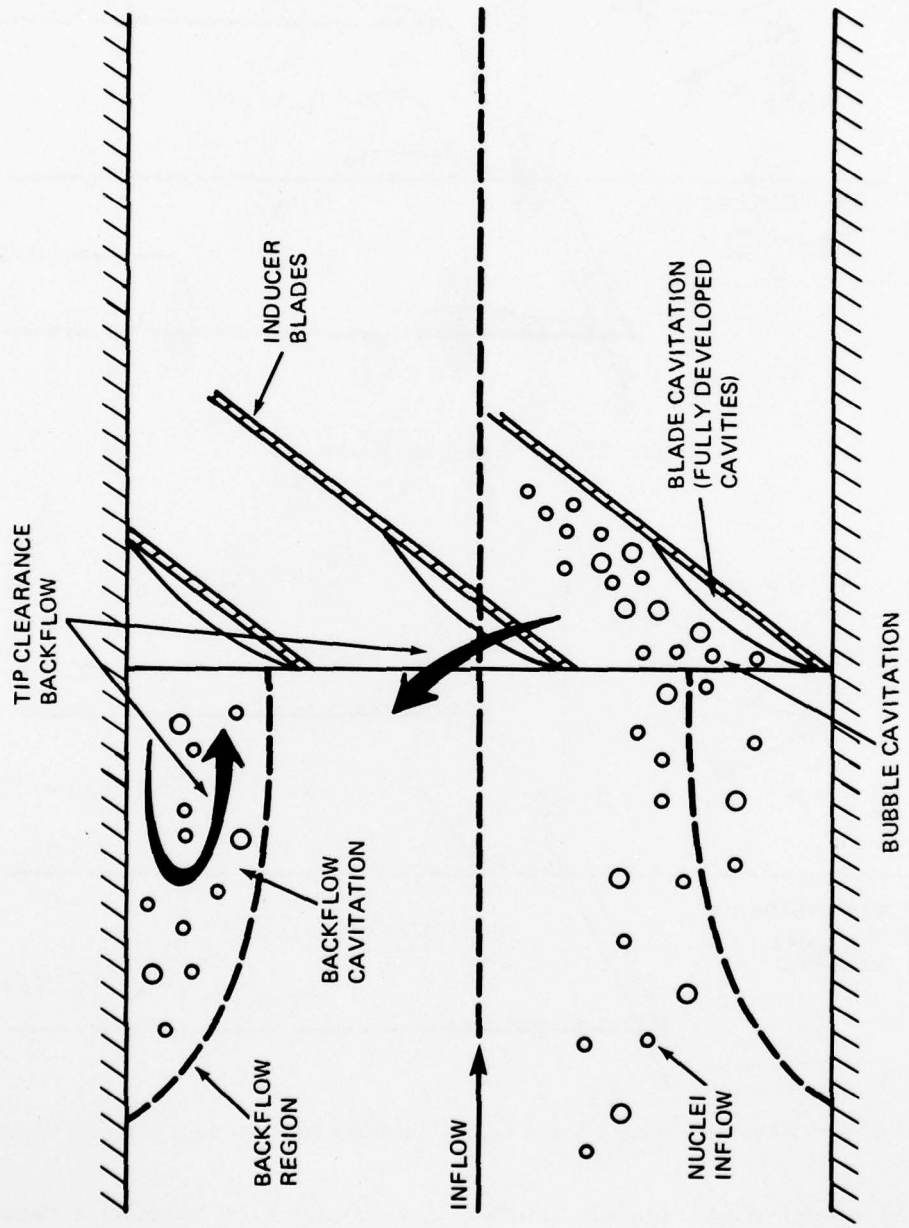


Figure 36 - Forms of Cavitation in an Inducer Pump Blade Row

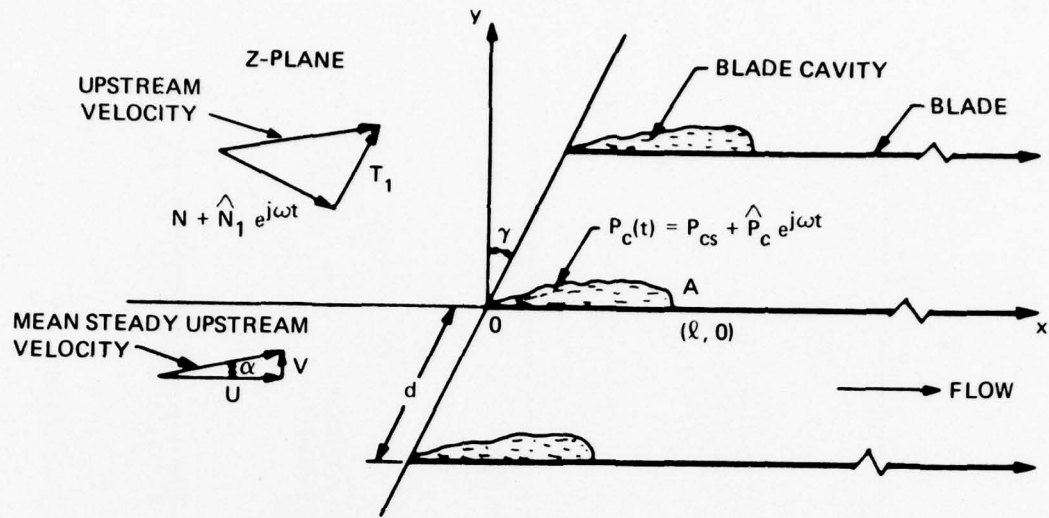


Figure 37a - Physical Plane

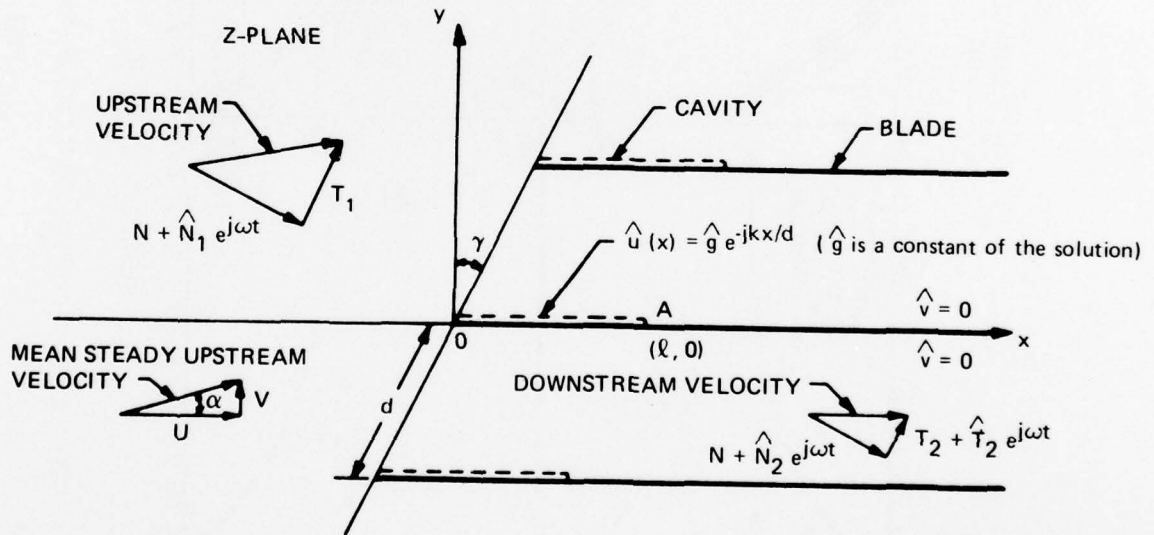


Figure 37b - Mathematical Plane (with linearized boundary conditions)

Figure 37 - Representation of Unsteady Cavitating Flow Through a Cascade of Inducer Blades Together with Linearized Boundary Conditions  
 (Kim and Acosta 1975)

$$p \rightarrow -j\omega\rho\hat{u}_1xe^{j\omega t} + \hat{p}_1e^{j\omega t} + p_{1s} \quad (35)$$

upstream and

$$p \rightarrow -j\omega\rho\hat{u}_2xe^{j\omega t} + \hat{p}_2e^{j\omega t} + p_{2s} \quad (36)$$

downstream. Here  $\omega$  is the frequency,  $j$ , the imaginary unit of time,  $u_1$  and  $u_2$ , the fluctuating velocities in Figure 37b, and  $x$ , the distance along the chord. The first term may be seen to be the pressure gradient due to the "mass oscillations" of the up and downstream flows. The terms  $p_{1s}$  and  $p_{2s}$  are the steady pressures across the cascade in the absence of motion, and  $\hat{p}_1$  and  $\hat{p}_2$  are the additional complex fluctuating pressures caused by the presence of the cascade.

These additional pressures are what are needed to account for the insertion of the cascade between the up and downstream flow regions. It turns out that these additional pressures can be simply related to the unsteady axial fluctuations by a linear equation of the form

$$\begin{pmatrix} \hat{p}_2 - \hat{p}_1 \\ \hat{N}_2 - \hat{N}_1 \end{pmatrix} = [z] \begin{pmatrix} \hat{p}_1 \\ \hat{N}_1 \end{pmatrix} \quad (37)$$

where  $z$  is a  $2 \times 2$  matrix with complex coefficients. This matrix, we can now see, is the transfer function for the cascade. Before discussing some of the terms of this transfer function, we need to mention some of the difficulties in finding practical evaluations of the implied formal solution.

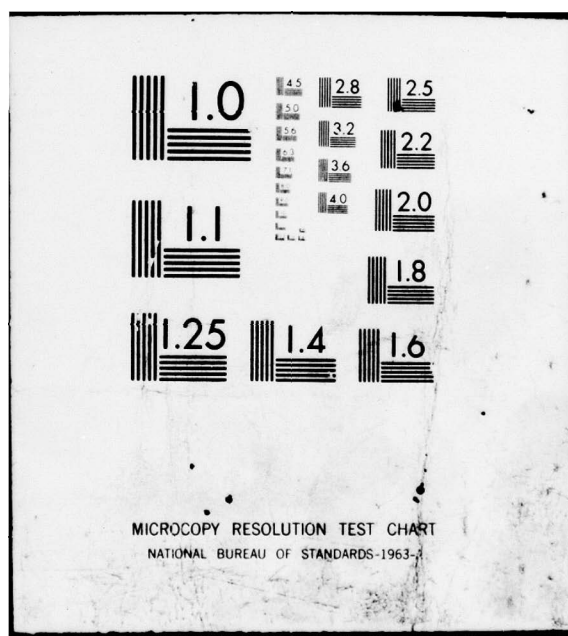
Even in the linearized free streamline theory, we need to be concerned about the physical significance of the cavity model. It has become acceptable to think of steady flow cavity models as having an ultimate "wake" to account for the momentum deficiency of the cavitating drag. Unsteady cavitation models have not, however, received as much attention.

AD-A075 893 DAVID W TAYLOR NAVAL SHIP RESEARCH AND DEVELOPMENT CE--ETC F/G 20/4  
CAVITATION INCEPTION AND INTERNAL FLOWS WITH CAVITATION. THE FO--ETC(U)  
OCT 79 A J ACOSTA  
UNCLASSIFIED DTNSRDC-79/011

2 OF 2  
AD  
A075893

NL

END  
DATE  
FILED  
11-79  
DDC



In water tunnels, we observe that attached cavities grow and shrink in response to system pressure changes. To the eye, at least for slow changes, the cavity appears to be a closed body of changing shape and length. It is actually a material surface. In the linear theory the coordinate,  $Y$ , of the end of the cavity, is

$$Y(t) = \int_0^{\ell(t)} \frac{v}{U_o} \left( \xi, t - \frac{\ell(t)}{U_o} + \frac{\xi}{U_o} \right) d\xi \quad (38)$$

where  $\ell(t)$  is the fluctuating end of the cavity,  $v$  is the perturbation velocity component normal to the cavity, and  $U_o$  is the reference speed. For steady flows,  $Y = 0$  is Tulin's closed cavity model;  $Y \neq 0$  corresponds to an open wake model. For unsteady flows, Equation (38) is actually quite a difficult integral to evaluate, even in simple flows. Most of these problems were foreshadowed by Parkin's work on unsteady hydrofoils (Parkin 1957). As it has turned out, most work in the field since then has avoided direct use of Equation (38), and, because of these formal difficulties, other approaches have been adopted. Among these, two are well-known;\* Guerst permitted no change in cavity volume, whereas Leehey assumed that the end of the cavity remained at its steady value (thereby circumventing Equation (38)), but allowed the cavity volume to change. This approach was also used later by Kim and Acosta (1975) to evaluate the terms of the transfer matrix,  $z$ . Still, this seemed not entirely a satisfactory resolution because it was clear that very slow oscillations should approach known "quasi-steady" values, wherein, the actual changes in cavity length that are seen, are properly modeled. It has been shown more recently (Acosta and Furuya) that application of Equation (38), with  $Y = 0$  for small frequency, does, in fact, lead to the quasi-steady limit of Tulin's closed cavity model. It was also shown that the fixed-terminus cavity model for unsteady flow had a rather unnatural singular behavior of one of the coefficients of  $z$ . To appreciate this we now need to comment on each of the terms of the cascade transfer function  $z$ .

---

\*Refer to the review by Wu for details.

### The Transfer Function

The sample problem of this section is in the form of the flow across a moving cascade. The static pressure rise across such a cavitating cascade is a function of the upstream pressure and the upstream flow velocity. In the absence of fluid losses, an infinitely long cascade has no change in pressure rise with inlet pressure for a steady flow. An unsteady flow is a different matter, however, and the component,  $z_{11}$ , may not be expected to be zero. The fluid losses in steady flow are due primarily to mixing caused by the drag due to cavitation. This "momentum" loss increases with decreasing pressure, and thus, we may expect quasi-steady cascade experimental data to show a positive value of  $z_{11}$ . Pump cascades, as sketched in Figures 36 and 37, create a static pressure rise through diffusion of the relative velocity. This pressure rise decreases with increased axial speed (and thereby reduced angle of attack) so that on a quasi-steady basis we may expect the term  $z_{12}$  to be negative, i.e., a fluctuating increase in flow should result in a fluctuating decrease in pressure rise. Additional complex terms may be expected in unsteady flow.

We have repeatedly focused attention on the volume change of cavitation with pressure; the rate of volume change is seen to be proportional to the differences of down and upstream speed across the cascade. From experience with steady cavitating flows, we expect the volume of cavitation to increase with a decrease in upstream pressure, and to increase with an increase of angle of attack or a decrease in inlet flow velocity. We expect that, for vanishing frequency, the terms  $z_{21}$  and  $z_{22}$  will both be negative and imaginary, and proportional to frequency, as this is the appropriate behavior in the quasi-steady limit. The term  $z_{21}$  is of particular interest; it is related to what has been termed the "compliance" by hydraulic system analysts. The compliance is the negative rate of change of cavity volume with pressure. In fact, in dimensional units,  $z_{21}$  is equal to the negative of this compliance times  $j\omega$  divided by the pump inlet area. It is an important system parameter, since the period of an inlet pipe line oscillation is proportional to the square root of the

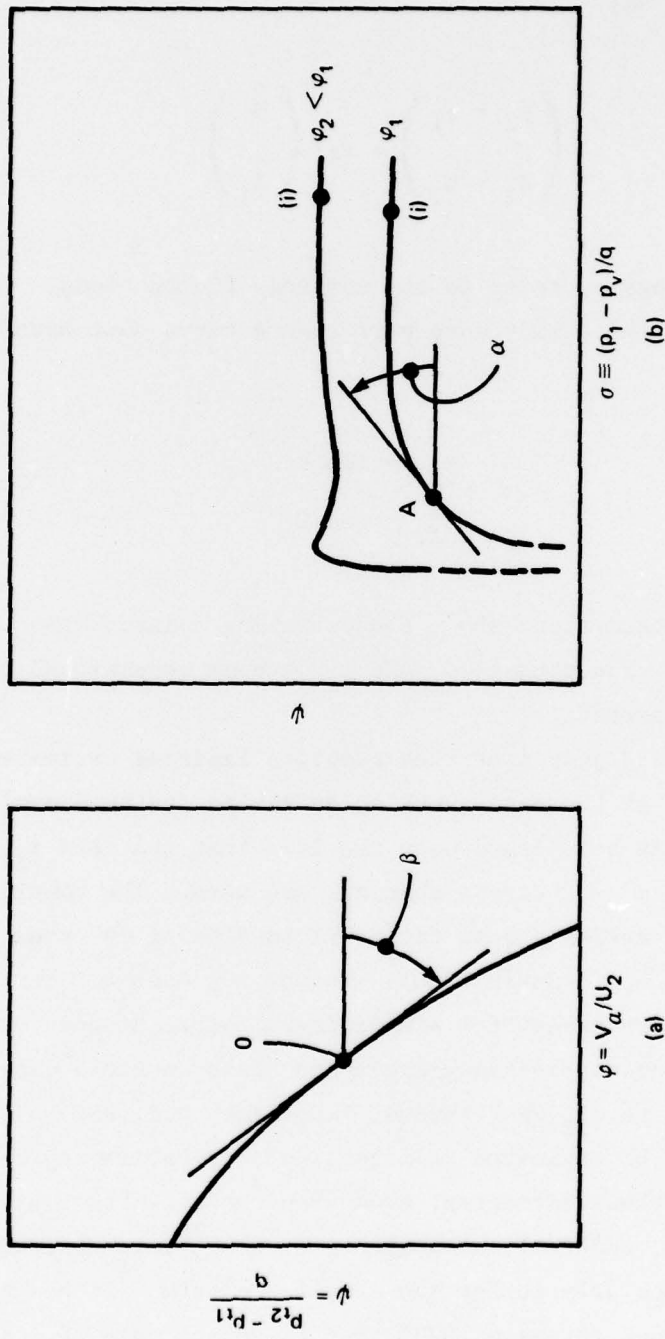
compliance times the inertance of the inlet line. It is the compliance that becomes singular for the fixed-terminus cavity model, thereby showing this model to be unsuitable for an unsteady internal flow.

Thus far, in discussing unsteady flow interactions, we have focused on the cascade idea. This was, primarily, because the natural form of the solution led immediately into the transfer function description, more common in system analysis. As mentioned in Table 5, not all flows of interest are attached cavity flows; in fact, these may not be, dynamically, the most important forms. Observations of some pump inflows reveal a significant number of microbubbles. These undergo growth and collapse histories within the impeller which are modified by the fluctuating inlet pressure. The "compliance" of a stream of microbubbles undergoing such a growth and collapse process can be determined from bubble mechanics. This is, in fact, what Brennen, in a most influential paper, has carried out in great detail (Brennen 1973), using, for want of a better choice, microbubble distributions derived from water tunnel measurements. The results are most interesting in that the response of individual bubbles shows that the compliance slowly decreases from its quasi-static value as frequency increases with a gradually increasing phase lag. Thus, in the present notation,  $z_{21}$  becomes complex with increase in frequency. We defer these interesting results for comparison later with cavitating pump applications.

#### Application to Pumps

Pump engineers, historically, have carried out two types of steady tests; namely, a performance test in which the (total) pressure difference at fixed rotative speed is measured as a function of flow rate, and then, a cavitation test in which the pressure rise at fixed speed and flow rate is measured as a function of inlet pressure. It is customary to normalize the total pressure rise by the quantity  $(q)$ , and the inlet pressure by  $(q)$ , where  $q$  is the dynamic pressure based on tip speed. The axial inlet velocity is normalized by the tip speed (different, thereby, by  $\pi$  from the advance ratio of propellers). Curves, representative of the performance of real pumps, are sketched in Figure 38. From our previous discussion of

Figure 38 - Pump Performance Curves



unsteady flows across cavitating pump cascades, we can see that a plausible form of the transfer function for a pump would be (with reference to the notation of Figure 38)

$$\begin{pmatrix} \hat{\psi}_2 - \hat{\psi}_1 \\ \hat{\phi}_2 - \hat{\phi}_1 \end{pmatrix} = [z] \begin{pmatrix} \hat{\sigma} \\ \hat{\phi}_1 \end{pmatrix} \quad (39)$$

the circumflexes, again, refer to the unsteady fluctuations. In the limit of zero frequency, the steady pump performance curve must have the result that

$$\begin{aligned} z_{11} &\rightarrow \tan \alpha \\ z_{12} &\rightarrow \tan \beta \end{aligned} \quad (40)$$

for infinitesimal excursions about the operating point. When the frequency is not zero we may expect that  $z_{11}$  and  $z_{12}$  become complex and that  $z_{21}$  and  $z_{22}$  will become important

The steady state pump test then provides limiting estimates of  $z_{11}$  and  $z_{12}$ . Much of the early work on hydraulic system dynamics involving cavitating pumps has been based upon the idea that the term  $z_{21}$  is precisely a "compliance" effect and that  $z_{22}$  was zero. The compliance was then determined by making a best fit to field data of observed system oscillations (see, e.g., Rubin 1966). It was, of course, not necessary to assume  $z_{22}$  to be zero except for simplicity. Later, Brennen et al., (1976) showed from limiting quasi-steady arguments based on field data, that the term corresponding to  $z_{22}$  was, indeed, important, and that this term, as well as  $z_{21}$ , could be estimated from quasi-steady cavitating cascade theory. As it turned out, these estimates, even when the effects of blade thickness were included, underestimated the results of field observations by a fair amount, particularly so for the compliance term. It had been shown previously by Brennen (Brennen 1973) that the compliance effect due to

travelling microbubbles alone could account for much of the observed behavior. We reproduce here in Figure 39 his summary results using the water-tunnel derived estimates of microbubble populations. Plainly although much remains to be learned about the cavitating environment of these flows, bubbly cavitation is evidently an important factor in them. From all of this work, it was clear that new experimental methods had to be devised to measure the transfer function of a pump.

#### Experiments in Unsteady Pump Dynamics

There has been growing concern by many workers with the proper representation of unsteady pump characteristics. We may mention, for example, the work of Kolesnikov and Kinelev (1973), Fanelli (1972), and Black and Santon (1975), who are all concerned in various respects with this problem. Experimental work is comparatively rare, however. Among the first of these is that of Ohashi (1968) and later Anderson et al. (1971), who carried out experiments on oscillating flow in fully wetted pumps. There, in principle, only the term  $z_{12}$  needs to be measured; this, of course, greatly simplified measurement demands. Rather similar problems have encroached into related fields of naval hydrodynamics, namely the response of lift fans of surface effect vehicles to periodic disturbances. There too, a transfer function approach is taken (Durkin and Luehr 1978). Durkin and Luehr did not carry out measurements of the transfer function itself, but based their conclusions, as did earlier workers, on lumped parameter system model tests. It would appear that the first direct attempt to measure the transfer function of a cavitating pump system is due to Ng (1976). The problem, as described there, is to determine the eight unknown coefficients of the transfer matrix  $[z]$  of Equation (39) from measurements of fluctuating inlet and outlet pressures and volumetric flow rates. Any given hydraulic system with a fixed method of excitation will produce a unique relation between input and output quantities, thereby providing insufficient data to determine  $[z]$ . The solution devised by Ng was to provide two sources of excitation to a test loop, these sources being locked in phase, but separated by an isolation section. Then, with

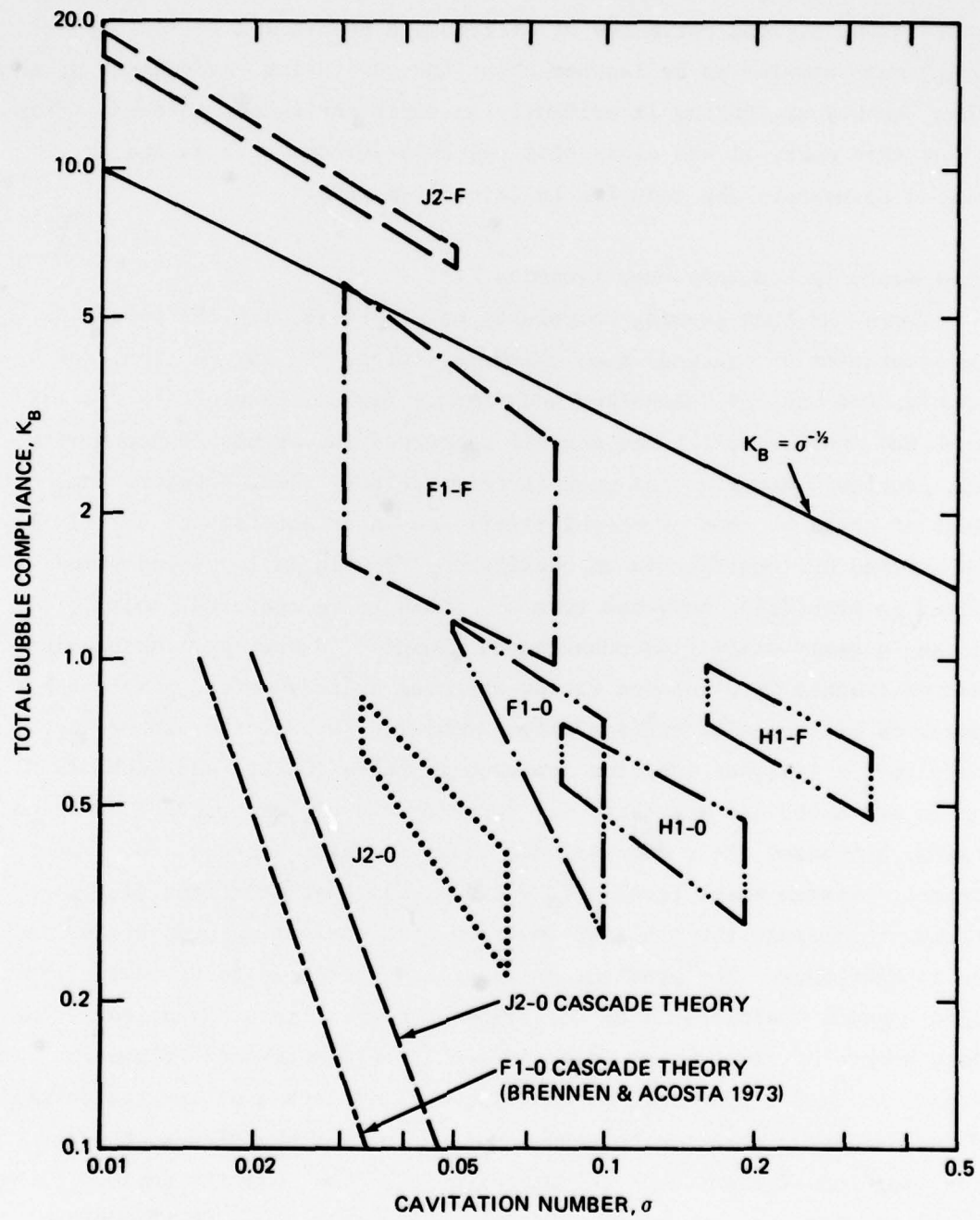


Figure 39 - Cavitation Compliance  $K_B$  Estimated from Microbubble Populations  
Measured in Water Tunnels versus Cavitation Index (Brennen 1973)

fixed operation parameters, variation of the phase between the sources provides the additional sets of relations needed to find  $[z]$ . In practice combinations of phase and amplitude were used. The excitation consisted of a "siren" like valve which provided a variable hydraulic resistance to the flow circuit.

Another notable feature of the Ng experiments was the use of laser velocimetry to measure up and downstream flows. This necessitated certain flow smoothing and conditioning not common in hydraulic circuits. These experimental features are shown in Figure 40, and an example of some of the first experimental results are shown in Figure 41 (Ng et al. 1976).

This rather involved figure shows two sets of data, one basically noncavitating and the other cavitating. The noncavitating results show that the terms  $z_{11}$ ,  $z_{21}$ , and  $z_{22}$  are small; in the absence of cavitation and elasticity of the fluid and supporting structure, and experimental error, these terms should be strictly zero. The term  $z_{12}$  is seen to have a negative real part. This corresponds fairly well to the slope of the total head performance curve, the angle  $\beta$  of Figure 38a, but shows some change with frequency. The term  $z_{12}$  also has an imaginary part which is equivalent (within experimental accuracy) to the inertia of a certain length of fluid. The fully wetted data are rather as expected.

The cavitating transfer function is, however, quite different. As our touchstone, the slope of the performance curve decreases (in magnitude) at higher frequency and the inertance part practically vanishes. We may mention that the cavitation number,  $\sigma = 0.046$ , results in a condition of extensive cavitation in the inducer portion of the pump. There is attached blade cavitation, but the extensive cavitation seen under strobe illumination is due primarily to bubbly-cavitating tip-clearance flows (see Figure 41). This extent of cavitation is a normal condition of operation for many inducer pumps. We see some change in the customary pressure rise-flow characteristic ( $z_{12}$ ) due to cavitation. But there are more important and striking changes in the other terms of the transfer function; the term  $z_{11}$ , for example, exhibits a large change with frequency, both in

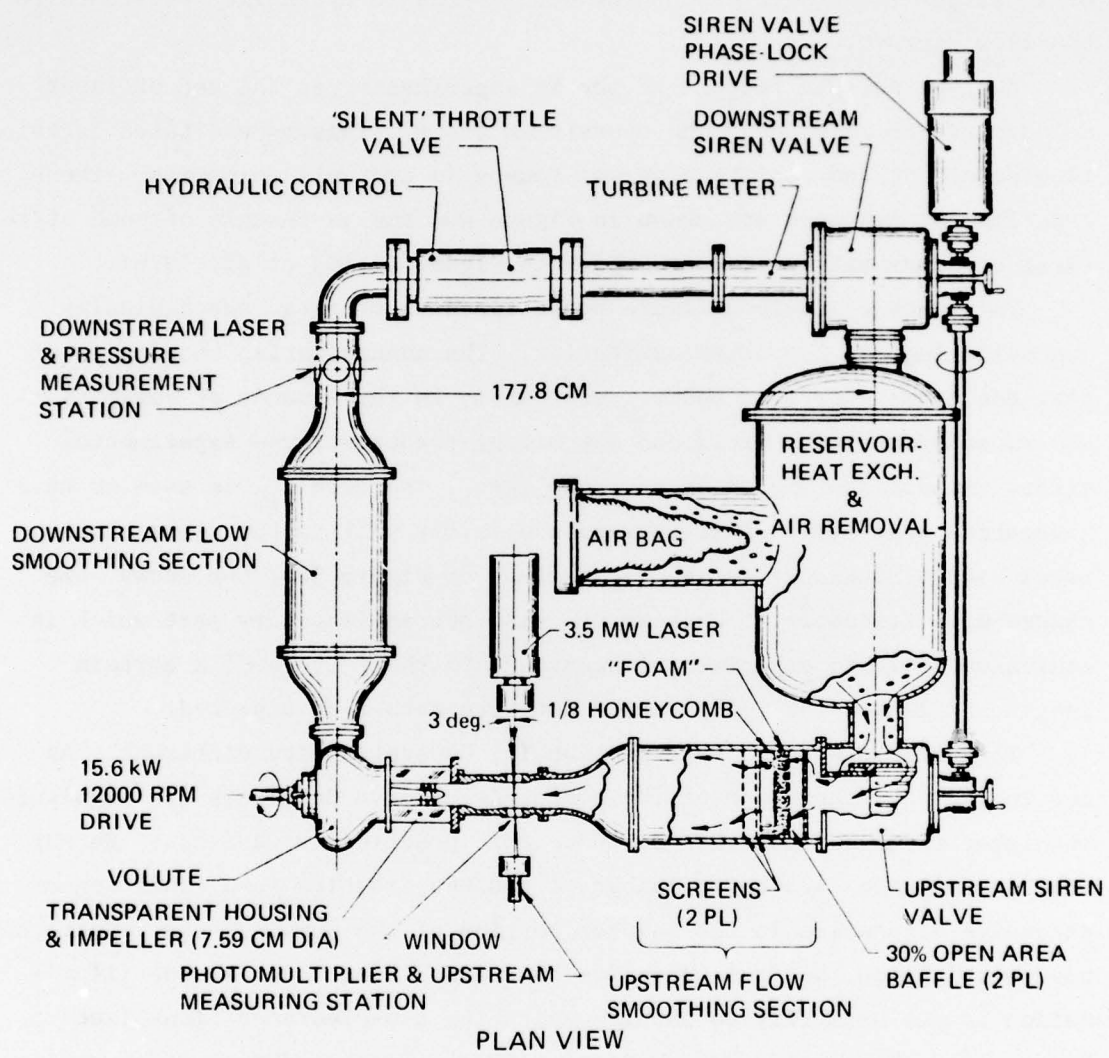


Figure 40 - Test Loop for Dynamic Transfer Function Measurement  
(Ng 1976)

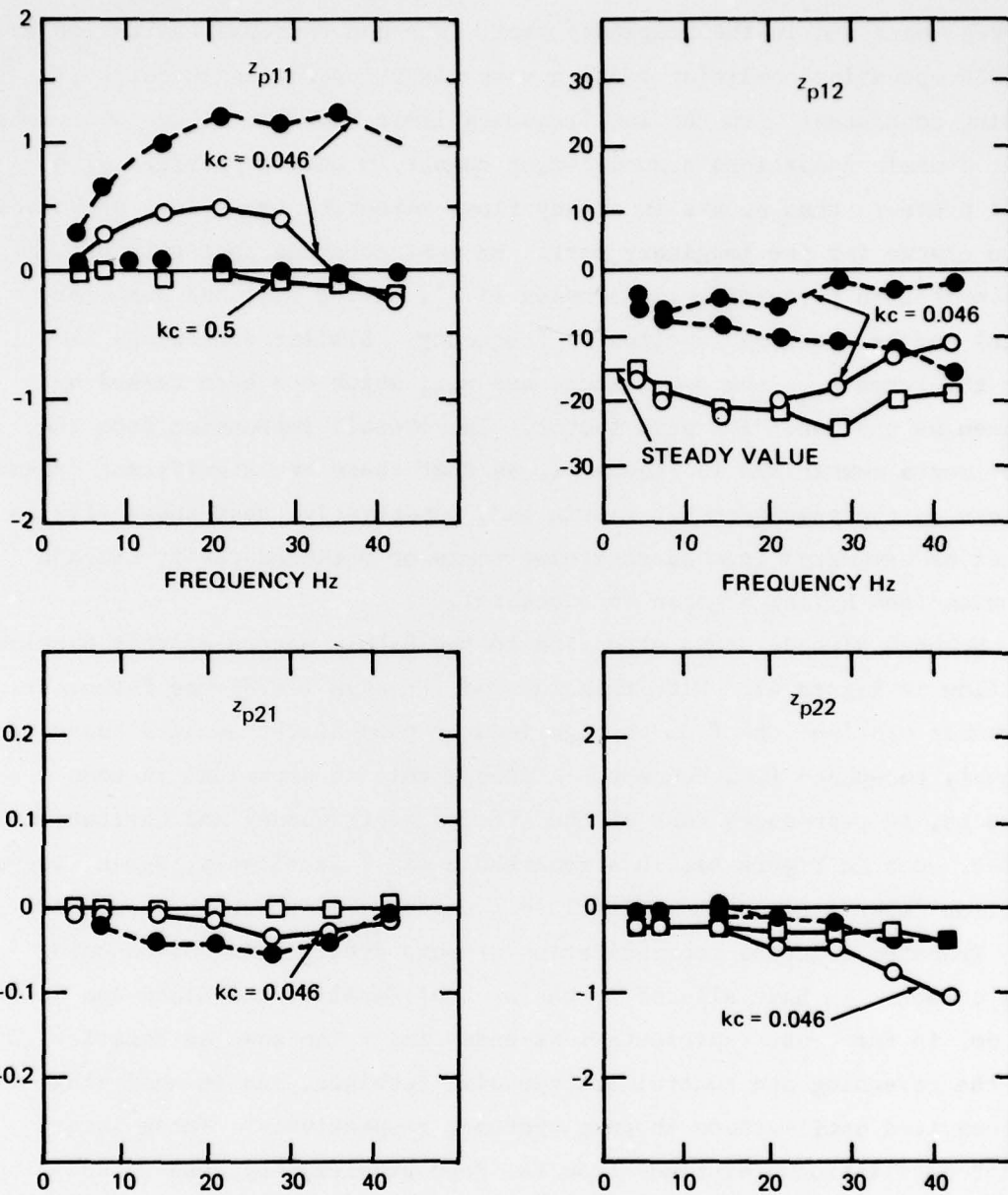


Figure 41 - Transfer Function for an Axial Inducer Pump at a Flow Coefficient of 0.07 (Inlet Value) (The value of the total pressure coefficient is about 0.50. The inducer consists of four cambered blades having a tip inlet angle of 7 degrees followed by 12 more heavily loaded tandem blades. The real part of the coefficients are shown solid and the imaginary dotted. Two sets of data are shown, fully wetted and for a cavitation index  $\sigma = 0.046$ .)

the real part and in the imaginary part. The conventional cavitation test at this operating condition shows a very slight reduction in output, a finding consistent with the low frequency limit shown in Figure 40. We see under dynamic conditions a much larger change in output pressure with inlet pressure than occurs in steady flow; moreover, there is a pronounced phase change for the imaginary part. We must conclude that this part of the cavitation performance is complex (i.e., having real and imaginary parts) and is a strong function of frequency. Similar deductions flow from the terms  $z_{21}$ , the compliance, and  $z_{22}$ , which has been termed by Brennen as the mass-flow gain factor. The overall impression from the experiments summarized in Figure 41, is that there are significant dynamic effects in the pump transfer matrix and, importantly, that these effects cannot be estimated from quasi-steady tests or attached cavity cascade theories (see Ng and Brennen for details).

We have already drawn attention to the bubbly nature of this particular flow in Figure 42. With this in mind, Brennen (1978) has formulated a dynamic model of the flow through inducer pump blade channels based upon a bubbly two-phase flow concept. Although this is empirical in some respects, it reproduces most of the effects of frequency and cavitation number, seen in Figure 41, in a remarkable way. Inevitably, again, the void fraction depends upon some initial (but unknown) microbubble population.

Transfer function representation of pump dynamics is now becoming more common. We have alluded to the work of Fanelli, and Black and Santos who do, in fact, use representations essentially the same as Equation (39) for the governing and control of hydraulic turbines, and in analyzing self-excited oscillations in pump systems, respectively. These later "auto"-oscillations (distinct from the Pogo problem) may lead to damaging levels of pressure fluctuations. The onset of such oscillations in a dynamically characterized hydraulic test loop has been shown recently to depend on the measured pump transfer function (Braisted and Brennen 1978). More importantly, Brennen (1978) has argued that the transfer function itself cannot be represented simply by a collection of passive elements such as compliance, resistance, and inertance, i.e., the conventional lumped parameters often used in analysis of mechanical linear systems.

Figure 42 - Cavitation in the Pump of Figure 41 at the Cavitation Index of  
 $\sigma = 0.040$



We conclude here, our discussion of cavitating internal flows; the field remains extremely active because of the thermo-hydraulic problems associated with nuclear power plants. We have stressed application of these internal flows to pumps because of the relative simplicity of the representation and because of the inherent importance of the subject. As we have seen there are somewhat analogous problems in naval hydrodynamics. Some of these are due to geometric confinement, such as in the testing of unsteady cavitating flows in water tunnels, and others have their common origin in the liquid environment itself.

#### SUMMARY

It has been nearly ten years since "Cavitation State of Knowledge" has appeared. Since then, many new lines of research have appeared and some older ones refined. There is now a much clearer understanding, than formerly, of the role of the viscous boundary-layer flow on smooth bodies in cavitation inception. Similarly, the necessity of carefully describing the form and extent of cavitation, both at its onset and developed states for the formulation of realistic physical models, seems well appreciated. New experimental techniques, including the measurement of freestream cavitation "nuclei," have appeared; these promise to put laboratory and field studies of cavitation on a new quantitative level. The presently available cavitation-inception scaling concepts are considerably improved and more physically based than formerly. With all these new advances it is still not possible to predict with certainty the location, form, and onset conditions required for cavitation in an arbitrary flow. This is particularly so for unsteady cavitating flows. These flows, in addition, because of the volume change of the cavitation itself, may experience large unsteady interactions with neighboring surfaces or flow fields. Initial attempts at sorting out these mutual effects for certain well-defined hydraulic systems have met with some success. As our observational and methodological techniques improve, there is every reason to believe that our understanding of unsteady cavitation phenomena will continue to improve, just as it has for cavitation-inception processes.

ACKNOWLEDGMENT

The preparation of this manuscript was made possible through funds from the David W. Taylor Naval Ship Research and Development Center and the Office of Naval Research. This support is gratefully acknowledged.

#### BIBLIOGRAPHY

Acosta, A.J. and B.R. Parkin, "Cavitation Inception--A Selective Review," *Journal of Ship Research*, Vol. 19, No. 4, pp. 193-205 (1975).

Acosta, A.J. and O. Furuya, "A Brief Note on Linearized Unsteady, Super-cavitating Flows," *Journal of Ship Research*, Vol. 23, No. 2, pp. 85-88 (1979).

Albrecht, K. and O. Bjorheden, "Cavitation Testing of Propellers in a Free Surface Tunnel Using Micro Bubble Control," in "Cavity Flows," B.R. Parkin and W.B. Morgan (Eds.), American Society of Mechanical Engineers Symposium, Minneapolis (1975).

Anderson, D.A. et al., "Response of a Radial-Bladed Centrifugal Pump for Sinusoidal Disturbances for Non-cavitating Flow," National Aeronautics and Space Administration TN-D-6536 (1971).

Arakeri, V.H., "Water Tunnel Investigations of Scale Effects in Cavitation Detachment from Smooth Slender Bodies and Characteristics of Flow Past a Bi-Convex Hydrofoil," Division of Engineering and Applied Science Report E 79A12, California Institute of Technology (1971).

Arakeri, V.H., "Viscous Effects in Inception and Development of Cavitation on Axi-Symmetric Bodies," Ph.D. Thesis, California Institute of Technology, also Division of Engineering and Applied Science Report E 183-1 (1973).

Arakeri, V.H., "Viscous Effects on the Position of Cavitation Separation from Smooth Bodies," *Journal of Fluid Mechanics*, Vol. 68, Part 4, pp. 779-799 (1975a).

Arakeri, V.H., "A Note on the Transition Observations on an Axi-Symmetric Body and Some Related Fluctuating Wall Pressure Measurements," *Journal of Fluid Engineering*, Vol. 97, Ser. I, No. 1, pp. 82-87 (1975b).

Arakeri, V.H. and A.J. Acosta, "Viscous Effects in the Inception of Cavitation on Axisymmetric Bodies," *Journal of Fluid Engineering*, American Society of Mechanical Engineers, Vol. 95, Ser. I, No. 4, pp. 519-528 (1973).

Arakeri, V.H. and A.J. Acosta, "Some Transition and Cavitation Inception Observations on a 1.5 Cal Ogive," 17th American Towing Tank Conference, California Institute of Technology (Jun 1974).

Arakeri, V.H. and A.J. Acosta, "Cavitation Inception Observations on Axisymmetric Bodies at Supercritical Reynolds Numbers," Journal of Ship Research, Vol. 20, No. 1, pp. 40-50 (1976).

Arakeri, V.H. and A.J. Acosta, "Viscous Effects in the Inception of Cavitation," to be presented at the International Symposium on Cavitation Inception, American Society of Mechanical Engineers (1979).

Arndt, R.E.A. et al., "A Note on the Inhibition of Cavitation in Dilute Polymer Solutions," in "Cavitation and Polyphase Flow Forum," R.L. Waid (Ed.), American Society of Mechanical Engineers, pp. 1-4 (1976).

Arndt, R.E.A. and A.P. Keller, "Free Gas Content Effects on Cavitation Inception and Noise in a Free Shear Flow," Conference on Two-Phase Flow and Cavitation in Power Generation Systems, Proceedings, International Association for Hydraulic Research, Grenoble, France, pp. 3-16 (1976).

Arndt, R.E.A., "Investigation of the Effects of Dissolved Gas and Free Nuclei on Cavitation and Noise in the Wake of a Sharp Edged Disk," Joint Symposium on Design and Operation of Fluid Machinery VII, American Society of Civil Engineers, American Society of Mechanical Engineers, International Association for Hydraulic Research, Ft. Collins, Colorado, pp. 543-556 (1978).

Arndt, R.E.A., "Cavitation on Model Propellers with Boundary Layer Trips," in "Cavitation and Polyphase Flow Forum," R.L. Waid (Ed.), American Society of Mechanical Engineers, pp. 30-33 (1976).

Bailey, A.B., "The Relationship Between Flow Separation and Cavitation," Department of Engineering Science, Oxford University, Report 1111/70 (1970).

Baker, E.S., "Review of Wall Effects on Fully Developed Cavity Flows," 18th American Towing Tank Conference, U.S. Naval Academy, Annapolis, MD (1977).

Bjorheden, O. and L. Astrom, "Prediction of Impeller Noise Spectra," Symposium on Hydrodynamics of Ship and Offshore Propulsion Systems, Sponsored by Det Norske Veritas, Høvik outside Oslo (1977).

Black, H.F. and L.-D. Santos, "Stability of Oscillations in Boiler Feed Pump Pipe-Line Systems," Institute of Mechanical Engineering Conference on Vibrations and Noise in Pump Fan and Compressor Installations, University of Southampton, U.K. (1975).

Blake, W.K. et al., "Effects of Boundary-Layer Development on Cavitation Noise and Inception on a Hydrofoil," David W. Taylor Naval Ship Research and Development Center Report 76-0051 (1976).

Braisted, D. and C. Brennen, "Observations on Instabilities of Cavitating Inducers," Cavitation and Polyphase Flow Forum, American Society of Mechanical Engineers, pp. 19-23 (1978).

Brennen, C., "The Dynamic Behavior and Compliance of a Stream of Bubbles," Transactions, American Society of Mechanical Engineers, Journal of Fluid Engineering, pp. 533-541 (1973).

Brennen, C., "The Unsteady Dynamic Characterization of Hydraulic Systems with Emphasis on Cavitation and Turbomachines," Joint Symposium on Design and Operation of Fluid Machinery, VI, American Society of Civil Engineers, American Society of Mechanical Engineers, International Association for Hydraulic Research, Ft. Collins, Colorado, pp. 97-107 (1978).

Brennen, C. and A.J. Acosta, "The Dynamic Transfer Function for a Cavitating Inducer," Journal of Fluid Engineering, Vol. 98, pp. 182-191 (1976).

Brockett, T., "Some Environmental Effects on Headform Cavitation Inception," Naval Ship Research and Development Center Report 3974 (1972).

Clay, C.S. and H. Medwin, "Acoustical Oceanography," Wiley (1977).

Daily, F.W. and V.E. Johnson, Jr., "Turbulence and Boundary-Layer Effects on Cavitation Inception From Gas Nuclei," Transactions, American Society of Mechanical Engineers, Vol. 78, pp. 1695-1706 (1956).

Durkin, J.M. and L.W.H. Luehr, "Dynamic Response of Lift Fans Subject to Varying Backpressure," American Institute of Aeronautics and Astronautics, Society of Naval Architects and Marine Engineers, Advanced Vehicles Conference, San Diego (1978).

Ellis, A.T. et al., "Cavitation Suppression and Stress Effects in High-Speed Flows of Water with Dilute Macromolecular Additives," Transactions, American Society of Mechanical Engineers, Journal of Basic Engineering, Ser. D, Vol. 92, No. 3, pp. 459-466 (1970).

Fanelli, M., "Further Considerations on the Dynamic Behavior of Hydraulic Turbomachinery," Water Power, pp. 208-222 (1972).

Gaster, M., "The Structure and Behavior of Laminar Separation Bubbles," Advisory Group for Aerospace Research and Development Proceedings, No. 4, Part 2, pp. 813-854, London (1966).

Gates, E.M., "The Influence of Freestream Turbulence, Freestream Nuclei Populations and a Drag-Reducing Polymer on Cavitation Inception on Two Axisymmetric Bodies," Division of Engineering and Applied Science, California Institute of Technology, Report 183-2 (1977).

Gates, E.M. and J. Bacon, "Determination of Cavitation Nuclei Distributions by Holography," Journal of Ship Research, Vol. 22, No. 1, pp. 29-31 (1978).

Gates, E.M. and A.J. Acosta, "Some Effects of Several Freestream Factors on Cavitation Inception on Axisymmetric Bodies," 12th Symposium on Naval Hydrodynamics, Washington, D.C. (1978).

Gavrilov, L.R., "Free Gas Content of a Liquid and Acoustical Techniques for Its Measurement," Soviet Physics-Acoustics, Vol. 15, No. 3, pp. 285-295 (1970).

Hall, D.J. and J.C. Gibbings, "Influence of Stream Turbulence and Pressure Gradient upon Boundary Layer Transition," Journal of Mechanical Engineering Science, Vol. 14, No. 2, pp. 134-146 (1972).

Holl, J.W., "Limited Cavitation," article in "Cavitation State of Knowledge," American Society of Mechanical Engineers, J. Robertson and G.F. Wislicenus (Eds.) (1969).

Holl, J.W. and A.L. Kornhauser, "Thermodynamic Effects on Desinent Cavitation on Hemispherical Nosed Bodies in Water of Temperatures from 80°F to 260°F," Journal of Basic Engineering, American Society of Mechanical Engineers, pp. 44-58 (Mar 1970).

Hoyt, J., "The Effects of Additives on Fluid Friction," Journal of Basic Engineering, Transactions, American Society of Mechanical Engineers, Vol. 94, Ser. D, No. 2, pp. 258-285 (1972).

Hsieh, D.Y. and M.S. Plesset, "Theory of Rectified Diffusion of Mass into Gas Bubbles," Acoustical Society of America Journal, Vol. 33, No. 2, pp. 206-215 (Feb 1961).

Huang, T.T. and D.E. Hannan, "Pressure Fluctuations in Regions of Flow Transition," David W. Taylor Naval Ship Research and Development Center Report 4723 (1975).

Huang, T.T. and F.B. Peterson, "Influence of Viscous Effects on Model Full-Scale Cavitation Scaling," Journal of Ship Research, Vol. 20, No. 4, pp. 215-223 (1976).

Huang, T.T. and N. Santelli, "Cavitation Inception Observations on Two Axisymmetric Headforms," David W. Taylor Naval Ship Research and Development Center Report SPD-807-01 (1977).

Johnson, V.E., "Investigation of Cavity Flows by Experimental Means," International Union of Theoretical and Applied Mechanics Symposium on Non-Steady Flow of Water at High Speeds, Nauka, pp. 60-83, Lenningrad (1972).

Johnson, V.E., Jr. and T. Hsieh, "The Influence of Entrained Gas Nuclei Trajectories on Cavitation Inception," 6th Symposium on Naval Hydrodynamics, Washington, D.C. (1966).

Johnsson, C.A., "Cavitation Inception on Headforms, Further Tests," 12th International Towing Tank Conference, Rome, pp. 381-392 (1969).

Katz, J.K., "Determination of Solid Nuclei and Bubble Distributions in Water," Division of Engineering and Applied Science, California Institute of Technology, Report E 183-3 (1978).

Kaups, K., "Transition Prediction on Bodies of Revolution," Douglas Aircraft Co., Long Beach, CA, Report MDL J6530 (1974).

Keller, A., "Experimentelle und Theoretische Untersuchungen Zum Problem Der Modellmässigen Behandlung Von Strömungskavitation," Bericht NK. 26, Miller Inst. Tech. Univ. Munich. See also English Summary Report Umich 01357-28-T, University of Michigan, Department of Mechanical Engineering (Mar 1973) and Transactions, American Society of Mechanical Engineers, Journal of Basic Engineering, Vol. 94, Ser. D, No. 4, pp. 917-924 (1972).

Keller, A. and E.A. Weitendorf, "Influence of Undissolved Air Content on Cavitation Phenomena at the Propeller Blades and on Induced Hull Pressure Amplitudes," International Association for Hydraulic Research Symposium on Two Phase Flow and Cavitation in Power Generation Systems, Grenoble, pp. 65-77 (1976).

Kim, J.H. and A.J. Acosta, "Unsteady Flow in Cavitating Turbopumps," Transactions, American Society of Mechanical Engineers, Vol. 97, Ser. I, No. 4, pp. 412-419 (1975).

Knapp, R.T., "Cavitation Mechanics and Its Relation to the Design of Hydraulic Equipment," Institute of Mechanical Engineers, Proceedings A, Vol. 166, pp. 150-163 (1958).

Knapp, R.T. et al., "Cavitation," McGraw-Hill (1970).

Knapp, R.T. and A. Hollander, "Laboratory Investigations of the Mechanism of Cavitation," Transactions, American Society of Mechanical Engineers, Vol. 70, pp. 419-435 (1948).

Kolesnikov, K.S. and V.G. Kinelev, "Mathematical Model of Cavitation Phenomena in Heliocentric Pumps," Ivestiga VUZ Aviat. Tekh., Vol. 16, No. 4, pp. 87-92 (1973).

Kuiper, G., "Scale Effects on Propeller Cavitation Inception," 12th Symposium on Naval Hydrodynamics, Washington, D.C. (1978).

Lindgren, H. and C.A. Johnsson, "Cavitation Inception on Headforms I.T.T.C. Comparative Experiments," Proceedings of the 11th International Towing Tank Conference, Tokoyo, pp. 219-232. Also Pub. No. 58, Swedish State Shipbuilding Experimental Tank, Göteborg (1966).

Mack, L.M., "Transition Prediction and Linear Stability Theory," Paper No. 1, Advisory Group for Aerospace Research and Development Proc. 224, "Laminar Turbulent Transition (1978).

McCarthy, J. et al., "Roles of Transition, Laminar Separation and Turbulence Stimulation in the Analysis of Axisymmetric Body Drag," 11th Symposium on Naval Hydrodynamics, London (1976).

Medwin, H., "In Situ Acoustic Measurements of Microbubbles at Sea," Journal of Geo. Physical Research, Vol. 75, pp. 599-611 (1977).

Morgan, W.B., "Air Content and Nuclei Measurements," 13th International Towing Tank Conference, Berlin/Hamburg (1972).

Morgan, W.B., (Ed.) "17th American Towing Tank Conference," Cavitation Report, Pasadena, Calif. (1974).

Morgan, W.B. and F.B. Peterson, "Cavitation Inception," 18th American Towing Tank Conference Report, U.S. Naval Academy (1977).

Narita, H. and Y. Kunitake, "Investigation on the Ducted Propeller Cavitation and the Duct Erosion Prevention by the Air Injection System," Symposium on Hydrodynamics of Ship and Offshore Propulsion Systems, Sponsored by Det Norske Veritas, Høvik outside Oslo (1977).

Ng, S.L., "Dynamic Response of Cavitating Turbomachines," Ph.D. Thesis, Division of Engineering and Applied Science, California Institute of Technology (1976).

Ng, S.L. et al., "The Dynamics of Cavitating Inducer Pumps," International Association of Hydraulic Research Symposium, Grenoble, pp. 383-399 (1976).

Ng, S.L. and C. Brennen, "Experiments on the Dynamic Behavior of Cavitating Pumps," submitted to Journal of Fluid Engineering (1978).

Noordzij, L., "Some Experiments on Cavitation Inception with Propellers in the NSMB Depressurized Towing Tank," Publication 526, Netherlands Ship Model Basin. Also International Ship Building Progress, Vol. 23, No. 265, Netherlands (1976).

O'Hashi, H., "Analytical and Experimental Study of Dynamic Characteristics of Turbopumps," National Aeronautics and Space Administration TND-4298 (1968).

Parkin, B.R., "Scale Effects in Cavitating Flows," Ph.D. Thesis, Division of Engineering and Applied Science, California Institute of Technology (1952).

Parkin, B.R. and J.W. Holl, "Incipient Cavitation Scaling Experiments for Hemispherical and 1.5 Caliber Ogive-nosed Bodies," Joint CIT/Penn. State Ordnance Research Laboratory Report NORD 7958-264 (1953).

Parkin, B.R. and R.W. Kermeen, "Incipient Cavitation and Boundary Layer Interaction on a Streamlined Body," Division of Engineering and Applied Science California Institute of Technology, Report E-35-2 (1953). See also Kermeen, R.W. et al., "Mechanism of Cavitation Inception and the Related Scale Effects Problem," Transactions, American Society of Mechanical Engineers, Vol. 77, pp. 533-541 (1955).

Parkin, B.R., "Fully Cavitating Hydrofoils in Nonsteady Motion," Division of Engineering and Applied Science, California Institute of Technology, Report 85-2 (1957).

Peterson, F.B., "Water Tunnel High-Speed Basin Cavitation Inception Comparison," 12th International Towing Tank Conference, Rome, pp. 519-523 (1969).

Peterson, F.B., "Hydrodynamic Cavitation and Some Considerations of the Influence of Free-Gas Content," 9th Symposium on Naval Hydrodynamics, Paris (1972).

Peterson, F.B. et al., "Determination of Bubble and Particulate Spectra and Number Density in a Water Tunnel with Three Optical Techniques," 14th International Towing Tank Conference, Ottawa (1975).

Peterson, L.L., "The Propagation of Sunlight and the Size Distribution of Suspended Particles in a Municipally Polluted Ocean Water," Ph.D. Thesis, California Institute of Technology (1974).

Plesset, M.S., "The Dynamics of Cavitation Bubbles," Transactions, American Society of Mechanical Engineers, Journal of Applied Mechanics, Vol. 16, pp. 228-231 (1949).

Plesset, M.S., "Effect of Dissolved Gases on Cavitation in Liquids," Zeit. für Flugwissenschaften, 19 Heft 3, pp. 120-121 (1971).

Plesset, M.S. and S.A. Zwick, "Dynamics of Small Vapor Bubbles in Liquids," Journal of Mathematics and Physics, Vol. 33, p. 309 (1955).

Power, J.L., "Drag, Flow Transition, and Laminar Separation on Nine Bodies of Revolution Having Different Forebody Shapes," David W. Taylor Naval Ship Research and Development Center Report 77-0065 (1977).

Reshotko, E., "Boundary Layer Stability and Transition," Annual Review of Fluid Mechanics, Vol. 8, pp. 311-349 (1976).

Ripkin, J.F. and J.M. Killen, "A Study of the Influence of Gas Nuclei on Scale Effects and Acoustic Noise for Incipient Cavitation in a Water Tunnel," Technical Paper 27, Ser. B, St. Anthony Falls Hydraulic Laboratory, University of Minnesota (1959).

Robertson, J.M. and G.F. Wislicenus (Eds.), "Cavitation State of Knowledge," American Society of Mechanical Engineers (1969).

Rubin, S., "Longitudinal Instability of Liquid Rockets Due to Propulsion Feedback (POGO)," Journal of Spacecraft and Rockets, Vol. 3, No. 8, pp. 1188-1195 (1966).

Schiebe, F.R., "Cavitation Occurrence Counting--A New Technique in Inception Research," "Cavitation Forum," American Society of Mechanical Engineers, New York, pp. 8-9 (1966).

Schiebe, F.R., "The Influence of Gas Nuclei Size Distribution on Transient Cavitation Near Inception," Report 107, St. Anthony Falls Hydraulic Laboratory, University of Minnesota (1969).

Schiebe, F.R., "The Measurement of the Cavitation Susceptability of Water Using Standard Bodies," Report 118, St. Anthony Falls Hydraulic Laboratory, University of Minnesota (1972).

Silberman, E., "The Use of Equivalent Gas Bubble Nuclei to Measure the Cavitation Susceptability of Water," 14th International Towing Tank Conference, Ottawa, Vol. 2, pp. 248-251 (1975).

Takahashi, H., "Appendix 2 -- Basic Mechanisms of Cavitation Inception," 14th International Towing Tank Conference, Ottawa Proceedings VII, pp. 53-75 (1975).

Van Driest, E.R. and C.B. Blumer, "Boundary Layer Transition: Freestream Turbulence and Pressure Gradient Effects," American Institute of Aeronautics and Astronautics Journal, Vol. 1, No. 6, pp. 1303-1306 (1963).

Van Ingen, J.L., "On the Calculation of Laminar Separation Bubbles in Two-Dimensional Incompressible Flow," in AGARD CP-168 "Flow Separation," Göttingen (1975). See also Paper 20 AGARD Proceedings 224, "Transition, Pressure Gradient, Suction, Separation and Stability Theory" (1977).

van der Meulen, J.H.J., "The Influence of Polymer Injection on Cavitation," Conference of Cavitation, Heriot-Watt University, Institute of Mechanical Engineering, London (1974).

van der Meulen, J.H.J., "Holographic Study of Polymer Effect on Cavitation," Polyphase and Cavitation Forum, American Society of Mechanical Engineers, New Orleans. See also, "A Holographic Study of Cavitation on Axisymmetric Bodies and the Influence of Polymer Additives," Publication 509, Netherlands Ship Model Basin, Wageningen, Netherlands (1976).

van der Meulen, J.H.J., "A Holographic Study of the Influence of Boundary Layers and Surface Characteristics on Incipient and Developed Cavitation on Axisymmetric Bodies," 12th Symposium on Naval Hydrodynamics, Washington, D.C. (1978).

van der Walle, F., "On the Growth of Nuclei and the Related Scaling Factors in Cavitation Inception," 4th Symposium on Naval Hydrodynamics, Washington, D.C., ONR/ACR-92, pp. 357-404 (1962).

Van Driest, E.R. and C.B. Blumer, "Boundary Layer Transition: Freestream Turbulence and Pressure Gradient Effects," American Institute of Aeronautics and Astronautics Journal, Vol. 1, No. 6, pp. 1303-1306 (1963).

Wallis, G., "One-Dimensional Two-Phase Flows," McGraw-Hill (1969).

Wazzan, A.R. et al., "Spatial and Temporal Stability Charts for the Falkner-Skan Boundary Layer Profiles," DAC 67086. See also American Institute of Aeronautics and Astronautics Journal, Vol. 8, No. 2, pp. 301-308 (1968).

Wazzan, A.R. and C. Gazley, Jr., "The Combined Effects of Pressure Gradient and Heating on the Stability and Transition of Water Boundary Layers," Rand Report R-2175-ARPA. See also "Low-Speed Boundary Layer Transition Workshop II," Rand Corp., Santa Monica, CA (1978).

Weitendorf, E.A., "Cavitation and Its Influence on Induced Hull Pressure Amplitudes," Symposium Hydrodynamics of Ship and Offshore Propulsion Systems, Sponsored by Det Norske Veritas, Høvik outside Oslo (1977).

Wu, T.Y., "Cavity Flow Theory," Annual Review of Fluid Mechanics, Vol. 4, pp. 243-284 (1972).

Yamaguchi, M., "Experimental Investigation on Propeller Exciting Forces," Symposium on Hydrodynamics of Ship and Offshore Propulsion Systems, Sponsored by Det Norske Veritas, Høvik outside Oslo (1977).

INITIAL DISTRIBUTION

Copies	Copies
1 US Army Waterways Experiment Station Res Center Lib	1 NAVSWC DAHLGREN VA/Lib
2 CNR 1 R. Lundegard 1 Code 438/R. Cooper	1 NAVSWC SILVER SPRING MD/Lib
1 ONR/Boston	1 NUSC NEWPORT RI
1 ONR/Chicago	1 NUSC NEW LONDON CT
1 ONR/Pasadena	1 NAVSHIPYD BREMERTON WA/Lib
1 USNA/B. Johnson	1 NAVSHIPYD CHARLESTON SC/Lib
1 NAVPGSCOL	1 NAVSHIPYD PEARL HARBOR HI/Lib
1 NROTCU & NAVADMINU MIT	1 NAVSHIPYD PHILADELPHIA PA/Lib
1 NAVWARCOL	1 NAVSHIPYD PORTSMOUTH NH/Lib
1 NRL/Lib	1 NAVSHIPYD PORTSMOUTH VA/Lib
12 NAVSEASYS COM 2 03D 1 05R 1 32 1 32R 2 312 1 321 1 521 1 525/Burke 2 99632	1 NAVSEC NORFOLK VA/SEC 6660.03 D. Blount 12 DDC 1 AFFDL/FDDS/J. Olsen 2 AFFDL/FYS 1 D. Cooley 1 S. Pollock
1 NAVFACENGC COM	2 COGARD
1 NAVOCEANO/Lib	1 COM (E), STA 5-2
1 NAVAIRDEV CEN	1 Div of Merchant Marine Safety
1 NAVWPNC EN	1 LC/SCI & TECH DIV
1 NAVOCEANSYSC EN	1 MARAD/Adv Ship Prog Off

Copies		Copies	
1	MMA/Tech Lib	1	Florida Atlantic U/Ocean Eng Lab
1	NASA AMES RES CEN R. Medan, MS 221-2	1	Harvard U/Dept of Math G. Birkhoff
4	NASA Langley RES CEN 1 Brooks 1 D. Bushnell 1 J. Lamar, Ms 404A 1 E. Yates, Jr., Ms 340	1	U Hawaii/Library
1	NASA Sci & Tech Info Facility	1	U Illinois/College of Eng Theoretical & Applied Mech J. Robertson
1	NSF/Eng Div	3	State U Iowa/Iowa Inst of Hyd Res 1 J. Kennedy 1 L. Landweber 1 V. Patel
1	U Bridgeport/Mech Eng Dept Prof. E. Uram	1	Johns Hopkins U/Mech Dept
4	U California, Berkeley College of Eng, NA Dept 1 J. Paulling 1 W. Webster 1 J. Wehausen 1 Library	1	Kansas State U/Eng Exp Sta D. Nesmith
23	CIT 20 A. Acosta 1 M. Plesset 1 T. Wu 1 Library	1	Lehigh U/Fritz Lab Lib
3	City College, Wave Hill 1 A. Peters 1 W. Pierson, Jr. 1 J. Stoker	1	Long Island U/Grad Dept of Marine Science
1	Colorado State U/Dept of Civ Eng M. Albertson	4	U Maryland 1 P. Cunniff 1 Plotkin 1 C. Sayre 1 Eng Library
1	U Connecticut/Hyd Res Lab V. Scottron	6	MIT/Dept of Ocean Eng 1 M. Abkowitz 1 J. Kerwin 1 P. Leehey 1 P. Mandel 1 N. Newman 1 F. Noblesse
1	Cornell U/Grad School of Aero Eng W. Sears	3	U Mich/Dept NAME 1 H. Benford 1 R. Couch 1 T. Ogilvie
1	Delaware U/Math Dept		

Copies		Copies	
5	U Minnesota/St. Anthony Falls 1 A. Arndt 1 J. Killen 1 F. Schiebe 1 C. Song 1 J. Wetzel	1	Woods Hole/Ocean Eng Dept SNAME
1	U Notre Dame A. Strandhagen	1	Aerojet-General W. Beckwith
2	Penn State U/Ordnance Res Lab	1	Bolt, Beranek & Newman, MA
3	Southwest Res Inst 1 H. Abramson 1 G. Transleben, Jr. 1 Applied Mech Review	2	Boeing Company/Commercial Airplane Group 1 P. Rubbert 1 G. Saaris
1	Stanford Res Inst/Library	1	CALSPAN, INC./ Applied Mech Dept
3	Stanford U/Dept of Civ Eng 1 B. Perry 1 R. Street 1 Dept of Aero and Astro J. Ashley	1	Dynamics Technology
3	SIT/Davison Lab 1 J. Breslin 1 S. Tsakonas 1 Library	1	Flow Research, Inc.
1	Utah State U/College of Eng R. Jeppson	1	Eastern Res. Group
2	U Virginia/Aero Eng Dept 1 J. Haviland 1 Y. Yoo	2	General Dynamics Corp. 1 Convair Aerospace Div/ A. Cunningham, Jr. 1 Electric Boat Div/ V. Boatwright, Jr.
2	UPI 1 Nayfeh 1 Schetz	1	Gibbs & Cox, Inc. Tech Info Control Section
2	Webb Institute 1 E. Lewis 1 L. Ward	1	Grumman Aircraft Eng Corp./ Grumman Marine W. Carl, Mgr.
1	Worcester Poly Inst/Alden Research Lab	3	Hydronautics, Inc. 1 P. Eisenberg 1 T. Tsu 1 M. Tulin
		2	Lockheed Aircraft Corp./ Lockheed Missiles & Space 1 R. Lacey 1 R. Waid
		1	Marquadt Corp/ General Applied Sci Labs

Copies		Copies	Code	Name	
1	Martin Marietta Corp./Rias P. Jordan	1	1507	D. Cieslowski	
		1	1508	F. Peterson	
2	McDonnell-Douglas Corp., Douglas Aircraft Company 1 J. Giesing 1 Library	1	152	G. Cox (Acting)	
		1	1521	P. Pien	
		4	1524	W. Lin	
1	Newport News Shipbuilding/ Library	3	1532	G. Dobay	
		1	154	M. Ochi (Acting)	
1	Nielsen, NA Rockwell	1	1541	P. Granville	
		1	1542	B. Yim	
1	North American Rockwell, Los Angeles Div., Dept 056-015 J. Tulinius	4	1544	R. Cumming	
		1	1548	R. Folb	
		20	1552	J. McCarthy	
2	Northrop Corp./Aircraft Div. 1 J. Gallagher 1 J. Stevens	4	1556	G. Santore	
		1	156	G. Hagen	
		1	1564	J. Feldman	
1	Oceanics, Inc. P. Kaplan	1	1568	G. Cox	
		1	1572	M. Ochi	
1	Sperry Sys. Mgmt.	1	1576	W.E. Smith	
1	Robert Taggart, Inc.	1	16	H. Chaplin	
1	Tracor	1	166	R. Englar	
		1	17	W. Murray	
<b>CENTER DISTRIBUTION</b>					
Copies	Code	Name	Code	Name	
1	11	W. Ellsworth	3	1843	H. Haussling
1	115	R. Johnston	1	19	M. Sevik
1	1151	W. O'Neill	1	1901	M. Strasberg
1	1152	W. Stolgitis	1	1905.1	W. Blake
1	1154	L. Tedeschi	1	273	W. Blumberg
1	15	W. Morgan (Acting)	1	2732	
1	1504	V. Monacella	10	5211.1	Reports Distribution
1	1505		1	522.1	Library (C)
1	1506		1	522.2	Library (A)

